

# Dynamic Testing of Structures Using Scale Models

Anshuman Jha

A Thesis

In

The Department

of

Mechanical and Industrial Engineering

Presented in Partial Fulfillment of the Requirements  
for the Degree of Master of Applied Science (Mechanical Engineering) at  
Concordia University  
Montreal, Quebec, Canada

August 2004

© Anshuman Jha, 2004



Library and  
Archives Canada

Published Heritage  
Branch

395 Wellington Street  
Ottawa ON K1A 0N4  
Canada

Bibliothèque et  
Archives Canada

Direction du  
Patrimoine de l'édition

395, rue Wellington  
Ottawa ON K1A 0N4  
Canada

*Your file* *Votre référence*  
ISBN: 0-612-94727-0

*Our file* *Notre référence*  
ISBN: 0-612-94727-0

The author has granted a non-exclusive license allowing the Library and Archives Canada to reproduce, loan, distribute or sell copies of this thesis in microform, paper or electronic formats.

L'auteur a accordé une licence non exclusive permettant à la Bibliothèque et Archives Canada de reproduire, prêter, distribuer ou vendre des copies de cette thèse sous la forme de microfiche/film, de reproduction sur papier ou sur format électronique.

The author retains ownership of the copyright in this thesis. Neither the thesis nor substantial extracts from it may be printed or otherwise reproduced without the author's permission.

L'auteur conserve la propriété du droit d'auteur qui protège cette thèse. Ni la thèse ni des extraits substantiels de celle-ci ne doivent être imprimés ou autrement reproduits sans son autorisation.

---

In compliance with the Canadian Privacy Act some supporting forms may have been removed from this thesis.

Conformément à la loi canadienne sur la protection de la vie privée, quelques formulaires secondaires ont été enlevés de cette thèse.

While these forms may be included in the document page count, their removal does not represent any loss of content from the thesis.

Bien que ces formulaires aient inclus dans la pagination, il n'y aura aucun contenu manquant.

# Canadä



# **ABSTRACT**

## **DYNAMIC TESTING OF STRUCTURES USING SCALE MODELS**

Anshuman Jha

Dynamic testing is very useful in the design and development of products and systems. Although designers employ most powerful analysis tools, using the most elaborate electronic computers, actual testing is required in order to ensure the proper functioning of the designed system. For the structures that are extremely small such as the Micro Electromechanical Systems (MEMS) or that are very large such as civil and aerospace structures complex dynamic tests can be carried out on a replica of the system, called the *model*, made to larger or smaller scale, respectively, for reasons of economy, convenience and saving in time.

Similitude theory is employed to develop the necessary similarity conditions (scaling laws) for dynamic testing of scaled structures. Scaling laws provide relationship between a full-scale structure and its small scale model, and can be used to predict the response of the prototype by performing dynamic testing on inexpensive model conveniently. Such scaled models have been extensively used in wind tunnel testing of large structures such as automobiles, buildings and aircrafts structures. The difficulty of making completely similar small scale models often leads to certain types of relaxations and distortions from exact duplication of the prototype (partial similarity). Both complete and partial similarities are discussed. These scaling laws are then validated both by

carrying out finite element analysis using ANSYS 7.1, and by performing experiments in the laboratory for a simple structures.

The above methodology has also been applied to the design validation of a shipboard monitor console. The console is required to isolate the monitor from the shock and vibration inputs and ensure its proper functioning. The shipboard console and its scale model have been investigated for their dynamic response subjected to sinusoidal and shock loads and a good correlation has been found between the prototype and the model.

## **ACKNOWLEDGEMENTS**

I am sincerely grateful to my erudite supervisors Dr. Rama Bhat and Dr. Ramin Sedaghati for their enthusiastic guidance and continuous encouragement throughout my thesis work almost for two years.

I would like to express my thanks to Mr. Danius Juras and Mr. Jose Esteves for facilitating all the means and helping me in carrying out experiments in the laboratory.

Also I would like to thank my colleagues and friends for their help and useful discussions during the course of this work.

Last but not the least I would like to thank my parents, uncle, aunty and cousins for their moral support throughout the research period.

# TABLE OF CONTENTS

	PAGE NO.
<b>ABSTRACT</b>	iii
<b>ACKNOWLEDGEMENTS</b>	v
<b>TABLE OF CONTENTS</b>	vi
<b>LIST OF FIGURES</b>	x
<b>LIST OF TABLES</b>	xiv
<b>NOMENCLATURE</b>	xv
<b>CHAPTER 1 INTRODUCTION</b>	1
<b>1.1 INTRODUCTION</b>	1
<b>1.2 STATE OF THE ART</b>	4
1.2.1 Historical Development of Dimensional Analysis	4
1.2.2 Fields of Application	9
<b>1.3 MOTIVATION AND SCOPE OF PRESENT WORK</b>	18
<b>1.4 ORGANIZATION OF THE THESIS</b>	19
<b>CHAPTER 2 PRINCIPLES OF SCALED MODELING</b>	21
<b>2.1 MODELING BASED ON THE CONDITION OF SIMILARITY</b>	21
<b>2.2 DIMENSIONAL ANALYSIS</b>	22
2.2.1 Primary and Secondary Quantities in Dimensional Analysis	22

2.2.2 Dimensional Homogeneity	24
<b>2.3 PRINCIPLE OF SCALE MODELING</b>	<b>24</b>
2.3.1 Primary and Secondary Scale Factors	27
2.3.2 Representative Quantities and Pi-Numbers	28
<i>2.3.2.1 Law Approach</i>	31
<i>2.3.2.2 Characteristic Equation Approach</i>	32
<i>2.3.2.3 Parameter Approach</i>	34
<b>2.4 TYPES OF MODELS BASED ON SIMILARITY CONDITION</b>	<b>36</b>
2.4.1 Completely Similar Models	36
<i>2.4.1.1 Steps in Complete Similarity Modeling</i>	36
<i>2.4.2.1 Derivation of Scale Factors for Dynamic Analysis using Dimensional Analysis</i>	37
2.4.2 Relaxed or Distorted or Dissimilar Models	42
<i>2.4.2.1 Need of Relaxation</i>	42
<b>2.5 IDENTIFYING WEAK LAWS</b>	<b>45</b>
2.5.1 Disregarding Weak Laws	46
2.5.2 Self-Modeling Tests	47
2.5.3 Sequential Modeling	48
2.5.4 Regional Modeling	48
2.5.5 Directional Modeling	49
2.5.6 Circumventive Strong Laws	49
2.5.7 Restriction in Generality	50
2.5.8 Law Simulation	50
2.5.9 Dummy Weights	50

2.5.10 Dummy Spring	51
2.5.11 Temporally Integrated Effects	52
2.5.12 Use of Analytical Knowledge	52
2.5.13 Use of the Same Material	55
<b>2.6 VALIDATION OF SCALING LAWS ON SIMPLE STRUCTURES</b>	<b>56</b>
2.6.1 Neglecting Gravity Effects	56
<i>2.6.1.1 Modal Analysis</i>	58
<i>2.6.1.2 Harmonic Analysis</i>	61
<i>2.6.1.3 Transient Analysis</i>	65
2.6.2 Using Dummy Masses To Avoid Violating Gravity Effects	69
<i>2.6.2.1 Modal Analysis</i>	71
<i>2.6.2.2 Harmonic Analysis</i>	75
<i>2.6.2.3 Transient Analysis</i>	77
<b>CHAPTER 3 EXPERIMENTAL VERIFICATION OF SCALING LAWS</b>	<b>80</b>
<b>3.1 INTRODUCTION</b>	<b>80</b>
<b>3.2 FABRICATION OF PROTOTYPE AND MODEL STRUCTURE</b>	<b>81</b>
<b>3.3 EXPERIMENTAL SETUP AND RESULTS</b>	<b>82</b>
3.3.1 Natural Frequency Measurement	82
3.3.2 Mode Shape Measurement	86

<b>CHAPTER 4 NAVAL SHIPBOARD CONSOLE VIBRATION AND SHOCK ANALYSIS USING SCALED MODEL</b>	93
<b>4.1 GENERAL</b>	93
<b>4.2 DESCRIPTION OF THE SHIPBOARD MONITOR AND CONSOLE</b>	93
<b>4.3 SCALING OF SHIPBOARD MONITOR AND CONSOLE</b>	95
<b>4.4 FINITE ELEMENT MODELING AND MESHING</b>	96
<b>4.5 ANALYSIS</b>	98
4.5.1 Modal Analysis	98
4.5.2 Harmonic Analysis	100
4.5.3 Shock Test	104
<b>CHAPTER 5 CONCLUSIONS AND FUTURE WORK</b>	110
<b>5.1 SUMMARY</b>	110
<b>5.2 CONCLUSIONS</b>	111
<b>5.3 FUTURE WORK</b>	112
<b>REFERENCES</b>	113
<b>APPENDIX-1</b>	118
<b>APPENDIX-2</b>	119
<b>APPENDIX-3</b>	121

# LIST OF FIGURES

Fig. 1.1	Flow chart for problem analysis	1
Fig. 1.2	Segmented Model of Aircraft Carrier	11
Fig. 1.3	Deflection Curves Obtained from Vibration Generator Test	12
Fig. 1.4	Diffusion of Smoke Above and Within Shear Layer 1/400 Scale Model of Part of Downtown Montreal in 6-FT×9-FT Wind Tunnel	13
Fig. 1.5	Model and Full-Scale Saturn Vibration Test Vehicles	15
Fig. 1.6	First Bending Mode of Saturn, of Maximum Dynamic Pressure weight	16
Fig. 1.7	First Cluster Mode of Saturn, Maximum Dynamic Pressure weight	16
Fig. 1.8	Model Glacier Made from Kaolin. Faults and Fields Closely Resemble Those of Field Observations	17
Fig. 1.9	Acoustic Model Designed to Study Audience Absorption in Lecture Halls	18
Fig. 2.1	Prototype and Homologous (Scale) Model of Vibrating Beam	26
Fig. 2.2	Three Approaches to obtaining pi-numbers	30
Fig. 2.3	Simple spring-mass-dashpot system	33
Fig. 2.4	Summary of Relaxation Methods in Scaled Modeling	44
Fig. 2.5	Three Hypothetical Effects of $\pi_1$ on $\pi_3$	45
Fig. 2.6	Cantilever Beam Meshed with 40 BEAM3 Elements	57
Fig. 2.7	Amplitude Response for $\frac{1}{2}$ Scale Model Beam Under Harmonic Excitation	62
Fig. 2.8	Amplitude Response for Prototype Beam Under Harmonic Excitation	62
Fig. 2.9	Amplitude Response to Harmonic Excitation (Analytical & Predicted Response Using Model)	63
Fig. 2.10	Maximum Stresses ( $N/m^2$ ) Developed During Harmonic Excitation in $\frac{1}{2}$ Scale Model	64

Fig. 2.11	Maximum Stresses ( $N/m^2$ ) Developed During Harmonic Excitation in Prototype	64
Fig. 2.12	Rectangular Impulse for Transient Analysis	65
Fig. 2.13	Amplitude Response for $\frac{1}{2}$ Scale Model Beam Under Impulse Excitation	67
Fig. 2.14	Amplitude Response for Prototype Beam Under Impulse Excitation	67
Fig. 2.15	Amplitude Response for Impulse Excitation (Analytical & Predicted Response Using Model)	68
Fig. 2.16	Model Clamped Beam Meshed with Beam elements and Dummy Masses	71
Fig. 2.17	Amplitude Response for Model with Dummy Masses Under Harmonic Excitation	75
Fig. 2.18	Amplitude Response to Harmonic Excitation (Analytical & Predicted Response Using Model with Dummy Masses)	76
Fig. 2.19	Amplitude Response for Scale Model Beam with Dummy Masses Under Impulse Excitation	77
Fig. 2.20	Amplitude Response for Impulse Excitation (Analytical & Predicted Response Using Model)	78
Fig. 3.1	Basic Test Setup in Dynamic Testing	80
Fig. 3.2	Prototype 1018-Steel Beam and its $\frac{1}{2}$ Scaled 6061-T6 Aluminium Beam	81
Fig. 3.3	Prototype Beam Clamped at One End to Achieve Cantilever Boundary Condition	82
Fig. 3.4	Experimental Setup for Vibration Testing of Prototype Beam	83
Fig. 3.5	FRF for Prototype	84
Fig. 3.6	Experimental Setup with Laser Vibrometer for Model Beam	84
Fig. 3.7	FRF for Model	85
Fig. 3.8	Experimental Set up for Roving Impact Test to Obtain Mode Shape	87
Fig. 3.9	Imaginary part of FRF (H11) for Prototype Beam	89

Fig 3.10	Mode Shapes obtained Experimentally for Prototype and its $\frac{1}{2}$ Scale Model Beam	92
Fig. 4.1	Bridge Control Console Unit	94
Fig. 4.2	Part of Bridge Control Console which is modeled for FEM Analysis	96
Fig. 4.3	FEM Model of Console with CRT Monitor and Beam Cross Section	97
Fig. 4.4	Harmonic Input for Prototype	100
Fig. 4.5	Scaled Harmonic Input for Model	101
Fig. 4.6	Amplitude Response for $\frac{1}{2}$ Scale Model under Harmonic Excitation	102
Fig. 4.7	Amplitude Response for Prototype under Harmonic Excitation	102
Fig. 4.8	Amplitude Response for Harmonic Excitation (Analytical & Predicted Response using Model)	103
Fig. 4.9	Hammer Falls Through a Height ‘h’, and Impacts the Base of the Anvil on which the Console-Monitor Assembly is Mounted	105
Fig. 4.10	Amplitude Response for $\frac{1}{2}$ Scale Model under Impulse Excitation	107
Fig. 4.11	Amplitude Response for Prototype under Impulse Excitation	108
Fig. 4.12	Amplitude Response Under Impulse Excitation (Analytical & Predicted Response using Model)	109
Fig 6.1	Amplitude Response for $\frac{1}{2}$ Scale Model under Harmonic Excitation	118
Fig 6.2	Amplitude Response for Prototype under Harmonic Excitation	118
Fig 6.3	Amplitude Response for $\frac{1}{2}$ Scale Model under Impulse Excitation	121
Fig 6.4	Amplitude Response for Prototype under Impulse Excitation	121
Fig 6.5	Amplitude Response for $\frac{1}{2}$ Scale Model under Impulse Excitation	122

Fig 6.6	Amplitude Response for Prototype under Impulse Excitation	122
Fig 6.7	Amplitude Response for $\frac{1}{2}$ Scale Model under Impulse Excitation	123
Fig 6.8	Amplitude Response for Prototype under Impulse Excitation	123
Fig 6.9	Amplitude Response for $\frac{1}{2}$ Scale Model under Impulse Excitation	124
Fig 6.10	Amplitude Response for Prototype under Impulse Excitation	124
Fig 6.11	Amplitude Response for $\frac{1}{2}$ Scale Model under Impulse Excitation	125
Fig 6.12	Amplitude Response for Prototype under Impulse Excitation	125

## LIST OF TABLES

Table 2.1	Dimensions of Measured Quantities for Dynamic Analysis	37
Table 2.2	Parameters used for Prototype a Model Beam	57
Table 2.3	Natural Frequencies and Mode Shapes with Aluminium Model and Steel Prototype	60
Table 2.4	Harmonic Input for Prototype	61
Table 2.5	Scaled Harmonic Input for Model	61
Table 2.6	Parameters used for Model Beam with Dummy Masses	69
Table 2.7	Natural Frequencies and Mode Shapes with Aluminium Model and Steel	74
Table 2.8	Scaled Harmonic Input for Model	75
Table 3.1	Prototype Natural Frequencies obtained Experimentally and from Simulation	83
Table 3.2	Model Natural Frequencies obtained Experimentally and from Simulation	85
Table 3.3	Comparison of the Predicted Natural Frequency using Experimental Results of the Model Beam with Experimental Natural Frequencies for Prototype	86
Table 3.4	Imaginary Values of FRF at obtained Experimentally at First Three Natural Frequencies for Prototype Beam	91
Table 3.5	Imaginary Values of FRF obtained Experimentally at First Three Natural Frequencies for $\frac{1}{2}$ Scale Model Beam	91
Table 4.1	Natural Frequencies with Same material Model	99
Table 4.2	Harmonic Input for Prototype	100
Table 4.3	Scaled Harmonic Input for Model	101
Table 4.4	Medium Weight Test Heights	104

## NOMENCLATURE

$A_p$	Cross-Sectional Area of Prototype,	$m^2$
$C$	Material Constant,	$N.m/s$
$E$	Young's Modulus,	$N/m^2$
$E_m$	Young's Modulus of Model Material,	$N/m^2$
$E_p$	Young's Modulus of Prototype Material,	$N/m^2$
$F$	Force,	$N$
$F_m$	Model Representative Force,	$N$
$F_p$	Prototype Representative Force,	$N$
$I$	Cross-Sectional moment of inertia,	$m^4$
$I_H$	Impulse of the Hammer,	$N.s$
$I_s$	Impulse of the Structure,	$N.s$
$M$	Bending Moment,	$N.m$
$M_a$	Mass of Anvil,	$kg$
$M_h$	Mass of Hammer,	$kg$
$M_s$	Mass of Structures,	$kg$
$V_h$	Velocity of Hammer,	$m/s^2$
$V_c$	Common Velocity of Hammer, Monitor-Console Structure and Anvil,	$m/s^2$

$a$	Acceleration,	$m/s^2$
$a_m$	Model Representative Acceleration,	$m/s^2$
$a_p$	Prototype Representative Acceleration,	$m/s^2$
$c_m$	Model Damping Coefficient,	$N.m/s$
$c_p$	Prototype Damping Coefficient,	$N.m/s$
$g$	Gravitational Acceleration Constant,	$m/s^2$
$l_m$	Model Representative Length,	$m$
$l_p$	Prototype Representative Length,	$m$
$m$	Mass,	$kg$
$r$	Rank of Matrix,	-
$s$	Distance Traveled,	$m$
$t_m$	Model Representative Time,	$s$
$t_p$	Prototype Representative Time,	$s$
$\varepsilon$	Strain,	-
$\lambda_E$	Young's Modulus Scale Factor,	-
$\lambda_f$	Force Scale Factor,	-
$\lambda_a$	Acceleration Scale Factor,	-
$\lambda_c$	Damping Scale Factor,	-
$\lambda_l$	Length Scale Factor,	-
$\lambda_t$	Time Scale Factor,	-
$\lambda_\sigma$	Stress Scale Factor,	-

$\lambda_\rho$	Density Scale Factor,	-
$\lambda_\omega$	Frequency Scale Factor,	-
$\sigma$	Stress,	$N / m^2$
$\rho_m$	Density of Model Material,	$kg / m^3$
$\rho_{om}$	Real density of the Model structure,	$kg / m^3$
$\rho_p$	Density of Prototype Material,	$kg / m^3$
$\omega_m$	Model Representative Frequency,	$r / s$
$\omega_p$	Prototype Representative Frequency,	$r / s$
$\Delta m'$	Dummy Weight's Mass,	$kg$
$\Delta t$	Duration of Shock Pulse,	$s$
$\Delta v'$	Volume per Dummy Weight,	$m^3$

# CHAPTER 1

## INTRODUCTION

### 1.1 INTRODUCTION

Engineering analysis, design and research often need simulations, when the direct observation on the *prototype*, which is the actual system of interest, is not possible or is very costly. The steps involved in the simulation of the prototype are schematically illustrated in Fig. 1.1. In order to define the system precisely, usually many assumptions are made and the new system is referred to as idealized prototype. The assumptions made at this initial stage are not restrictive and are imposed only so that the problem can be well defined.

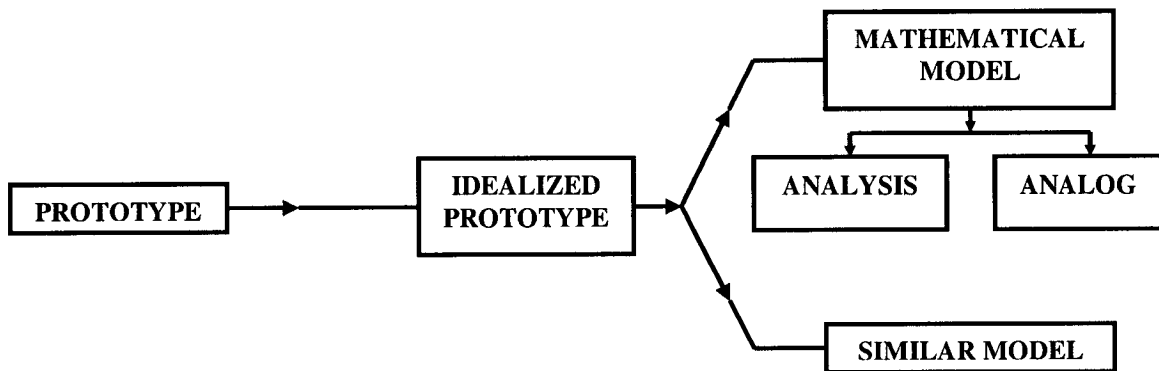


Fig.1.1 Flow chart for problem analysis [6].

Following the definition of the problem, the type of simulation technique to be used is decided. If the problem can be solved analytically, the mathematical model must be developed and subsequently solved either by mathematical analysis or by an analog.

When the analog approach is used, the system or model which is different in appearance to the original prototype is analyzed experimentally.

For the simulation of the prototype with a mathematical model, the characteristic equations describing the behavior of the system should be well known. This frequently adds more assumptions with regard to the behavior of the system. For example, while considering the deformation of structures, the most common assumption is that the material behaves elastically. Thus, a thorough understanding of the characteristics of the system, and the fundamental equations governing the behavior of the system, must be achieved, to have a well defined mathematical system. The main advantage of solving the problems in this manner is the possibility to obtain the complete and detailed solution without having any experimental expenses. The major disadvantage is the large number of assumptions that are needed to establish a mathematical model. Moreover, in many instances, it becomes very difficult to obtain a solution analytically due to the complexity of the governing equations.

The alternative basic simulation technique is one of actually simulating the prototype, or the idealized prototype, with a similar *model*. A similar model is defined as the system which is similar in appearance to the prototype but not identical to it. In practice, such systems are referred to as models and are usually smaller in size than the prototype. In some instances, it may be advantageous to have a model that is larger than the prototype. It is frequently possible, through the use of similar models, to study very complex problems with relative ease, and this is one of the major advantages of the technique. In many cases, less number of assumptions are required when similar models for simulation are used than in simulating with mathematical model. The major

disadvantage of using similar models is that the solution is obtained experimentally which is expensive. Also the results obtained experimentally are frequently restrictive and limited in applicability.

A relationship between the model and prototype must be established regardless of the particular technique chosen to simulate the prototype. Through the development of mathematical models, this relationship evolves naturally and is readily apparent. However, when similar models are used, the relationship between model and the prototype must also be known. The establishment of this relationship and the fulfillment of the various similarity requirements, or model-design conditions, between the two systems are sometimes difficult to achieve [6].

For systems that are large and of a complex nature, dynamic testing and investigations can preferably be carried out on a replica of the system, called the *model*, made to a smaller scale for reasons of economy, convenience and savings in time. Such is the case with the design and development of aircraft, tall structures, oceanic vessels, large dams, harbors and bridges, and many other technologically advanced systems where performance and behavior have to be predicted with confidence to a high degree of accuracy. There are however, also instances such as micro electro mechanical systems (MEMS) where the original system, called the *prototype*, is very small and where a scaled-up model system can be used to advantage [2]. The use of small laboratory models for simulation of complex engineering problems has been found to be particularly valuable in three respects: *a)* To obtain experimental data for quantitative evaluation of a particular system behavior, *b)* to explore the fundamental behavior involved in the occurrence of little-understood and particular type of phenomena, *c)* to obtain

quantitative data for use in prototype design problems, particularly where the mathematical theory is overly complex or even nonexistent [3].

Those principles which enable the proper design and construction, operation, and interpretation of test results of these models comprise the theory of similitude. The theory of similitude includes a consideration of the conditions under which the behavior of two separate entities or systems will be similar, and the techniques of accurately predicting results on the one from the observations on the other [4].

## **1.2 STATE OF THE ART**

Engineers and scientists have been profitably using scale models for many years. Models for vibrating rods and plates were investigated by French mathematician A.L. Cauchy in 1829[5]. The first water basin model for designing watercraft was made by W. Froude in 1869[5]. O. Reynolds started using the concept of scaling in fluid machinery problem and he published classical model experiments on fluid motion in pipes in 1883 [5]. Model tests have many limitations but still they are invaluable for engineers and the use of model testing is increasing steadily.

### **1.2.1 Historical Development of Dimensional Analysis**

Two methods commonly used to establish the similarity relationship between the model and prototype are based on 1) the analysis of the characteristic equation of the system and 2) dimensional analysis [6]. In the former, the system is first described in terms of a mathematical model and then the scaling laws, model-design conditions, or similarity requirements are developed from the model on the other hand in the latter, derivation of the scaling laws by dimensional analysis requires that all system parameters

be listed in and that Buckingham's Theorem be applied to obtain the functional relationship between dimensionless quantities [7]. Dimensional analysis is a technique that enables identification of the fundamental quantities that describes a physical phenomenon or system, and it has been utilized effectively in engineering modeling. The principal purpose of dimensional analysis from engineering viewpoint is the arrangement of the variables of a physical relation so that, without destroying the generality of the relationship, it may be more easily determined experimentally [8]. Thus, the complexity and extent of an experiment may be greatly simplified by this approach. The genesis of the modern theory of dimensional analysis is rooted in the concept of geometric similitude used first by Galileo for determining elastic properties of a single structural member as a function of their geometric dimensions. Newton used it in the study of the Laws of Motion, and Mariotte for work on shock and on fluid flow [9]. Great contributions were made to the analysis of physical phenomena during the eighteenth century, and yet very little attention was paid to matters of physical dimensions during most of that period. Euler broke this trend and showed in several of his numerous writings the meaning of quantities and the mathematical expression of physical relationship [10]. In *Theoria motus corporum solidorum seu rigidorum* (1765), Euler devoted a chapter to questions of units and homogeneity; although his discussions are somewhat obscure, it is evident that Euler was aware that there is nothing absolute in the matter of systems of units and dimensions of physical quantities [10]. Lagrange and Laplace continued the work that was initiated by Euler and formulated the principles of dimensional analysis; Fourier, in the last of his three successive versions (1807, 1811, and 1822) of the *Analytical Theory of Heat*, established the foundations of dimensional

analysis [10]. Fourier also not only showed exceptional mathematical powers but also deep concerns about physical aspects of the problem of heat transfer. He concluded that, to determine numerically most varied movements of heat, it is sufficient to submit each substance to three fundamental measurements [10]. Although Fourier did not draw most of the consequences with which we are familiar now, he recognized the existence of dimensionless groups in his equations. All the basic elements pertaining to the principles of dimensional analysis are in Fourier's *Théorie Analytique de la Chaleur*, but the derivation of relations between variables involved was not foreseen by him [10]. In the works of Fourier, consideration is also given to the flow of heat in similar bodies. Much confusion between similarity and dimensional analysis has now existed for a century, and Fourier did not establish any connection between the two questions. After Fourier, no important development in dimensional analysis took place for half a century. There were considerations and discussions about system of units for old and newly created physical quantities; moreover- from both analytical treatments and considerations of similarity – dimensionless groups, or so-called “abstract coefficients”, started to appear in the literature. In the Index of subjects of *Theory of Sound (1877-8)* by Lord Rayleigh, an entry “Method of Dimensions” is found which marks the beginning of application of principles enunciated by Fourier fifty years ago [10]. The first detailed application of the method of dimensions is to be found at the beginning of the first volume (1877) after discussing the theoretical solution of the problem of the vibration of a mass attached to the center of a stretched string [10]. The corresponding differential equation for vibrations of small amplitude is

$$M \ddot{x} + 2T(x/a) = 0, \quad (1.1)$$

in which  $M$  is the mass,  $x$  is the displacement,  $T$  is the tension of the spring, and  $a$  is half the length of the string. After expressing the time period as

$$\tau = 2\pi\sqrt{(aM/2T)} \quad (1.2)$$

Equation (1.2) expresses the manner in which  $\tau$  varies with each of the independent quantities  $T, M, a$ : results which may all be obtained by considering the dimension of the quantities involved. After emphasizing the importance of the “argument of dimensions” in acoustics, the Lord Rayleigh indicated that the solution of the problem may be written as [10]

$$\tau = f(a, M, T) \quad (1.3)$$

It was explained that the equation must retain its original form unchanged, whatever may be the fundamental units with which the four quantities are numerically expressed. Because  $T$ , the only variable in the function  $f$  that involves time, has dimensions (mass)(length)(time)<sup>-2</sup>, Rayleigh concluded that, when  $a$  and  $M$  are constant, one must have  $\tau$  proportional to  $T^{-1/2}$  as the only way of preventing changes in units from disturbing the functional relationship (1.3). Rayleigh also indicated in detail the procedure of assuming the dependent variable to be proportional to a product of unknown powers of the independent variables and of solving the system of linear algebraic equations which results from the requirement of the same dimension on both sides of the original equation. Carvallo and Vaschy were the first to attempt a formulation of a general theorem for the method of dimensions [10]. Therein Carvallo showed that the equation for the power of a dynamo could be expressed as a relation between two dimensionless variables [10]. The dimensionless equation for the power  $W$ ,

$$W^2 = E^2 I^2 - (4\pi^2 L^2 I^4 / T^2) \quad (1.4)$$

given by Lucas, was transformed by Carvallo into

$$y^2 = x^2 - x^4 \quad (1.5)$$

in which the terms

$$x = 2\pi LI/ET \text{ and } y = 2\pi LW/E^2T \quad (1.6)$$

are dimensionless groups. In these expressions,  $E$ ,  $I$ ,  $L$  and  $T$  indicate electromotive force, current intensity, self-inductance and period of alternating current. Much work was carried out by Carvallo, Vaschy, and Riabouchinsky before Buckingham [11] in 1914 developed the Pi Theorem that forms the basis for investigating physical relationships within the framework of similarity. If, some physical system called prototype, about which it is desired to make certain predictions or draw certain conclusions is considered then for such a system,  $n$  physical parameters which are significant, lead to the relationship of the form

$$f(Q_1, Q_2, \dots, Q_n) = 0 \quad (1.7)$$

If this equation is unique in the sense that only one relation exists between the parameters, then the need for dimensional homogeneity leads to the requirement that there exists an equivalent relation

$$\psi(\pi_1, \pi_2, \dots, \pi_m) = 0 \quad (1.8)$$

This relation is among  $m$  independent dimensionless groups ( $\pi$ ) of the original dimensional parameters where  $m = n - s$  and  $s$  is the minimum number of physical dimensions necessary for the description of the  $n$  parameters. This is general statement of the well known Buckingham  $\pi$  theorem [3]. In 1915, Rayleigh [12] published a paper stimulating the use of his method in dimensions among engineers; he gave several examples, including an analysis of Boussinesq's on the steady passage of heat from a

solid conducting body immersed in a stream of fluid moving with a velocity  $v$  at infinity. Rayleigh assumed that the total heat  $h$  passing in the unit of time was a function of only the linear dimension  $a$  of the solid, the temperature difference  $\theta$ , the velocity  $v$ , the specific heat of the fluid  $c$ , and the conductivity  $k$ . He discarded the density of the fluid, because it “clearly does not enter into the question”. His analysis led to

$$h = ka\theta.F(avc/k). \quad (1.9)$$

Riabouchinsky commented (Nature July 29, pp. 591) that heat, temperature, length, and time are treated in the deduction as independent units; and that if it's supposed that only three of these units to be “really independent”, different results are obtained [13]. Bridgman [14] also presented his contribution on the methods of dimensional analysis that he presented in his book of 1922. The past many decades of dimensional analysis have been studied mainly as the period of increasing application, with the refinement of techniques that always follows the period of development [10]. In reference [8] an algorithm has been developed to calculate a complete optimized set of dimensional products of the variables associated with a physical phenomenon from any complete set of dimensionless products. The developed algorithm is non exhaustive and is readily adaptable for digital computers. Alternative formulation of Buckingham's pi-theorem was also presented by Pankhurst [15], in which exploitation of “orthogonal independence” properties were studied.

### 1.2.2 Fields of Application

Historically dimensional analysis and similarity theory were first used to study hydraulics and the flow of fluids in pipes and channels. Empirical rules were developed through model tests before laws of viscous flow were known. Since many areas of fluid

dynamics are still too complicated and accurate analysis is mathematically very difficult, lot of effort has been devoted to develop accurate similarity methods for fluid dynamics, hydraulics, aerodynamics, and naval hydrodynamics [16]. Model test on water wheels were conducted in the eighteenth century by Smeaton [17]. At the beginning of the twentieth century model tests again began to be carried out by manufacturers for the development of modern types of hydraulic turbines and they are still carried out at the primary stage of the construction when modifications are possible. Hydraulic scaled models are frequently used in pump, turbine, hydraulic torque converters and other turbo machines. These scaled models are used to design the sump or intake, to establish head, flow, efficiency, cavitation characteristics to ensure compliance with specified rated conditions, obtain flow patterns, and to acquire the best efficiency value [18-22].

The best known and perhaps one of the oldest applications of scale model experiments is in the field of naval architecture. Historical records show that experiments with models of ships have been performed since the time of Leonardo da Vinci [23]. However, it was not until W.E. Froude (1874) that model test predictions were established as a valuable engineering tool. He used it to obtain the resistance of a full-scale ship from model resistance experiments in a towing tank. The accurate extrapolation of model test results to full scale was not possible until the principles of spectral and transfer functions were established, as presented by St Dennis and Pierson (1953). Over the years, model tests have demonstrated their usefulness in solving problems relating to both preliminary design and retrofitting. The successful model test program leads to an optimum hydrodynamic and/or structural design which will enhance the economic performance of the marine structure. For many decades model-testing tank,

or water basin have been used for ship designing [3]. Frictional and wave making resistance, propeller performance, ship maneuverability in smooth and rough water, cavitation, ship bending vibrations due to wave impact and slamming, seakeeping, and many other performance would be impossible to predict without model experiments [3].

A 136:1 scale model of 820 feet World War II ESSEX-Class aircraft prototype as shown in Fig 1.2 was tested at the David Taylor Model Basin in regular and irregular seas [24]. Model test objective required that the measurement of elastic response be permitted at any point along the hull. A segmented model joined by a continuous beam was developed and all the scaling laws were found.

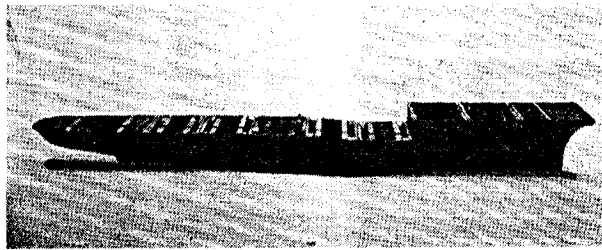


Fig. 1.2 Segmented Model of Aircraft Carrier [24].

Transient vibrations of an unexpected severity were found to result from the wave impact loads on the aircraft carriers. The lack of preliminary knowledge on this type of impact load prompted model tests and computational studies to examine the hull girder response to such loads. It was indicated that agreeable correlation with full scale as shown in Fig 1.3 exists and also revealed the need of complementary model tests.

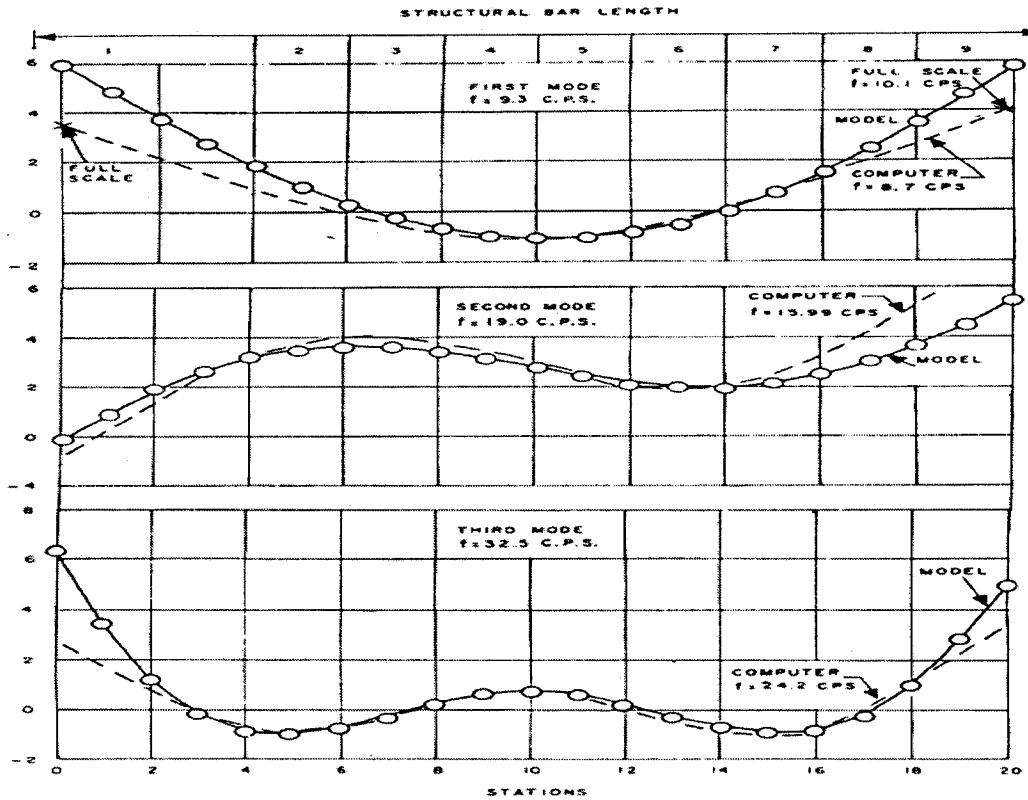


Fig. 1.3 Deflection Curves Obtained from Vibration Generator Test [24].

Just as the water basin was used in studying structural behavior in fluids, the wind tunnel was used to study the structural behavior in subsonic, supersonic, hypersonic, and hypervelocity air flow. Wind tunnels can simulate velocities ranging from a light breeze to many times the speed of sound. They can accommodate the scaled models of buildings and structures that are sensitive to winds [25], aircraft, and spacecraft for studies of turbulence, drag, lift, pressures, buffeting, flutter, and other phenomena [3]. After the dramatic and catastrophic failure of Tacoma Narrows Bridge in 1940, intensive study of the aerodynamic stability of suspension bridges was carried out. Investigators used wind tunnels in order to study the aerodynamics of bridge sections. Use of dynamic “sectional” models, as opposed to complete or full bridge models, is now commonly accepted [26].

Larger model scale and lower modeling cost are advantages offered by sectional approach. The scale ratio for sectional models may be in the region of 1:30 or 1:50, and for full models in conventional wind tunnels may be 1:200 or higher. A 1/400 - Scale model shown in Fig. 1.4 of about one mile of downtown Montreal was used in the 6-ft $\times$ 9-ft low speed wind tunnel to obtain mean pressures and the spectrum on unsteady pressures at different locations on a tall building in a simulated wind shear layer [27].

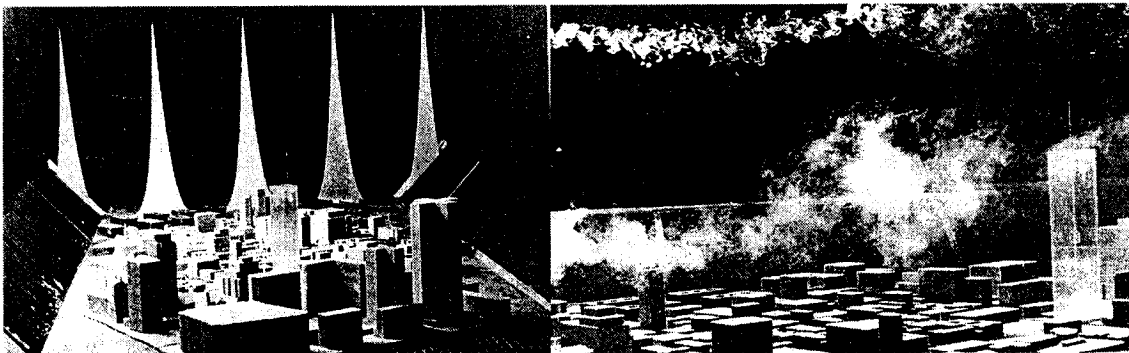


Fig. 1.4 Diffusion of Smoke Above and Within Shear Layer 1/400 Scale Model of Part of Downtown Montreal in 6-FT $\times$ 9-FT Wind Tunnel [27].

Again scaled models have been used extensively in the aeronautical field. In the past decades, dynamic models has made possible many refinements and helped in solving many problems which otherwise would have been impossible to solve economically. Dynamic scaled models have also been used extensively in the development of large launch vehicles in order to study fuel slosh, and the primary natural frequencies of the vehicle, buffet and response to ground winds, and also the determination of response due to acoustic excitation [28]. The importance of dynamic scaled models in aerospace research and development is demonstrated in reference [28]. Much of the work on

dynamic scaled models in aerospace has been carried out at Langley Research center of NASA.

In 1950 a one-tenth dynamic scaled model of large helicopter with a rotor diameter of about 13 feet was tested [29]. This model was designed to study the ground resonance and flutter problems. However, during the investigation, it was found that at 3 per revolution large vibratory stresses were developed which is unusual for a two-blade rotor since the blade stresses are usually at the rotor frequency and frequencies which are integral multiples of the number of blades. These stresses at 3 per revolution were discounted; however, when the actual prototype was flown they also appeared in the prototype and proved as high as to severely limit the flight time. The model was then used in a program to reduce the stresses by changing the mass distribution in the blades. Scaled models are used in the investigation of flutter problems. A 1/6<sup>th</sup> scale model, equipped with wing tip tanks and representative of unswept fighter-type of conventional plan form, was tested for flutter [30]. For the design of the model, the model was dynamically scaled to flutter at the same speed as a full scale; in addition the principles followed in the scaling required that non-dimensional parameters important in flutter, such as mass ratio, frequency ratio, and reduced frequency, remain the same on the model as on the full-scale counter part. No attempt was made to scale the stiffness in the tip-tank or wing-tip-tank-attachment. The results of the flutter experiments were compared with the results of flutter calculation performed by utilizing Rayleigh-Ritz analysis. The propeller whirl flutter was investigated on a model at Langley Transonic Dynamics Tunnel. The phenomenon of propeller whirl flutter is the instability resulting from the coupling of the aerodynamic and gyroscopic forces of the propeller with the stiffness and

inertia forces of the mount [31]. The model test revealed that the weakened mount could cause accidents. Subsequently the aircrafts were redesigned to provide greater margins with respect to this type of flutter. A 1/5<sup>th</sup> scale dynamic replica of Saturn SA-1 launch vehicle was constructed again at Langley Research Center to establish the feasibility of obtaining the required experimental vibration data with a model [32]. Since lateral bending vibrations were of primary interest, exact simulation of effects such as panel flutter, longitudinal vibrations, and fuel sloshing were neglected. In this case mass-stiffness ratios were appropriately scaled, with certain masses being treated as concentrated. For the resulting model which was 32 feet high (as compared to 160 feet full scale) and weighed about 7,500 pounds (as compared to 935,000 pounds on full scale) as shown in Fig. 1.5, good agreements were obtained with the prototype results for the first bending mode as shown in Fig. 1.6. However the first cluster mode results as shown in Fig. 1.7 show discrepancies between model and prototype indicative of the increased difficulty of modeling higher modes.

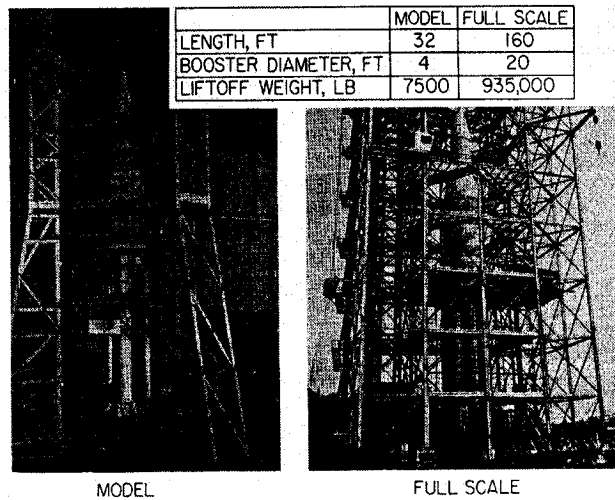


Fig. 1.5 Model and Full-Scale Saturn Vibration Test Vehicles [32].

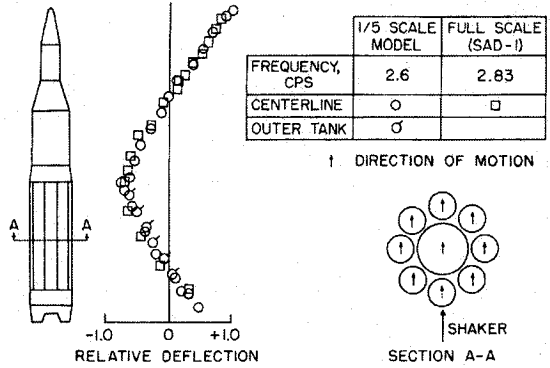


Fig. 1.6 First Bending Mode of Saturn, Maximum Dynamic Pressure weight [32].

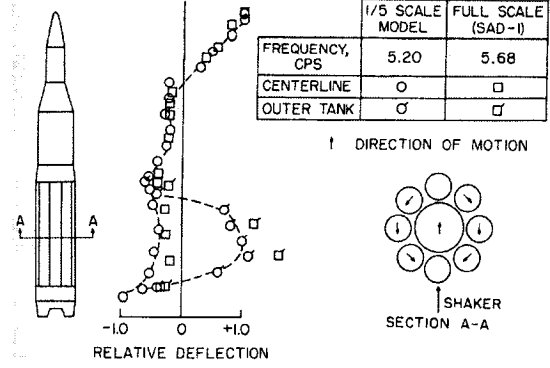


Fig. 1.7 First Cluster Mode of Saturn, Maximum Dynamic Pressure weight [32].

The modeling of concrete structures has received its greatest impetus in the post World War II years when many structural problems dealing with dynamic loads had to be resolved. Time dependent loadings, because of their complex nature and effects on structures, have enabled the experimental technique of using small-scaled models to compete on an equal basis with more traditional analytical methods. Scaled models have been used for evaluating the dynamic properties of concrete material [33], response behavior of multi-storey building structures, dams and bridges due to earthquake [34-37], response due to wind pressures, soil mechanics, pile foundations, underground explosions [3]. Scaled models are now being used for wide applications by building engineers; recently the feasibility study on the application of passive and active stack systems to enhance natural ventilation in public housing in Singapore was carried out using 1:5 scale model to effectively simulate the air flow in each room primary [38]. Objective of this work was to assess the status of natural ventilation in a typical four-room HDB flat using scaled model in the wind tunnel, and to develop an effective passive or active stack system to enhance natural ventilation in the flat.

Meteorologists and geophysicists are another group long interested in model experiments. As early as the late eighteenth century, an attempt was made to construct a laboratory model for cyclone. Now the study of geophysical phenomena in the laboratory on a miniature scale is well advanced. A model of extremely slow fluid flow, a miniature glacier composed of water and kaolin is shown in Fig. 1.8 [3].

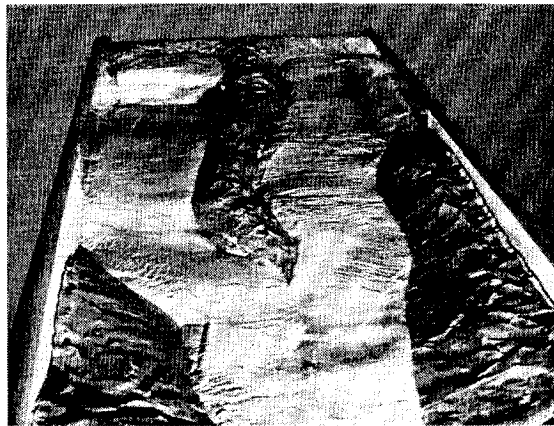


Fig. 1.8 Model Glacier Made from Kaolin. Faults and Fields Closely Resemble Those of Field Observations [3].

There is no limit to scale model experimentation within the realm of quantifiable physical phenomena. Scaled models are used in every field that needs experimental results for the approximation of behavior of phenomena. Acoustic models have contributed to the improvement of auditorium; 1:8 scale model of auditorium was developed to investigate the effect of clothing worn by people on absorption of sound shown in Fig. 1.9 [39]. Using 1:7.5 scale, the complete model of aircraft and the outer section of an A320 full scale wing were made to provided a baseline data set for the development, of noise (during landing) prediction schemes [40].

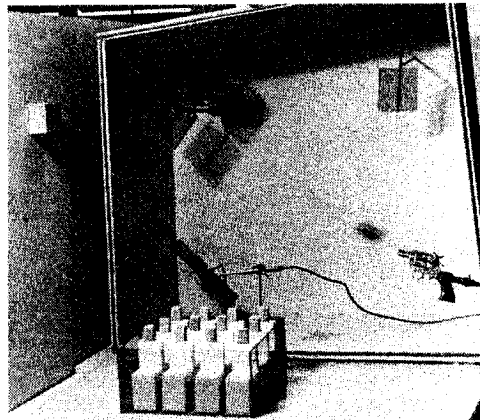


Fig. 1.9 Acoustic Model Designed to Study Audience Absorption in Lecture Halls [39].

### 1.3 MOTIVATION AND SCOPE OF PRESENT WORK

Scale modeling techniques seem to have lost its luster for past three decades. Scale modeling was quite popular till the decade of late 70's, however not much research work has been carried out since then in the area of scaled modeling as it reached its peak of the time. Literature review suggests that scale modeling has proved to be very useful in the fields of naval testing, wind tunnel testing, aerospace applications, earthquake engineering, and performance testing of hydraulic machines. Scale model principles can be very effectively used on many occasions to avoid costly full scale experimentation or just analytical verification of a problem where full scale experiments are not either feasible or possible. Scaled models are not restrictive to any particular field and can provide economic, convenient and time saving experimental results in laboratory with ease. With the development in the field of MEMS, composites scaled modeling can be effectively used in these new areas. Scaled modeling technique also provides researchers the opportunity to carry out experiments in the laboratory at universities which often have limited resources for full scale testing to validate the design requirements. This old

technique of scaled modeling still has many benefits to offer to the new emerging fields thus provides the motivation to further explore this area.

Thorough study of scale modeling techniques has been covered in the present work. Particular scaling laws have been derived for dynamic analysis of structures with different types of possible relaxations taken into consideration to meet the scaling conflicts encountered for dynamic analysis. The scaling laws are validated by carrying out finite element analysis using ANSYS 7.1. The prototype and half scaled model of simple cantilever beam are experimentally verified to compliment the proposed relaxation. The methodology has been applied to the design validation of a shipboard monitor console. The console is required to isolate the monitor from the Shock and Vibration inputs and ensure its proper functioning. The shipboard console and its scale model have been investigated for its dynamic response subjected to sinusoidal and Shock loads and a good correlation has been found between the prototype and the model.

#### **1.4 ORGANIZATION OF THE THESIS**

In chapter 1, historical development of Pi theorem which forms the basis of scaled model experiments and previous works carried out in the use of scaled models have been studied. It also provides the motivation and scope of the thesis undertaken.

In Chapter 2, detailed dimensional analysis and similitude theory has been presented. With the sound background of similitude theory discussed, specific scaling factors for dynamic analysis are derived and verified for a simple cantilever beam by carrying out finite element analysis. Although scaled modeling is an art, a few guidelines and possible relaxations are also discussed in chapters 2 which are often required when complete similarity is not feasible due to practical reasons.

Chapter 3, discusses experimental verification of scaling laws for dynamic analysis using a simple cantilever beam derived in chapter 2, and verifies that the relaxation suggested does not practically affect the response of structure.

In Chapter 4, application of developed methodology has been applied for dynamic testing of shipboard monitor console. The shipboard console and its half scale model have been investigated using finite element analysis in ANSYS 7.1 for its dynamic response subjected to sinusoidal and Shock loads and a good correlation has been found between the prototype and the model.

Chapter 5 presents the conclusions of the work undertaken and recommendations for the future work.

## CHAPTER 2

### PRINCIPLES OF SCALED MODELING

#### 2.1 MODELING BASED ON THE CONDITION OF SIMILARITY

Experimental modeling is based on the fact that the model and the prototype systems obey the same physical laws. The model must be constructed so as to embody all the relevant features and parts of the prototype system. The unique relationship between the model and prototype is broadly referred to as *similarity*. The condition of similarity can be achieved by following the procedure called Dimensional Analysis. This procedure is based on the fact that all general relationships in physics and engineering are expressed by dimensionally homogeneous equations. When methods or time for finding a general valid solution of a problem are not immediately available, dimensional analysis may be applied with advantage, i.e. use may be made of this property of dimensional homogeneity which allows a problem to be attacked solely from the ‘outside’.

The technique that provides the relationship between model and a prototype is called *modeling*. Modeling is an experimental technique and its application is based on the dimensional consideration. The technique employs certain dimensional properties of the variables appearing in the problem which are arranged in the non-dimensional form. The effectiveness of this technique can be enhanced through the use of information about the system under investigation that has analytical or empirical origin. When such information about the system can be found, both model design and experimental work can be simplified to a degree, depending upon the amount of information available [2].

## 2.2 DIMENSIONAL ANALYSIS

Dimensional analysis is a mathematical operation which involves units or dimensions. It is used for the following reasons:

- 1) *Deduction of laws* – physics and engineering demands dimensional consistency in equations. We can reduce the number of variables by writing them in dimensionless form.
- 2) *Scale up/down of experimental results*
  - a) It does not require a full understanding of the physical process to be scaled.
  - b) Suitable (dimensionless) scaling relationships can be easily derived.

### 2.2.1 Primary and Secondary Quantities in Dimensional Analysis

Any physical situation can be described by certain familiar physical quantities, for example length, velocity, area, volume, acceleration etc. These are all known as *dimensions*. The dimensions are however of no use without a magnitude being attached. Dimensions are properties which can be measured. Units are the standard elements used to quantify these dimensions. In dimensional analysis only the nature of the dimension is of concern, i.e. its quality and not its quantity. Only three physical quantities: Mass, Length and Time are required to define both dimension and quantity in Mechanics, i.e. any quantity in Mechanics can be defined by these three *basic quantities*. The following common abbreviations are used:

1	Length	L
2	Mass	M
3	Time	T
4	Temperature	$\theta$
5	Current	I

However, in Mechanics we are only concerned with L, M and T, while  $\theta$  and  $I$  are required for problems in thermodynamics, heat and mass transfer, electrostatics, electrodynamics, electromagnetics and magnetohydrodynamics. Nature or *dimension* and magnitude of all the physical quantities in Mechanics can be expressed as the product of powers of these three basic quantities L, T and M. For example, the nature of physical quantities velocity, acceleration and force are defined as follows:

$$\text{Velocity } v = \text{Length} \times \text{Time}^{-1},$$

$$\text{Acceleration } a = \text{velocity} \times \text{Time}^{-1} = \text{Length} \times \text{Time}^{-2},$$

and the dimension of force is give by Newton's second law as:

$$\text{Force, } F = \text{Mass} \times \text{acceleration} = \text{Mass} \times \text{Length} \times \text{Time}^{-2}.$$

These expressions give no indication of the magnitude of the respective physical quantities, but give solely their relationship to the basic quantities, the latter are also called the ***primary quantities***. In order to signify that the relationship such as the above express only the nature or *dimension* of a physical quantity, regardless of magnitude. Square bracket symbols are often used, so that the above relationships can be expressed as

$$[v] = [L \times T^{-1}]$$

$$[a] = [L \times T^{-2}]$$

$$[F] = [M \times L \times T^{-2}]$$

These are read as the *dimension* of velocity is length divided by time and so on. The so derived quantities like velocity, acceleration, force etc. are called as ***secondary quantities*** [2].

### 2.2.2 Dimensional Homogeneity

Any equation describing a physical situation will only be true if both sides have the same dimensions. In other words it must be dimensionally homogenous. If all the terms in an equation reduce to the same basic quantities (have the same dimension), the equation is said to be dimensionally homogeneous. For example, the well known equation of distance traveled by a freely falling body starting from the rest may be written as

$$s = \frac{1}{2} g t^2 \quad (2.1)$$

the dimensional equation becomes

$$L \doteq LT^{-2}T^2$$

or  $L \doteq L$  (2.2)

which is correct. Hence the coefficient  $\frac{1}{2}$  is dimensionless. Dimensional homogeneity in

any equation expresses a fundamental relationship between a number of different physical quantities, and each term in the equation must have the same dimensions [4].

### 2.3 PRINCIPLE OF SCALED MODELING

The general concept of scaled modeling can be visualized by considering small elements of the prototype and their corresponding elements in the model. In studying the prototype elements, the physical data of interest such as geometry, pressure, weight, stress, velocity, acceleration, frequency etc. is accounted. The homologous behavior of corresponding model elements is secured if each quantity of prototype can be transformed into the corresponding quantity of the model elements through multiplication

by a respective constant factor called **scale factor** [5]. The similarity condition expresses linearity between the corresponding variables of the prototype and the model which can be defined by a constant of proportionality named scale factor  $\lambda$ , which is the ratio

$$\lambda_i = \frac{\text{Magnitude of } i^{\text{th}} \text{ variable in prototype}}{\text{Magnitude of } i^{\text{th}} \text{ variable in model}}$$

where  $\lambda_i$  is the scaling factor corresponding for  $i^{\text{th}}$  physical quantity. Therefore the ratio of the corresponding dimensional variables of prototype and model at corresponding points are constant. For instance length scale factor can be defined as

$$\lambda_l = \frac{(L)_{\text{prototype}}}{(L)_{\text{model}}} = \text{constant}$$

If length scale factor  $\lambda_l = 2$ , then all geometrical lengths of model will be half that of prototype. However measurements or observations on prototype and model are made on homologous points. Homology deals with the relation between corresponding points, corresponding events and corresponding variables in each similar systems, i.e. the homology applies to the geometry as well as other physical characteristics. Therefore, in a correctly conceived design, there must exist for each point on the model where measurements are taken, a uniquely defined position on the prototype to which these measurements apply [2]. For example, consider two structural beams, a prototype and model subjected to periodically changing load as shown in Fig. 2.1.

If all corresponding lengths are linked by length scale factor,

$$\lambda_l = \frac{x_L}{x_L'} = \frac{x_1}{x_1'} = \frac{x_2}{x_2'} = \frac{y_2}{y_2'} = \frac{y_{2 \text{ max}}}{y_{2' \text{ max}}},$$

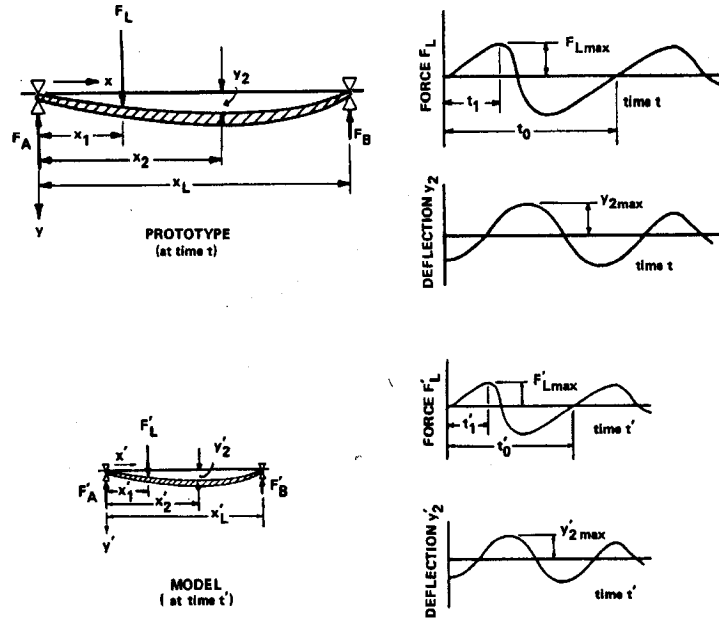


Fig. 2.1 Prototype and Homologous (Scale) Model of Vibrating Beam [5]

all corresponding times, by the time scale factor

$$\lambda_t = \frac{t_1}{t'_1} = \frac{t_o}{t'_o},$$

and all corresponding forces by the force scaling factor

$$\lambda_F = \frac{F_L}{F'_L} = \frac{F_A}{F'_A} = \frac{F_B}{F'_B} = \frac{F_{L\max}}{F'_{L\max}},$$

then the shapes, forces and times of the model and prototype will be similar. If the time axis of model is expanded by time scale factor \$\lambda\_t\$, and model's deflection by the length scale factor \$\lambda\_l\$, then the model's deflection-time axis curve, \$y'\_2(t')\$, measured at a distance \$x'\_2\$, will collapse with prototype's deflection-time curve, \$y\_2(t)\$, measured at distance \$x\_2\$. Or, if the model's time axis is expanded by the time scale factor \$\lambda\_t\$ and the model's force axis by force scale factor \$\lambda\_F\$, then the model's force-time curve, \$F'\_L(t')\$,

measured at distance  $x_1'$ , will coincide with the prototype's force-time curve,  $F_L(t)$ , measured at distance  $x_1$  [5].

Similarity in scale modeling generally includes three basic classifications:

- (1) ***Geometric similarity***: All linear dimensions of the model are related to the corresponding dimensions of the prototype by a constant length scale factor  $\lambda_l$ .
- (2) ***Kinematic similarity***: The velocities at 'corresponding' points on the model and prototype are in the same direction and differ by a constant velocity scale factor  $\lambda_v$ .
- (3) ***Dynamic similarity***: This is basically met if model and prototype forces differ by a constant scale factor at similar points.

### 2.3.1 Primary and secondary scale factors

In scale modeling, we are concerned only with quantities defined as product of five (or less) "primary" quantities, each raised to appropriate power. Therefore only the ***primary*** scale factors of these five quantities need to be accounted for; all other, ***secondary*** scale factors are easily derived from them. In dynamic analysis problems, two primary scale factors need to be decided:

- 1) Length scale factor  $\lambda_l$
- 2) Time scale factor  $\lambda_t$

For instance scale factor for velocity  $\lambda_v$ , which is secondary can be easily derived from primary scale factors of length  $\lambda_l$  and time  $\lambda_t$ . Speed can be expressed as the first derivative of length with respect to time, so that

$$\lambda_v = \frac{V_p}{V_m} = \frac{dl_p/dt_p}{dl_m/dt_m}$$

Geometric and temporal homology requires, however, that

$$l_p = \lambda_l l_m \text{ and } t_p = \lambda_t t_m$$

so that

$$\lambda_v = \frac{\lambda_l}{\lambda_t}$$

In the same way, any secondary scale factor can be derived from two or more primary ones such as:

Area scale factor  $\lambda_A = \lambda_l^2$

Acceleration scale factor  $\lambda_a = \frac{\lambda_l}{\lambda_t^2}$

Moment scale factor  $\lambda_M = \lambda_F \lambda_l$

In general, secondary scale factor may be written as [5]:

$$\text{Secondary Scale Factor} = \lambda_l^{n_1} \lambda_t^{n_2} \lambda_F^{n_3} \lambda_\theta^{n_4} \lambda_i^{n_5}$$

### 2.3.2 Representative quantities and Pi-numbers

In practical problems modeling becomes difficult as every element of reduced or enlarged model must repeat every instance of prototype on different but constant primary scales.

If  $\psi_p$  and  $\psi_m$  represents any two corresponding quantities of the same kind in prototype and model, respectively then scaling requirement can be written as

$$\lambda_\psi = \frac{\psi_p}{\psi_m}$$

For instance  $\lambda_l = \frac{l_p}{l_m}$  indicates that any corresponding lengths, distance, deformations, or

displacements of model and prototype must obey the same length scale factor. Likewise,

$\lambda_\omega = \frac{\omega_p}{\omega_m}$  means that any two corresponding frequency, natural frequency, forcing

frequency must follow the same frequency scale factor.

The quantities, like  $l_p$  and  $l_m$ ,  $\theta_p$  and  $\theta_m$ ,  $\omega_p$  and  $\omega_m$  that are involved in the study of prototype and model are called **representative quantities** and they are very important in scale modeling. Any scale factor can be expressed in terms of representative quantities.

For instance,

$$\lambda_v = \frac{\lambda_l}{\lambda_t} \text{ can be expressed as } \frac{v_p}{v_m} = \frac{l_p t_m}{l_m t_p}$$

This relation can be easily converted into the statement of

$$\frac{v_p t_p}{l_p} = \frac{v_m t_m}{l_m}$$

with all representative quantities of the prototype transferred to one side and the corresponding representative quantities of the model to other. In scale modeling, dimensionless products of this kind play a key role and they are called “pi-number” and denoted by the Greek letter  $\pi$  [5]. A pi-number is a pure number without any physical unit. Such a number is typically defined as a product or ratio of quantities that have units, in such a way that the product itself is dimensionless [41].

Thus, for instance the fore mentioned relation may be expressed by:

$$\pi = \frac{vt}{l}$$

A representative quantity in a pi-number can be substituted by any similar quantity of the given phenomenon to be modeled. W. For instance, if the pi-number  $\pi = vt/l$  is applied to the vibrating beam, we can place representative velocity  $v$  by the peak velocity of the imposed external load; representative time  $t$ , by the period of vibration; and the representative length, by the length of the beam. However in practical modeling, these steps are substantially shortened by converting all quantities of a governing relation directly into representative quantities. Hence, the governing relation of  $v = dl/dt$  can be converted into  $v \triangleq dl/dt$ . The sign " $\triangleq$ " (read as equivalent to) indicates that all terms are representing terms where speed  $v$  is a representative speed; the length differential,  $dl$  is a representative length; and the differential time  $dt$ , into a representative time. It also indicates that if all terms are assembled in the product form, it constitutes a pi-number [5].

Pi-Numbers can be derived in following three ways summarized in fig. 2.2

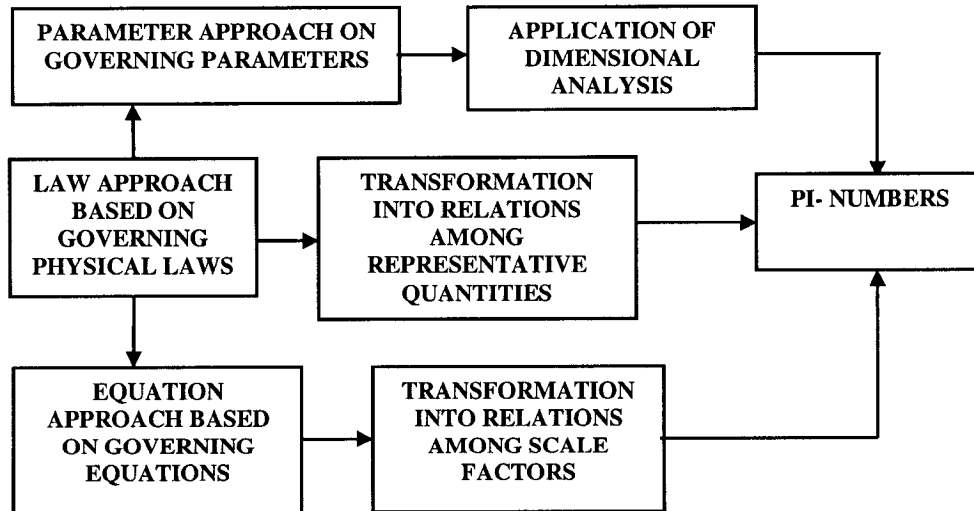


Fig. 2.2 Three Approaches to obtaining pi-numbers [5].

### 2.3.2.1 Law Approach

To have a scaled model, prototype and model should follow the same governing law, and pertinent pi-numbers are directly derived from the governing laws. The law approach can be explained with the example of a vibrating beam model that would predict the damp-out time of the prototype's free vibration. Since the phenomenon of the vibrating beam is one of elasticity, inertia, and internal friction, the model must conform to three physical laws.

- 1) Elasticity is described by Hooke's Law. Assuming negligible influence of Poisson's ratio, stress and strain can be related through

$$\sigma = E\epsilon$$

- 2) The inertial force on any element is ruled by Newton's second Law,

$$dF = dm.a$$

- 3) Internal friction, as expressed by energy loss per unit volume and per cycle, is (hypothetically) proportional to the third power of maximum stress,  $\sigma_m$

$$dU = dV.C.\sigma_m^3$$

To derive pi-numbers from these three laws, governing laws can be first expressed in representative terms; and then, in the form of pi-numbers [5].

Governing Law	In Representative Terms	As Pi-Numbers
$\sigma = E\epsilon$	$\sigma \simeq E\epsilon$	$\pi_1 = \frac{\sigma}{E\epsilon}$
$dF = dm.a$	$F \simeq ma$	$\pi_2 = \frac{F}{ma}$
$dU = dVc\sigma_m^3$	$U \simeq Vc\sigma^3$	$\pi_3 = \frac{U}{Vc\sigma^3}$

In the given form, the three pi-numbers are hardly useful for model design. It would be useful to have these numbers in terms of length, velocity, and force as they are easier to work with than in terms of stress, mass, and energy. The necessary modifications are accomplished with the help of representative relations among primary and secondary, quantities.

Representative laws	Modifying relations	Representative laws in terms of primary quantities	Pi-numbers
<b>Hooke's law</b> $\sigma \hat{=} E\varepsilon$	$\sigma = \frac{F}{l^2}$	$F \hat{=} l^2 E\varepsilon$	$\pi_e = \frac{F}{l^2 E\varepsilon}$
<b>Newton's law of inertia</b> $F \hat{=} ma$	$m \hat{=} \rho V$ $a \hat{=} l/t^2$	$F \hat{=} \rho \frac{l^4}{t^2}$	$\pi_i = \frac{F t^2}{\rho l^4}$
<b>Empirical law of internal damping</b> $U \hat{=} Vc\sigma^3$	$V \hat{=} l^3$ $U \hat{=} Fl$	$F \hat{=} \frac{l^2}{\sqrt{c}}$	$\pi_d = \frac{F \sqrt{c}}{l^2}$

### 2.3.2.2 Characteristic Equation Approach

The characteristic equations describing physical phenomenon are often differential equations and these equations combined with initial conditions and boundary conditions describe the problem. Essentially, similarity conditions from characteristic

approach are achieved by rewriting the characteristic equation in non-dimensional form, and determining from the transformed equations the conditions under which the behavior of two systems will be similar. For instance consider the spring-mass-damper system as shown in Fig. 2.3

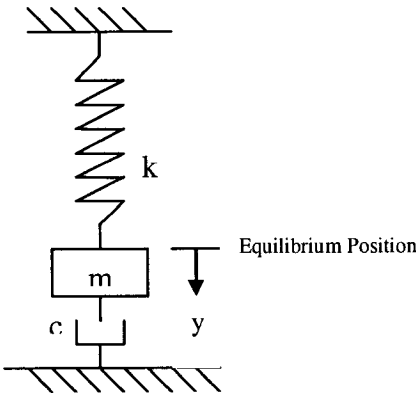


Fig. 2.3 Simple spring-mass-dashpot system

The displacement  $y$ , as a function of time can be studied by means of model study. The well known equation of motion of the mass can be represented as:

$$m \frac{d^2 y}{dt^2} + c \frac{dy}{dt} + ky = 0 \quad (2.3)$$

along with initial conditions of  $y = y_o$  and  $\frac{dy}{dt} = v_o$  at  $t = 0$

If we now introduce two dimensionless parameters

$$y^* = \frac{y}{y_o} \text{ and } t^* = \frac{t}{\tau} \text{ where } \tau = \sqrt{\frac{m}{k}}$$

$$\text{Eqn (2.3) can be written as } \frac{d^2 y^*}{dt^{*2}} + \frac{c}{\sqrt{mk}} \frac{dy^*}{dt^*} + y^* = 0 \quad (2.4)$$

Subsequently, the initial condition becomes  $y^* = 1$  and  $\frac{dy^*}{dt^*} = \frac{v_o}{y_o} \sqrt{\frac{m}{k}}$ . From Eqn (2.4),

it is noted that for any two systems governed by an equation of this form, the solution for

$y^*$  will be the same, i.e.  $y^* = y_m^*$  if  $\frac{c}{\sqrt{mk}} = \frac{c_m}{\sqrt{m_m k_m}}$ . Then  $\frac{v_o}{y_o} \sqrt{\frac{m}{k}} = \frac{v_{om}}{y_{om}} \sqrt{\frac{m_m}{k_m}} \Rightarrow$

$t \sqrt{\frac{k}{m}} = t_m \sqrt{\frac{k_m}{m_m}}$  where subscript  $m$  refers to the model. The last condition specifies the

time scale of the problem which can also be converted into pi number, i.e.,  $\pi = t \sqrt{\frac{k}{m}}$

which is dimensionless.

It is clear that, if the characteristic equation(s) are known for the system, the procedure described above can be systematically followed to establish necessary relationships between the prototype and model. However in many problems, the characteristic equations are more complicated or even unknown and therefore this method cannot be readily used [6].

### 2.3.2.3 Parameter Approach

In any problem, there are usually several variables,  $x_1, x_2, x_3 \dots x_k$ , required to describe the physical phenomenon of interest. A number of dimensionless quantities can be formed by combining the variables of the form  $x_1^{n_1}, x_2^{n_2}, x_3^{n_3} \dots x_k^{n_k}$  where exponents  $n_1, n_2, n_3 \dots n_k$  are selected so that the resulting product is dimensionless.

Thus, if we assume one of the variables, say  $x_i$  has the basic dimension  $x_i = L^{a_i} T^{b_i} M^{c_i}$ , the product can be expressed as  $(L^{a1} T^{b1} M^{c1})^{n1} (L^{a2} T^{b2} M^{c2})^{n2} \dots (L^{ak} T^{bk} M^{ck})^{nk}$ . In order to have the product dimensionless, the exponents of the various basic dimensions must combine to give zero value for each basic dimension. Thus

$$a_1 n_1 + a_2 n_2 + \dots + a_k n_k = 0$$

$$b_1 n_1 + b_2 n_2 + \dots + b_k n_k = 0 \quad (2.5)$$

$$c_1 n_1 + c_2 n_2 + \dots + c_k n_k = 0$$

There will be as many equations as the number of basic dimensions, say  $m$ , and  $k$  unknown  $n$ 's, where  $k$  is equal to the number of original variables in the problem. From the theory of equations, it is known that  $k - r$  linearly independent solution to Eqn's (2.5) exists where  $r$ , is the rank of the matrix of coefficients

$$\begin{pmatrix} a_1 & a_2 & \dots & a_k \\ b_1 & b_2 & \dots & b_k \\ c_1 & c_2 & \dots & c_k \end{pmatrix}$$

The matrix is commonly called dimensional matrix. Since the rank of a matrix is the highest order of non-zero determinant contained in the matrix, it is apparent that the rank cannot exceed the number of equations but may be smaller. Thus, the number of independent dimensionless products that can be formed is equal to  $k - r$ . Such a set of dimensionless products is called a complete set. Once a complete set of dimensionless products are found, all other possible dimensionless combinations can be formed as products contained in the complete set. Thus **Buckingham Pi Theorem** can be stated as follows:

If an equation involving  $k$  variables is dimensionally homogeneous,

$$q_1 = f(q_2, q_3, \dots, q_k) \quad (2.6)$$

it can be reduced to a relationship among  $k - r$  independent dimensionless products,

$$\pi_1 = f(\pi_2, \pi_3, \dots, \pi_{k-r}) \quad (2.7)$$

where  $r$  is the rank of the dimensional matrix [6].

## 2.4 TYPES OF MODELS BASED ON SIMILARITY CONDITIONS

Based on the similarity conditions models can be classified as:

- a) Completely similar models b) Dissimilar or relaxed models.

### 2.4.1 Completely Similar Models

Complete similarity between two systems exists if the values of all corresponding  $\pi$ -factors for prototype and model are equal. Complete similarity stated above does not necessarily require geometric similarity. Two systems may appear different in shape and size, yet may be completely similar. Complete similarity thus requires, according to the condition stated above, that

$$(\pi_1)_{\text{prototype}} = (\pi_1)_{\text{model}} \quad (2.8)$$

$$\text{and} \quad (\pi_i)_{\text{prototype}} = (\pi_i)_{\text{model}} \quad (i = 2, 3, 4, \dots, k - r) \quad (2.9)$$

These conditions are also called as model design parameters [2].

#### 2.4.1.1 Steps in Complete Similarity Modeling

To be able to model a given prototype system, each of the characteristics must be symbolized as a characteristic variable, which together with other variables, may be subjected to Dimensional Analysis. Next, the practical decisions have to be made with regard to model size, model material, model time, manufacturing, assembly and other issues. They are mainly dictated by the facilities and the resources available for model making and testing, such as available space, commercially available size and shapes of materials, power supplies, instrumentation etc. On the basis of these decisions the most suitable scaling factor values for all the variables involved may then be found.

To maintain the complete similarity, the modeling procedure may be confined to the following steps that will lead to scaling factor values, on which the model design may then be based [2]:

- 1) List all relevant variables involved in the physical problem.
- 2) Establish by Dimensional Analysis all  $\pi$ -factors.
- 3) List the given values and/or ranges of prototype variables.
- 4) Establish the scaling factors for all variables from the condition

$$(\pi_i)_{\text{prototype}} = (\pi_i)_{\text{model}} \quad (i = 1, 2, 3, 4, \dots, k - r)$$

#### **2.4.1.2 Derivation of Scale Factors for Dynamic Analysis using Dimensional Analysis**

The first step in the analysis is to list down all the relevant variables and their basic dimensions involved by neglecting the effect of Poisons ratio. These variables are tabulated in table 2.1.

Table 2.1 Dimensions of Measured Quantities for Dynamic Analysis

SYMBOL	MEASURED QUANTITY	DIMENSION
$l$	Characteristic Length	L
$\rho$	Density	ML <sup>-3</sup>
$E$	Modulus of Elasticity	ML <sup>-1</sup> T <sup>-2</sup>
$t$	Characteristic Time	T
$\omega$	Characteristic Frequency	T <sup>-1</sup>
$\sigma$	Stresses	ML <sup>-1</sup> T <sup>-2</sup>
$F$	Force	MLT <sup>-2</sup>
$a$	Characteristic Acceleration	LT <sup>-2</sup>
$c$	Damping Coefficient	MT <sup>-1</sup>

To proceed with Dimensional analysis we form the product

$$l^{x_1} \rho^{x_2} E^{x_3} t^{x_4} \omega^{x_5} \sigma^{x_6} F^{x_7} a^{x_8} c^{x_9} \quad (2.10)$$

Substituting the basic dimension for each variable we obtain

$$(L)^{x_1} (ML^{-3})^{x_2} (ML^{-1}T^{-2})^{x_3} (T)^{x_4} (T^{-1})^{x_5} (ML^{-1}T^{-2})^{x_6} (MLT^{-2})^{x_7} (LT^{-2})^{x_8} (MT^{-1})^{x_9}$$

Equating the exponent of the basic dimensions (M, L and T) to zero, we may have the following equations:

$$M : 0 + x_2 + x_3 + 0 + 0 + x_6 + x_7 + 0 + x_9 = 0$$

$$L : x_1 - 3x_2 - x_3 + 0 + 0 - x_6 + x_7 + x_8 + 0 = 0 \quad (2.11)$$

$$T : 0 + 0 - 2x_3 + x_4 - x_5 - 2x_6 - 2x_7 - 2x_8 - x_9 = 0$$

The dimensional matrix is

	$l$	$\rho$	$E$	$t$	$\omega$	$\sigma$	$F$	$a$	$c$
M	0	1	1	0	0	1	1	0	1
L	1	-3	-1	0	0	-1	1	1	0
T	0	0	-2	1	-1	-2	-2	-2	-1

Considering now the determinant formed by the last three columns of the matrix:

$$\begin{vmatrix} 1 & 0 & 1 \\ 1 & 1 & 0 \\ -2 & -2 & -1 \end{vmatrix} = 1$$

Since this is nonzero, it follows that the rank of the dimensional matrix is **three** and according to Buckingham's theorem there are  $9 - 3 = 6$  dimensionless products required to describe the problem.

To find the suitable set of dimensionless products called "Pi-Numbers", suitably chosen three parameters such as  $x_1$ ,  $x_2$  and  $x_4$  are expressed in term of  $x_3, x_5, x_6, x_7, x_8$  and  $x_9$  as

$$\begin{aligned}
x_1 &= -2x_3 - 2x_6 - 4x_7 - x_8 - 3x_9 \\
x_2 &= -x_3 - x_6 - x_7 - x_9 \\
x_4 &= 2x_3 + x_5 + 2x_6 + 2x_7 + 2x_8 + x_9
\end{aligned} \tag{2.12}$$

Substituting these values of  $x_1$ ,  $x_2$  and  $x_4$  from Eqn (2.12) in Eqn (2.10) we get

$$l^{(-2x_3 - 2x_6 - 4x_7 - x_8 - 3x_9)} \rho^{(-x_3 - x_6 - x_7 - x_9)} E^{x_3} t^{(2x_3 + x_5 + 2x_6 + 2x_7 + 2x_8 + x_9)} \omega^{x_5} \sigma^{x_6} F^{x_7} a^{x_8} c^{x_9} \tag{2.13}$$

Combining the similar powers in above equation we obtain

$$\left(\frac{Et^2}{\rho l^2}\right)^{x_3} (t \omega)^{x_5} \left(\frac{t^2 \sigma}{\rho l^2}\right)^{x_6} \left(\frac{Ft^2}{\rho l^4}\right)^{x_7} \left(\frac{t^2 a}{l}\right)^{x_8} \left(\frac{t c}{\rho l^3}\right)^{x_9} \tag{2.14}$$

To have one set of dimensionless numbers  $x_3, x_5, x_6, x_7, x_8$  and  $x_9$  are assumed to be one which leads to six dimensionless numbers as follows

$$\pi_1 = \frac{Et^2}{\rho l^2}, \pi_2 = t \omega, \pi_3 = \frac{t^2 \sigma}{\rho l^2}, \pi_4 = \frac{Ft^2}{\rho l^4}, \pi_5 = \frac{t^2 a}{l}, \text{ and } \pi_6 = \frac{t c}{\rho l^3} \tag{2.15}$$

It is apparent that the specific form of the pi terms depends on which of the “ $x$ ’s” are assigned values and the values themselves. However, it should be emphasized that, once an independent set is determined, all other possible independent set can be formed as product of powers of the original set.

Modeling or scaling laws can now be readily developed by applying similarity condition on these pi numbers. To have the similarity between the prototype and model, it is assumed that both these systems are described by equations

$$f_p(\pi_{1p}, \pi_{2p}, \pi_{3p}, \pi_{4p}, \pi_{5p}, \pi_{6p}) = 0 \quad (\text{Prototype}) \tag{2.16}$$

$$f_m(\pi_{1m}, \pi_{2m}, \pi_{3m}, \pi_{4m}, \pi_{5m}, \pi_{6m}) = 0 \quad (\text{Model}) \tag{2.17}$$

We further assume that the specific phenomenon under consideration is the same for the prototype and model. The function,  $f_p$ , for the prototype is the same as the function,  $f_m$ , for the model. Considering this, it can be concluded that:

$$\pi_{1p} = \pi_{1m}, \pi_{2p} = \pi_{2m}, \pi_{3p} = \pi_{3m}, \pi_{4p} = \pi_{4m}, \pi_{5p} = \pi_{5m}, \text{ and } \pi_{6p} = \pi_{6m} \quad (2.18)$$

Now the scale factors can be extracted (assuming different material for the prototype and model) as follows:

$$\begin{aligned} 1) \quad \pi_{1p} &= \pi_{1m} \\ \Rightarrow \left( \frac{Et^2}{\rho l^2} \right)_p &= \left( \frac{Et^2}{\rho l^2} \right)_m \\ \Rightarrow \frac{E_p}{E_m} &= \left( \frac{l_p}{l_m} \right)^2 \left( \frac{\rho_p}{\rho_m} \right) \left( \frac{t_m}{t_p} \right)^2 \quad \Rightarrow \lambda_E = \frac{\lambda_t^2 \lambda_\rho}{\lambda_t^2} \end{aligned} \quad (2.19)$$

$$\begin{aligned} 2) \quad \pi_{2p} &= \pi_{2m} \\ \Rightarrow (t \omega)_p &= (t \omega)_m \\ \Rightarrow \frac{\omega_p}{\omega_m} &= \frac{t_m}{t_p} \quad \Rightarrow \lambda_\omega = \frac{1}{\lambda_t} \end{aligned} \quad (2.20)$$

$$\begin{aligned} 3) \quad \pi_{3p} &= \pi_{3m} \\ \Rightarrow \left( \frac{t^2 \sigma}{\rho l^2} \right)_p &= \left( \frac{t^2 \sigma}{\rho l^2} \right)_m \\ \Rightarrow \frac{\sigma_p}{\sigma_m} &= \left( \frac{\rho_p}{\rho_m} \right) \left( \frac{l_p}{l_m} \right)^2 \left( \frac{t_m}{t_p} \right)^2 \quad \Rightarrow \lambda_\sigma = \frac{\lambda_\rho \lambda_t^2}{\lambda_t^2} \end{aligned} \quad (2.21)$$

$$\begin{aligned}
4) \quad \pi_{4p} &= \pi_{4m} \\
\Rightarrow \left( \frac{Ft^2}{\rho l^4} \right)_p &= \left( \frac{Ft^2}{\rho l^4} \right)_m \\
\Rightarrow \frac{F_p}{F_m} = \left( \frac{l_p}{l_m} \right)^4 \left( \frac{\rho_p}{\rho_m} \right) \left( \frac{t_m}{t_p} \right)^2 &\Rightarrow \lambda_F = \frac{\lambda_t^4 \lambda_\rho}{\lambda_t^2} \tag{2.22}
\end{aligned}$$

$$\begin{aligned}
5) \quad \pi_{5p} &= \pi_{5m} \\
\Rightarrow \left( \frac{t^2 a}{l} \right)_p &= \left( \frac{t^2 a}{l} \right)_m \\
\Rightarrow \left( \frac{t_p}{t_m} \right)^2 = \left( \frac{l_p}{l_m} \right) \left( \frac{a_m}{a_p} \right) &\Rightarrow \lambda_t = \sqrt{\lambda_t \lambda_a} \tag{2.23}
\end{aligned}$$

The characteristic acceleration should be same for both model and prototype. However since prototype and model will be tested in the same environment, the gravitational acceleration cannot be changed due to practical reasons we are forced to have  $\lambda_a = 1$ . Consequently Eqn (2.23) can further be reduced to

$$\lambda_t = \sqrt{\lambda_t} \tag{2.24}$$

$$\begin{aligned}
6) \quad \pi_{6p} &= \pi_{6m} \\
\Rightarrow \left( \frac{t c}{\rho l^3} \right)_p &= \left( \frac{t c}{\rho l^3} \right)_m \\
\Rightarrow \frac{c_p}{c_m} = \left( \frac{l_p}{l_m} \right)^3 \left( \frac{\rho_p}{\rho_m} \right) \left( \frac{t_m}{t_p} \right) &\Rightarrow \lambda_c = \frac{\lambda_t^3 \lambda_\rho}{\lambda_t} \tag{2.25}
\end{aligned}$$

By substituting time scale factor from Eqn (2.24) in Eqn's (2.19, 2.20, 2.21, 2.22, and 2.25) scaling laws can be written as:

- i.  $\lambda_E = \lambda_l \lambda_\rho$
- ii.  $\lambda_\omega = \frac{1}{\sqrt{\lambda_l}}$
- iii.  $\lambda_\sigma = \lambda_\rho \lambda_l$  (2.26)
- iv.  $\lambda_F = \lambda_l^3 \lambda_\rho$
- v.  $\lambda_c = \lambda_l^{1/2} \lambda_\rho$

### 2.4.2 Relaxed or Distorted or Dissimilar Models

Often situations are encountered where it is impractical, if not impossible to maintain complete similarity. Particularly in dealing with dynamic analysis it becomes impractical to satisfy all the design conditions with only one length scale factor, which is not unity. Due to lack of availability of materials, or unavailability of specified dimension of members, it becomes necessary to adopt two or more different length scales and this leads to distortion of geometry, where we neglect some weak laws [5].

#### 2.4.2.1 Need of Relaxation

Correct scaling becomes cumbersome when more than one principal pi-numbers are involved in a scaling problem. For instance, consider a case of dynamic analysis, which proved to have six pi-numbers and yield the scale factor relations written in Eqn (2.26). The primary scale factors  $\lambda_F, \lambda_l, \lambda_\rho$  can be chosen arbitrarily. From a mathematical point of view; it would require to adapt three material properties to the three given scale factor products.

For instance, if we decide to use the same material for both model and prototype then  $\lambda_E = \lambda_\rho = 1$  and consequently  $\lambda_l = \lambda_t = 1$ , a condition that denies scaling altogether. Even with dissimilar materials, the scaling law relating modulus of elasticity and densities  $\lambda_E = \lambda_l \lambda_\rho$  is very difficult to achieve. If the modulus of elasticity of the model material is same as the prototype material, the model material density must be  $\lambda_l$  times the prototype material density. For any reasonable value of  $\lambda_l$ , the model density requirement is impossible to satisfy because of material unavailability. Hence it is not possible to maintain complete similarity as  $\pi_{l_p} \neq \pi_{l_m}$ .

Fortunately, conflicting problems associated with scale factors can be resolved by *relaxation*, a single word meaning the resolution of scaling conflicts by using prior knowledge of the phenomena to be scaled. Relaxations might consist, for instance, of studiously neglecting less important laws, or of infusing experiment with analytical knowledge, or even of dividing the whole phenomena into smaller, manageable parts.

Relaxation is rather an art than a formal process. Each problem must be diagnosed separately and there are only some general rules. In history of scaled modeling, a number of relaxation methods have been evolved, not systematically but in rather diverse ways geared to specific problems. These principles are summarized in Fig. 2.4. The relaxations applicable to dynamic analysis has been discussed in detail [5].

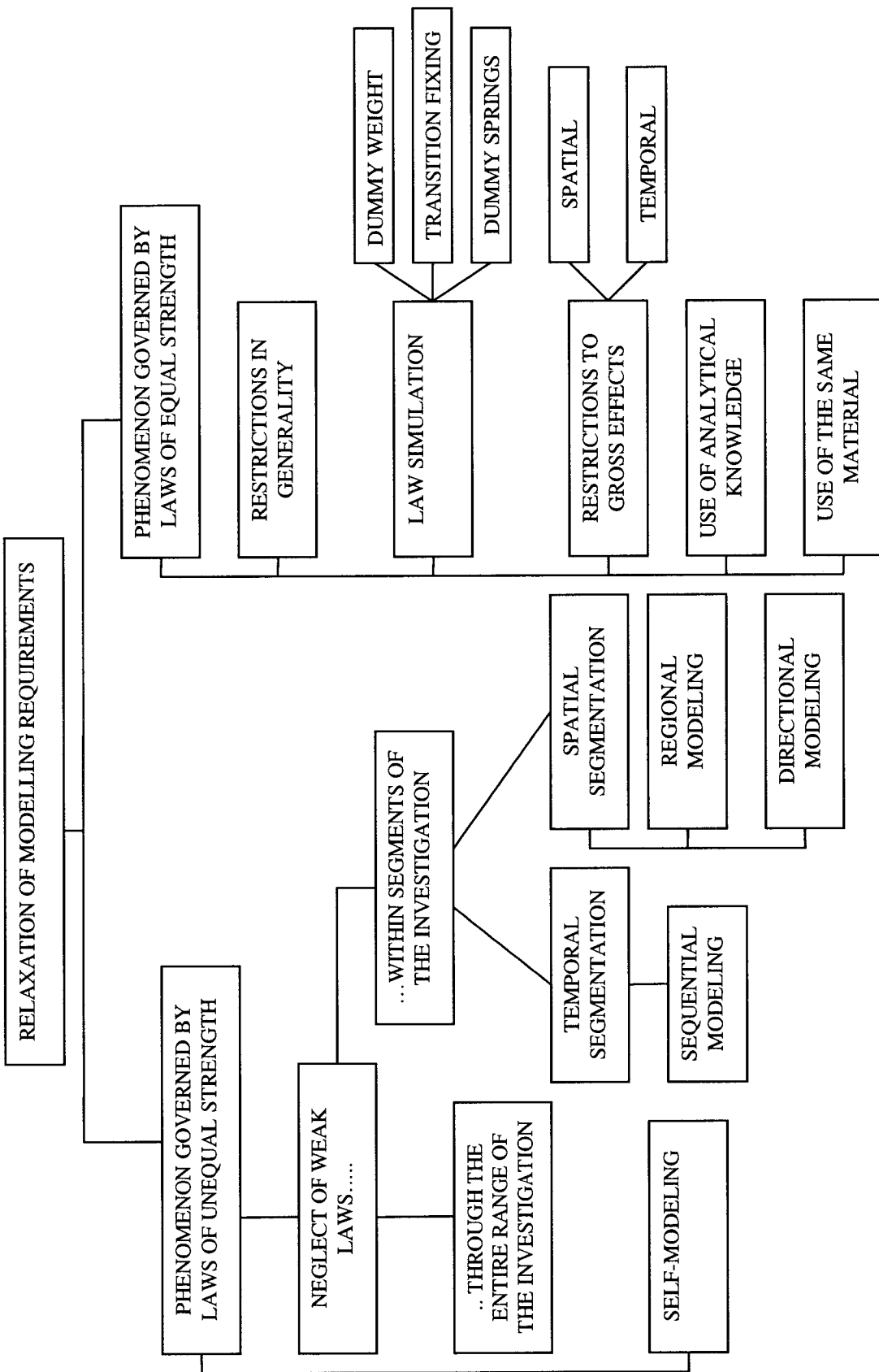


Fig. 2.4 Summary of Relaxation Methods in Scaled Modeling [5]

## 2.5 Identifying Weak Laws

As a first step of relaxation, it is helpful to determine whether the laws causing scaling conflicts are governing the given system with equal or unequal strength. If they govern it with unequal strength, the weakest law can perhaps be disregarded within segments of the investigation if not throughout its entire range. If their influences are equally strong, none can be neglected outright, but correct results may still be obtained by skillful circumvention of the most disturbing laws.

When the effect of governing law's on total performance is uncertain, tests with a pilot model may supply missing information. Suppose that three laws are known to govern a phenomenon; of the three, two are strong, but the third is allegedly weak. Three principal pi-numbers can be formulated, with one representing the weak law. In the pilot model tests, the "weak" pi-numbers will be revealed as weak or strong by checking its effect on the similarity between model and prototype results. Figure 2.5 shows hypothetical test to check the effect of  $\pi_1$  on the phenomena by plotting  $\pi_3$  versus  $\pi_1$ , with constant  $\pi_2$ . If the tests produce curve (1), we conclude that  $\pi_1$  exerts strong influence; if they produce curve (2), a weak influence; if they produce curve (3), we conclude that  $\pi_1$  exerts a strong influence at low  $\pi_1$  - values but a weak influence at high  $\pi_1$  - values [5].

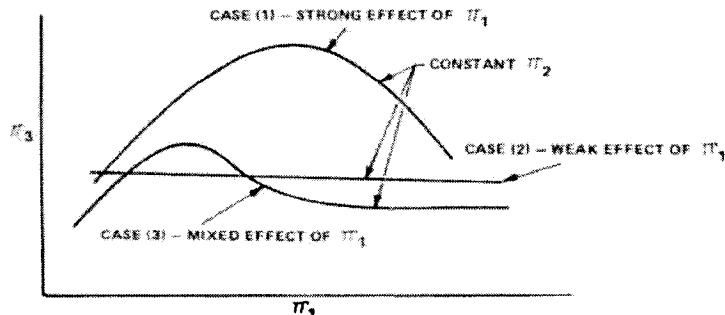


Fig. 2.5 Three Hypothetical Effects of  $\pi_1$  on  $\pi_3$  [5]

### 2.5.1 Disregarding Weak Laws

The technique of disregarding the weak law is perhaps the most common of all the relaxation methods. In most of vibrating structures, gravity exerts insignificant influence on the natural frequency that the law of gravitation need not be considered [5].

If the gravity effect is neglected then the scaling conflict in dynamic analysis can be easily resolved as follows:

If we do not maintain  $\lambda_a = 1$  in Eqn (2.23), then from Eqn (2.19) we have  $\lambda_E = \frac{\lambda_l^2 \lambda_\rho}{\lambda_t^2}$

and from Eqn (2.20) we have  $\lambda_\omega = \frac{1}{\lambda_t}$ . Now substituting  $\lambda_t = \frac{1}{\lambda_\omega}$  in Eqn (2.19) we have

$\lambda_E = \lambda_l^2 \lambda_\rho \lambda_\omega^2$ , from this we can re-write frequency scale factor  $\lambda_\omega$  as

$$\lambda_\omega = \frac{1}{\lambda_l} \sqrt{\frac{\lambda_E}{\lambda_\rho}} \quad (2.27)$$

Therefore time scale factor from Eqn (2.20) becomes

$$\lambda_t = \lambda_l \sqrt{\frac{\lambda_\rho}{\lambda_E}} \quad (2.28)$$

Substituting this new time scale factor into Eqn (2.21), the new stress factor can be obtained as:

$$\lambda_\sigma = \lambda_E \quad (2.29)$$

Substituting Eqn (2.28) in Eqn (2.22) provides new force scale factor as

$$\lambda_F = \lambda_l^2 \lambda_E \quad (2.30)$$

Now substituting Eqn (2.28) in Eqn (2.23) results in the following acceleration factor which is not unity as:

$$\lambda_a = \frac{\lambda_l \lambda_\rho}{\lambda_E} \quad (2.31)$$

Finally substitution of Eqn (2.28) into Eqn (2.25) results in the modified damping scale factor as  $\lambda_c = \lambda_l^2 \sqrt{\lambda_E \lambda_\rho}$

To summarize when the gravity effects are neglected, the scaling laws for dynamic analysis can be written as:

- i.  $\lambda_l = \lambda_l \sqrt{\frac{\lambda_\rho}{\lambda_E}}$
- ii.  $\lambda_\omega = \frac{1}{\lambda_l} \sqrt{\frac{\lambda_E}{\lambda_\rho}}$
- iii.  $\lambda_\sigma = \lambda_E$
- iv.  $\lambda_F = \lambda_l^2 \lambda_E$
- v.  $\lambda_a = \frac{\lambda_l \lambda_\rho}{\lambda_E}$
- vi.  $\lambda_c = \lambda_l^2 \sqrt{\lambda_E \lambda_\rho}$

### 2.5.2 Self-modeling tests

In self modeling, the prototype itself becomes the model; here the length scale factor is clearly unity and the materials are the same because model and prototype are the same. Any quantity other than length and material properties, however, can be changed in accordance with the ruling pi-numbers.

Self-modeling experiments are frequently used in fundamental heat and mass transfer experiments to clarify the influences of certain laws whose parameters can be varied without affecting the length and material properties [5].

### **2.5.3 Sequential Modeling**

Sequential modeling plays a major role when one phase follows another. In modeling automobile crashes, for instance, the crash phase can be clearly distinguished from the post-crash phase. During the crash phase, which usually lasts only for a fraction of a second, tire friction forces are negligibly small compared to the large inertial forces of the impacting cars. Hence, the crash phase is governed by inertial forces and by energy dissipation in partially elastic and imperfectly smooth bodies. Tire friction forces do not come into play until the beginning of the post-crash phase, which may last for several seconds. But then energy dissipation due to impact need no longer be modeled. Thus, dividing the whole phenomenon into two sequential phases greatly relaxes the modeling requirements [5].

### **2.5.4 Regional Modeling**

If a phenomenon can be treated as an assembly of separate regions, each governed by its own set of laws, it can be modeled regionally.

An example of regional modeling in the field of mechanical engineering is the dynamic response of a wheeled vehicle traversing undulating terrain. In a slowly moving off-road vehicle, vibrations are confined to frequencies between 1 and 10 Hz. At these low frequencies, sprung and unsprung masses behave like rigid bodies; consequently, those masses are subjected only to Newton's laws of inertia and gravitation. Furthermore,

all springs having negligibly small mass follow only Hooke's law of elasticity, and all shock absorbers having negligibly small mass also follow only the law of viscous friction. Hence, the whole vehicle can be partitioned into separate regions where different laws apply. Under these circumstances, modeling is considerably relaxed [5].

### **2.5.5 Directional Modeling**

When governing laws work in distinct directions instead of distinct regions, directional modeling can relieve stringent scaling requirements. For example, if the turbulent flow in rivers and estuaries were faithfully scaled in horizontal dimensions as well as in depth, river models would be so shallow that turbulent flow would be suppressed and unwanted surface tension would be exaggerated. With directional modeling, the depths of river and estuary models are very often disproportionately magnified or "intentionally distorted" geometrically for the following reasons: fully turbulent flow in a sloped channel is governed by Newton's law of inertia and the law of gravitation; but the inertial forces act predominantly in a horizontal direction, while the gravitational forces act in a vertical direction [5].

### **2.5.6 Circumventing Strong Laws**

If none of the conflicting laws can be disregarded, we must abandon the idea of modeling the whole phenomenon faithfully. Instead, we can try to circumvent the most troubling law by anyone of the following devices [5].

### **2.5.7 Restrictions in Generality**

The phenomenon is broken up in a number of special cases, each governed by fewer laws than the entire phenomenon. If enough special cases are investigated, and if they are all relatively independent of each other, an approximation of the total phenomenon can be obtained by superimposing results of the special cases

As an example, consider a ship in a severe storm at sea, a phenomenon sufficiently complex to warrant modeling special cases. Since the ship is operating in two distinctly different environments (water and wind), we may test two special cases: the ship in still water but exposed to wind forces, and the ship in still air but exposed to water forces. Another special case that can be investigated independently of water and wind resistance is the hull's structural response to wave impact. Each of these special cases allows more scaling freedom than is allowed by the phenomenon in its entirety [5].

### **2.5.8 Law Simulation**

Sometimes a disturbing but indispensable law can be substituted by a device that would simulate the desired effects and bypass the undesirable ones. Of the many possibilities, three are most frequently employed: dummy weight, transition fixing and dummy springs [5].

### **2.5.9 Dummy Weights**

One of the most practical approaches used in dynamic modeling of reinforced concrete structures is to augment the density of the structurally effective model material with high density material which is structurally not effective but permits the fulfillment of the similitude requirement  $\lambda_E = \lambda_l \lambda_p$  without violating the gravity effects. Practically,

this requires addition of suitably distributed weights which are attached to the structural elements in a manner that does not change the strength and stiffness characteristics. Since addition of weights alters the local stress histories close to attachment points, such models are not true models but provide satisfactory results. This is done with a series of equally and closely spaced dummy weights attached rigidly to the model structure. Now each section of the structure, with extra weight, can be considered to possess a density of

$$\rho_m = \rho_{om} + \frac{\Delta m'}{\Delta v'} \quad (2.34)$$

where  $\rho_{om}$  is the real density of model structure,  $\Delta m'$  is the mass of dummy weight and  $\Delta v'$  is the volume per dummy weight. Thus, the original restricting length scale factor relation that is  $\lambda_E = \lambda_l \lambda_\rho \Rightarrow \lambda_l = \lambda_E / \lambda_\rho$  becomes more flexible [5],

$$\lambda_l = \frac{\lambda_E}{\rho_p} (\rho_{om} + \Delta m' / \Delta v') \quad (2.35)$$

For instance, for 1:4 scale model using prototype material ( $\lambda_E = \lambda_\rho = 1$ ), the density will have to be increased by a factor of three.

Using dummy mass we can use previous derived scaling laws in Eqn (2.26) without violating gravity. Thus the scale factors in Eqn (2.26) are true and practically feasible with dummy mass simulation.

### 2.5.10 Dummy Spring

For modeling wind-induced vibrations of large elastic structures such as aircraft or suspension bridges, testing components rather than the entire model is often justifiable. The component must be scaled in shape and mass but it can be rigid and it must be

supported by springs that would simulate the elastic interaction of the component with the rest of the structure [5].

### **2.5.11 Temporally Integrated Effects**

If instantaneous data at a specific time are not needed --that is, if only the aggregate results of a phenomenon are to be modeled, we can find other means of relaxation. The scaling of cumulative effects depends very much on the given phenomenon. For instance, consider one model study focused on the kinematics of two cars after impact. During the collision, the cars exchange momentum so that, at the end of the crash phase when the cars separate and start following their own trajectories, each car is provided with a new set of velocities. These velocities, our sole interest, are fixed by the total momentum exchanged during the crash phase; therefore, we are not interested in the history of momentum exchange but only in the end result - the new set of car velocities. Consequently, only the end effect of the impact phase (the end momentum of each car) need be scaled. The same philosophy can be used for modeling the effects of explosions. The time history of the explosion itself is of no concern if the following events are slow. Thus, only the total amount of explosive energy requires to be modeled [5].

### **2.5.12 Use of Analytical Knowledge**

Scale model experiments are usually performed when analytical knowledge is lacking. However, when at least some analytical knowledge is available, it should be applied, depending on the given problem. The most violent impact suffered by a ship at sea is probably the heavy blow taken when the bow re-enters the water. After structural

failure was experienced by an aircraft carrier in rough seas, model tests were conducted to study the vibratory response of the carrier to wave impact loads. The ship's behavior was assumed to be governed by inertial forces of the ship and the water (Newton's law of inertia), by the weight of the ship and the water (law of gravitation), and the elastic forces of the ship (Hooke's law of elasticity). Since propulsion was of no immediate interest, resistance due to fluid friction was neglected. The three governing laws were transformed into the following principal pi-numbers and model rules.

Newton's law of Inertia

$$F \hat{=} ma \quad m \hat{=} \rho l^3 \quad Ne = \frac{F}{\rho l^2 v^2} \quad a \hat{=} \frac{v^2}{l}$$

Law of Gravitation

$$F \hat{=} mg \quad \pi_g = \frac{F}{\rho g l^3}$$

Hooke's Law of Elasticity

$$F \hat{=} \sigma l^2 \quad \sigma \hat{=} E \epsilon \quad \pi_e = \frac{F}{E \epsilon l^2}$$

Froude Number

$$Fr = \sqrt{\frac{\pi_g}{Ne}} = \frac{v}{\sqrt{gl}} \quad g_p = g_m \quad \left( \frac{v_p}{v_m} \right)^2 = \frac{l_p}{l_m} \quad \frac{l_p}{l_m} = \frac{E_p}{E_m} \frac{\rho_m}{\rho_p}$$

Cauchy Number

$$Ca = \frac{\pi_e}{Ne} = \frac{\rho v^2}{E \epsilon} \quad \epsilon_p = \epsilon_m \quad \left( \frac{v_p}{v_m} \right)^2 = \frac{E_p}{E_m} \frac{\rho_m}{\rho_p}$$

Hence, the length scale factor depends on the model's and prototype's material properties. Since model tests are usually performed in water,  $\rho_m = \rho_p$ . The density,  $\rho$ , however, being a representative quantity, stands not only for the density of water but also for the density of the ship's structure. The ship model was therefore to be constructed from a material of the density of steel but with a modulus,  $E_m$ , vastly smaller than that of steel ( $E_p/E_m = l_p/l_m$ ). Such a material did not exist. It was therefore decided to restrict the model study to bending vibrations. Then analytical knowledge could be infused by expressing Hooke's law as follows:

$$\text{From } M = EI \frac{d^2y}{dl^2} \longrightarrow F \simeq \frac{EI}{l^2} \longrightarrow \pi_e = \frac{Fl^2}{EI}$$

And the Cauchy number would assume the special form of

$$Ca = \frac{\pi_e}{Ne} = \frac{l^4 \rho v^2}{EI}$$

With this new Cauchy number, the length scale factor could be selected independent of material properties. For the same material for model and prototype, for instance,

$$\begin{aligned}
 Ca &\longrightarrow \left( \frac{v_p}{v_m} \right)^2 = \frac{I_p}{I_m} \left( \frac{l_m}{l_p} \right)^4 \\
 \rho_p = \rho_m &\quad \downarrow \\
 \varepsilon_p = \varepsilon_m & \\
 Fr &\longrightarrow \left( \frac{v_p}{v_m} \right)^2 = \frac{l_p}{l_m} \\
 &\quad \swarrow \quad \searrow \\
 &\quad \frac{I_p}{I_m} = \left( \frac{l_p}{l_m} \right)^5
 \end{aligned}$$

The selected length scale factor was 136. Therefore, a model had to be built, of the same material as that of the prototype, whose area moment of inertia was  $136^5$  times smaller

than that of the prototype. Such a model was built by composing the hull of nine segments, all joined by a continuous beam to allow flexures. The area moment,  $I$ , of the prototype was calculated in a separate computer study. The model's beam was varied to make it conform to the model rule of  $I_m = I_p / 136^5$  [5].

### 2.5.13 Use of the Same Material

Nature rarely provides the materials with the properties needed for scale modeling, and to synthesize materials having specified properties is a difficult task.

In most cases, attempts to scale material properties end in frustration. The isotropic Hookean solid, a seemingly easy material to scale, cannot be scaled at all if both its constitutive properties, Young's modulus,  $E$ , and Poisson's ratio,  $\nu$ , must be observed, as shown below:

For isotropic, homogeneous, energy-conservative materials, Hooke's law results in the two representative relations of  $\varepsilon \hat{=} \sigma/E$  and  $\varepsilon \hat{=} \nu\sigma/E$ . It is obvious that geometrical similarity between model and prototype (i.e.,  $\varepsilon_p = \varepsilon_m$ ) can be satisfied only if either the same material is used so that  $E_p = E_m$  and  $\nu_p = \nu_m$ ; or different materials are used with different moduli of elasticity but still the same Poisson's ratio so that  $\sigma_p/E_p = \sigma_m/E_m$  and  $\nu_p = \nu_m$ . These requirements again suggest use of the same material for model and prototype.

The condition of "same material" can be relaxed only if transverse deformations are disregarded. Then the influence of Poisson's ratio becomes less significant, a change that leaves only the requirement of  $\sigma_p/E_p = \sigma_m/E_m$  and permits the use of different materials for model and prototype. Neglecting Poisson's ratio is an important relaxation

in almost all structural problems. Most material constants are not real constants but complex functions of many variables. Hence, even if we use the same material in both the model and the prototype, we cannot ensure identical response of the material unless all participating variables in the constitutive relation of the material have the scale factor of unity [5].

## 2.6 VALIDATION OF SCALING LAWS ON SIMPLE STRUCTURES

Finite element analysis has been carried out using ANSYS on prototype and 1/2 scale model of a simple cantilever beam with rectangular cross section for the validation of scaling laws. The response obtained from the 1/2 scale model using ANSYS 7.1 is used to predict the response of the full scale prototype by using scaling laws. The results are compared with the response obtained for the full scale prototype again using ANSYS 7.1 to validate the scaling laws. Dynamic scaling laws have been verified for the following relaxations:

### 2.6.1 Neglecting Gravity Effects

BEAM3 ANSYS element has been used for the analysis which is a uniaxial element with tension, compression, and bending capabilities. The element has three degrees of freedom at each node: translations in the nodal x and y directions and rotation about the nodal z-axis. The x-degrees of freedom have been restrained to have pure bending modes in the analysis.

The cantilever beam for both model and prototype has been meshed with 40 BEAM3 elements as shown in Fig. 2.6.

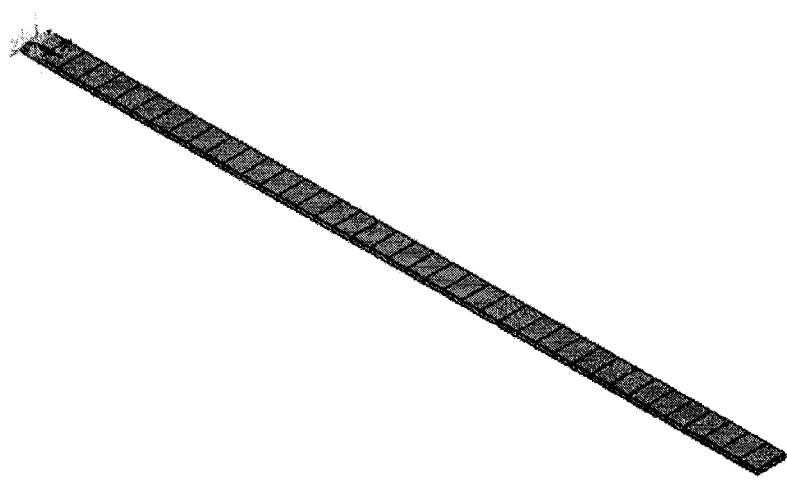
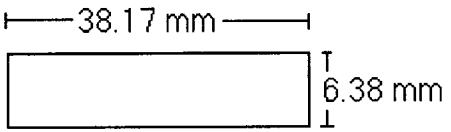
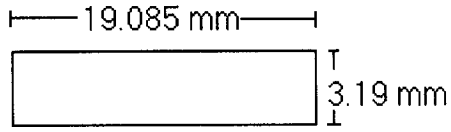


Fig. 2.6 Cantilever Beam Meshed with 40 BEAM3 Elements

The parameters used for the prototype and its  $\frac{1}{2}$  scale model is summarized in Table 2.2 below

Table 2.2 Parameters used for Prototype and Model Beam

PARAMETERS	Prototype	$\frac{1}{2}$ Scale Model
Length of Beam	$L_p = 1000 \text{ mm}$	$L_m = 500 \text{ mm}$
Material Used for Beam	1018-Steel	6061-T6 Aluminium
Modulus of Elasticity	$E_p = 2.05 \times 10^{11} \text{ N/m}^2$	$E_m = 69 \times 10^9 \text{ N/m}^2$
Density	$\rho_p = 7870 \text{ kg/m}^3$	$\rho_m = 2700 \text{ kg/m}^3$
Poisson's Ratio	$\nu_p = 0.29$	$\nu_m = 0.33$
Cross Section	 $38.17 \text{ mm}$ $6.38 \text{ mm}$	 $19.085 \text{ mm}$ $3.19 \text{ mm}$

Considering the parameters given in Table 2.2, scale factors  $\lambda_l = 2$ ,  $\lambda_E = 2.97101449$ ,  $\lambda_\rho = 2.91481481$  can be easily obtained. Now other scale factors for dynamic analysis when the gravity effects are neglected can be calculated as:

$$\lambda_t = \lambda_l \sqrt{\frac{\lambda_\rho}{\lambda_E}} = 1.9809937009$$

$$\lambda_\omega = \frac{1}{\lambda_l} \sqrt{\frac{\lambda_E}{\lambda_\rho}} = 0.5047971629$$

$$\lambda_\sigma = \lambda_E = 2.971014490$$

$$\lambda_F = \lambda_l^2 \lambda_E = 11.884057970$$

$$\lambda_a = \frac{\lambda_l \lambda_\rho}{\lambda_E} = 1.9621680210$$

### 2.6.1.1 Modal Analysis

Modal analysis is first performed to find out the natural frequencies which are the primary requirement in dynamic analysis. Using  $\frac{1}{2}$  scale model of the beam the fundamental natural frequency has been found to be 10.42 Hz. To predict the fundamental natural frequency of the full scale prototype from fundamental frequency of the scaled model using scaling laws, we have

$$\begin{aligned} \text{Predicted Natural Frequency of Prototype} &= \lambda_\omega \times \text{Natural Frequency of Model} \\ &= 0.5047971629 \times 10.42 \\ &= 5.259986 \text{ Hz.} \end{aligned}$$

To verify this, full scale prototype has also been modeled in ANSYS 7.1 and fundamental frequency of 5.26 Hz has been found out. Therefore, it can be realized that the predicted natural frequency using scaling law perfectly agrees with the natural frequency obtained from using full scale prototype beam parameters.

Table 2.3 summarizes first ten natural frequencies of the cantilever beam under consideration and it shows good correlation between the analytical and predicted natural frequencies exists, thus validating the frequency scale factor. Corresponding mode shapes are also shown in the last column of the Table 2.3. These mode shapes have been found to be identical prototype and its  $\frac{1}{2}$  scale model for the corresponding frequencies.

Sr. No.	Nat. Freq. (Hz) of $\frac{1}{2}$ Scale Model ANSYS ( $\omega_n$ ) <sub>M</sub>	Predicted Nat. Freq. (Hz.) of full Scale Prototype $\lambda_o \cdot (\omega_n)_M$	Nat. Freq.(Hz.) of Full Scale Prototype ANSYS ( $\omega_n$ ) <sub>P</sub>	Corresponding Mode Shape
1	10.42	5.259986	5.26	
2	65.298	32.96225	32.962	
3	182.82	92.28702	92.289	
4	358.22	180.8284	180.83	
5	592.09	298.8854	298.88	
6	884.33	446.4073	446.41	
7	1234.9	623.374	623.38	
8	1643.8	829.7856	829.76	
9	2110.8	1065.526	1065.5	
10	2636.1	1330.696	1330.7	

Table 2.3 Natural Frequencies and Mode Shapes with Aluminium Model and Steel Prototype  $\left( \lambda_o = \frac{1}{\lambda_i} \sqrt{\frac{\lambda_E}{\lambda_p}} = 0.50479716290892 \right)$

### 2.6.1.2 Harmonic Analysis:

Base excitation is applied at the clamped end of the beam in Y direction and the response is also observed in Y direction near the free end. The input is applied as different amplitude ranges in different frequency bands. The input for harmonic testing is known for prototype and is given in Table 2.4

Table 2.4 Harmonic Input for Prototype

Frequency Range (Hz) $\omega_p$	Amplitude in (mm) $\delta_p$	No of Sub-steps
0 to 15	0.762	150
15 to 25	0.508	100
25 to 33	0.254	80
33 to 40	0.127	70
40 to 50	0.0762	100

It is noted that for testing a scaled model, the above harmonic input has also to be scaled according to scaling laws. For the model, the harmonic input is scaled both for the frequency ranges and the corresponding amplitudes and is shown in Table 2.5

Table 2.5 Scaled Harmonic Input for Model

Frequency Range (Hz) $\omega_m = \omega_p / \lambda_\omega$	Amplitude in (mm) $\delta_m = \delta_p / \lambda_l$	No of Sub-steps
0 to 29.71	0.381	150
29.71 to 49.52	0.254	100
49.52 to 65.37	0.127	80
65.37 to 79.23	0.0635	70
79.23 to 99.04	0.0381	100

The amplitude response has been obtained for both model and prototype using ANSYS 7.1 is plotted in Fig. 2.7 and 2.8 respectively. Constant damping ratio of 0.02 has been assumed for harmonic analysis in both model and prototype.

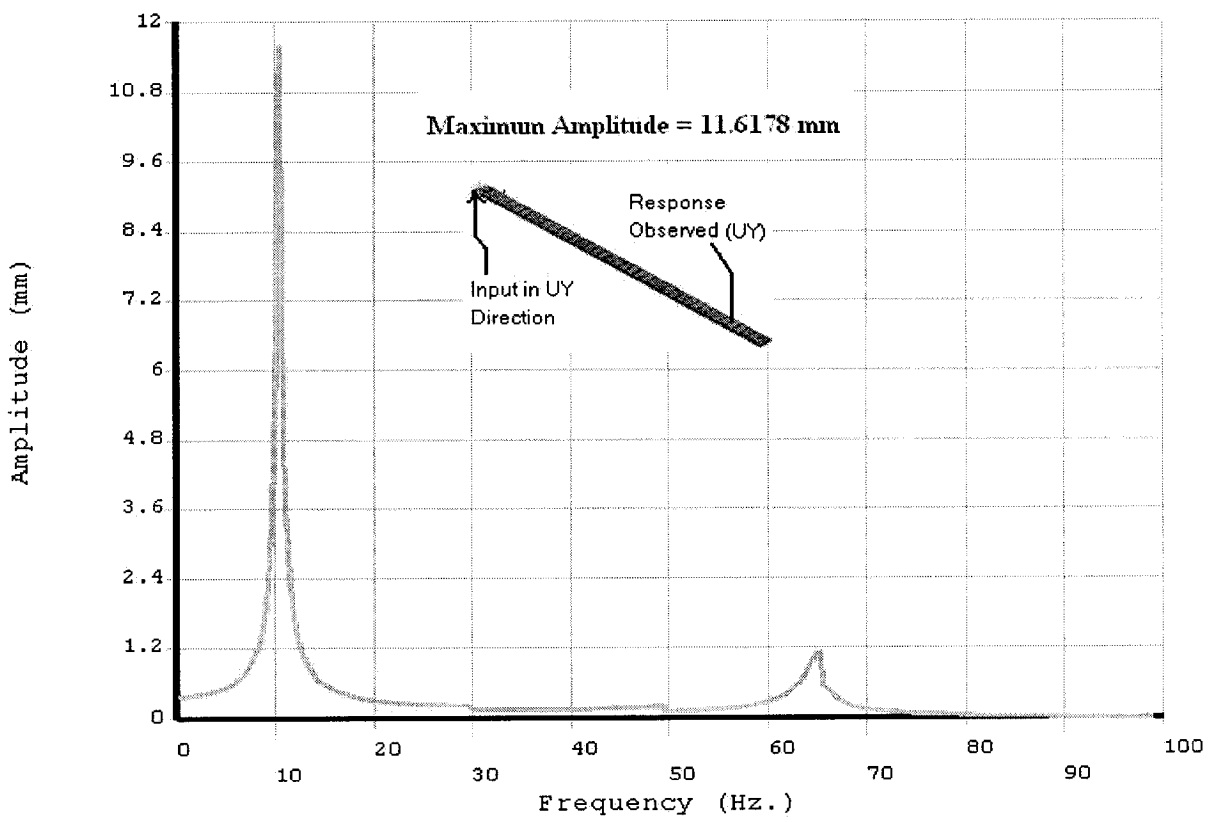


Fig. 2.7 Amplitude Response for  $\frac{1}{2}$  Scale Model Beam Under Harmonic Excitation

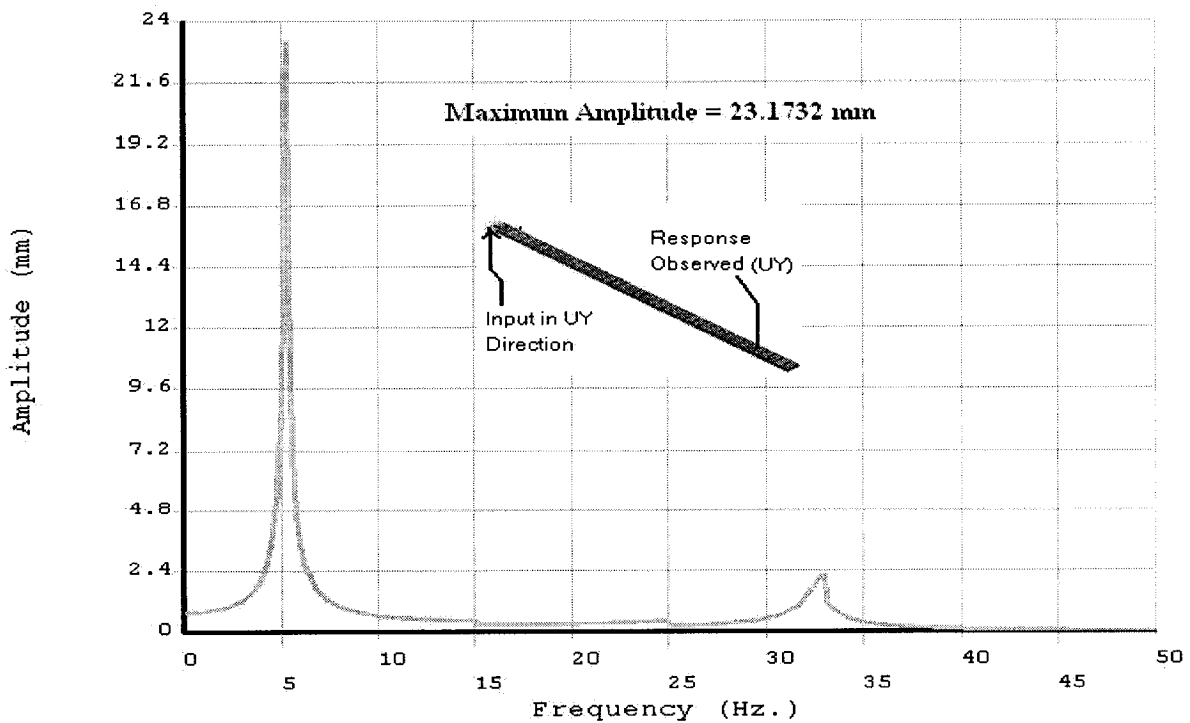


Fig. 2.8 Amplitude Response for Prototype Beam Under Harmonic Excitation

Now in Fig 2.7, the frequency of excitation of the model along the x-axis is expanded by  $\lambda_\omega$  and the amplitude response along y-axis is expanded by  $\lambda_t$  to obtain the predicted response of prototype. The Predicted response using model and response obtained from prototype is plotted in Fig. 2.9.

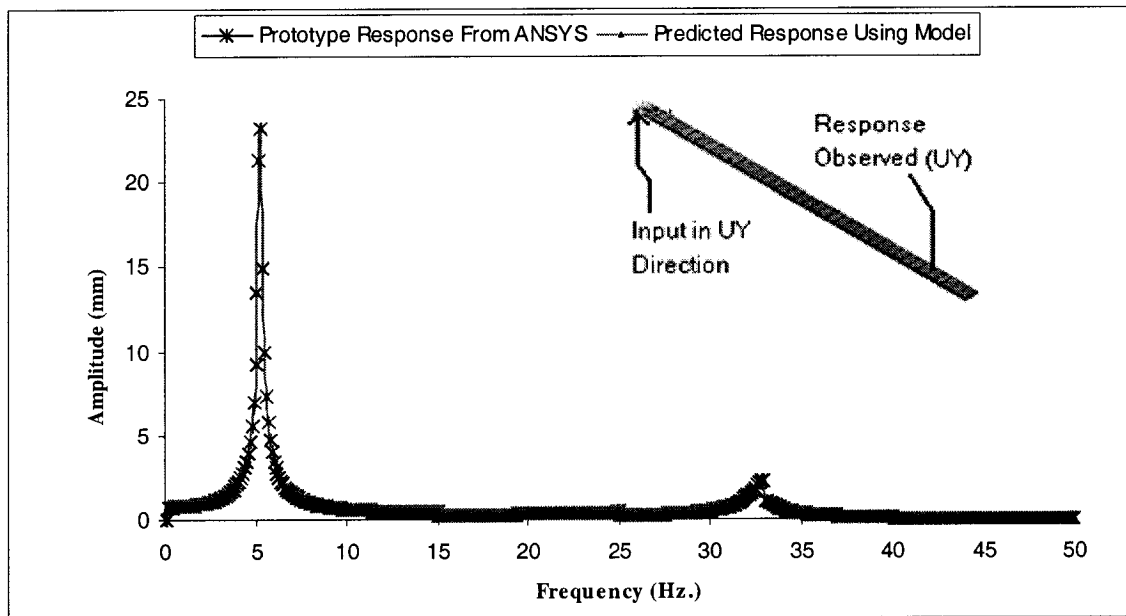


Fig. 2.9 Amplitude Response to Harmonic Excitation (Analytical & Predicted Response Using Model)

The maximum amplitude obtained for  $\frac{1}{2}$  scale model is 11.6178 mm. To predict the maximum response amplitude of prototype we have

$$\begin{aligned}
 \text{Predicted Amplitude of Prototype} &= \lambda_t \times \text{Amplitude of Model} \\
 &= 2 \times 11.6178 \\
 &= 23.2356 \text{ mm.}
 \end{aligned}$$

It is shown in Fig. 2.8 for the full scale prototype the maximum amplitude is 23.1732 mm. Therefore, the predicted response using scaling law is in excellent agreement with the response obtained from full scale prototype beam parameters.

The maximum stresses developed for model and prototype are shown in Fig. 2.10 and 2.11.

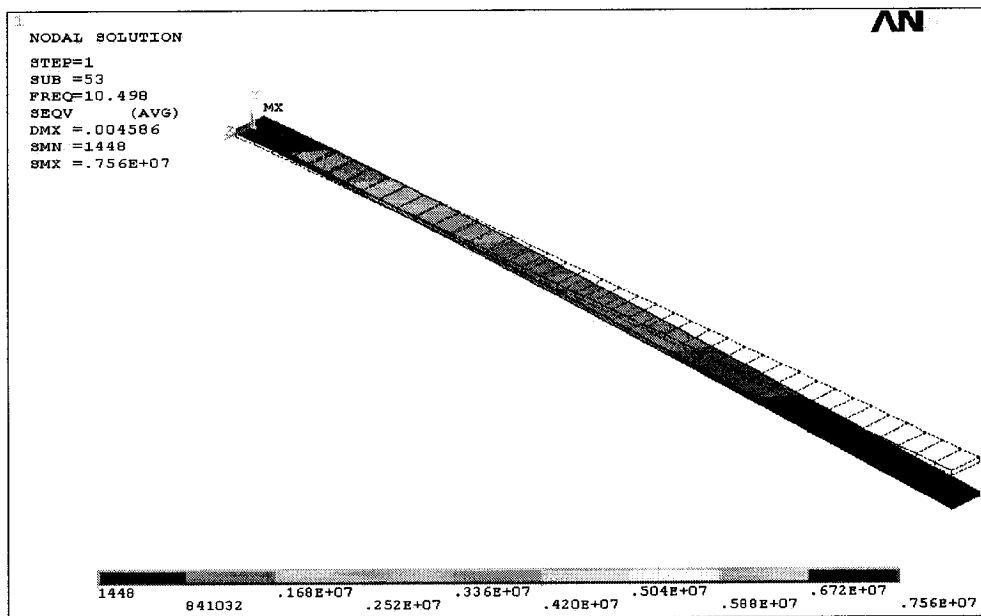


Fig. 2.10 Maximum Stresses ( $N/m^2$ ) Developed During Harmonic in Excitation in  $\frac{1}{2}$  Scale Model

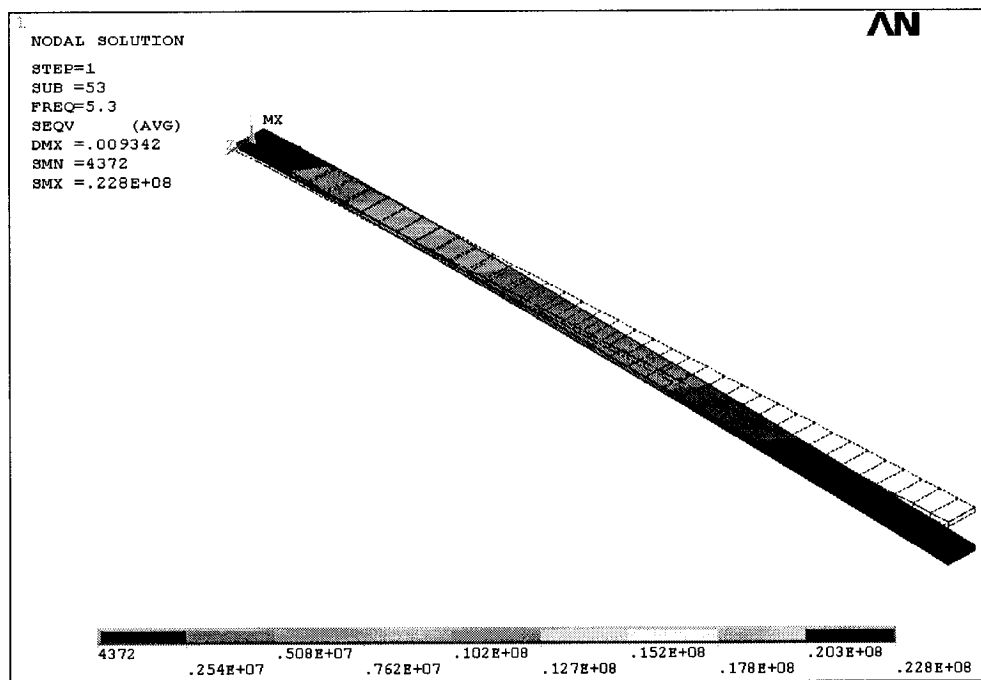


Fig. 2.11 Maximum Stresses ( $N/m^2$ ) Developed During Harmonic in Excitation Prototype

Maximum stress developed during Harmonic Excitation for  $\frac{1}{2}$  scale model is  $7.56 \times 10^6$  Pa. To predict the maximum response stress of prototype we have

$$\begin{aligned}\text{Predicted Stress in Prototype} &= \lambda_\sigma \times \text{Stress in Model} \\ &= 2.9710144902 \times 7.56 \times 10^6 \\ &= 2.246 \times 10^7 \text{ Pa.}\end{aligned}$$

Conducting the harmonic analysis with full scale parameters, the maximum stress amplitude has been found to be  $2.28 \times 10^7$  Pa which is in good agreement with the predicted stress in prototype. The error is less than 1.4% which is mainly due to rounding off of the values.

### 2.6.1.3 Transient Analysis

For transient analysis, the free end of the beam is impacted with an impulse and the response is taken at the location near the point of impact. Since an ideal impulse excites all the modes of a structure, the response of the beam should contain all the natural frequencies. However, we cannot produce an ideal impulse force numerically. We have to apply a load over a discrete amount of time  $dt$  as shown in Fig. 2.12.

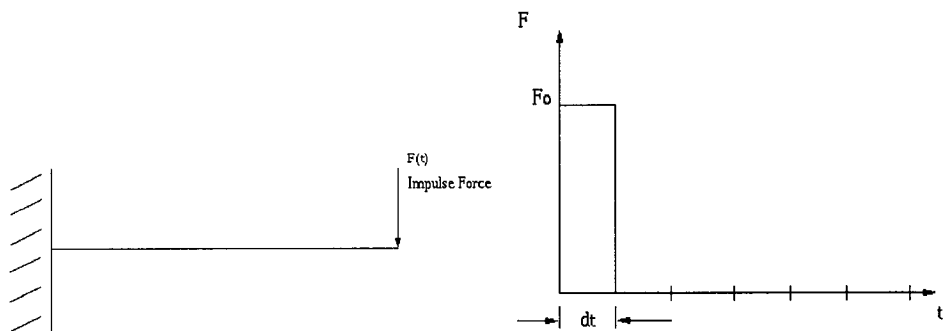


Fig. 2.12 Rectangular Impulse for Transient Analysis

The parameters for a rectangular pulse to have an impulse of 0.1 N.s on the prototype are

$(F_o)_p = 100N$  and  $(dt)_p = 0.001\text{sec}$ . For testing a  $\frac{1}{2}$  scale model these parameters are scaled

according to force and time scale factors as

$$(F_o)_m = \frac{(F_o)_p}{\lambda_F} = \frac{100}{11.884057970} = 8.41463414N$$

$$(dt)_m = \frac{(dt)_p}{\lambda_t} = \frac{0.001}{1.9809937009} = 5.04797162908 e^{-4} \text{ sec.}$$

Stiffness proportional damping is used for transient analysis. A damping ratio of 0.1 is considered in the first mode. In general, the mass and the stiffness proportional damping constant

is expressed as  $\zeta_i = \frac{\alpha}{2\omega_i} + \beta\omega_i$ . Since we have only stiffness proportional damping,  $\zeta_i = \beta\omega_i$ . For

prototype we have  $(\zeta_1)_p = \beta_p(\omega_1)_p$ . Therefore for 0.1 damping ratio in first mode, we

have  $\beta_p = 0.0060507$ . Similarly for  $\frac{1}{2}$  scale model stiffness proportional damping constant is

calculated as,  $(\zeta_1)_m = \beta_m(\omega_1)_m$  which gives  $\beta_m = 0.003054376$ .

The amplitude response obtained from model and prototype is shown in Fig. 2.13 and 2.14, respectively.

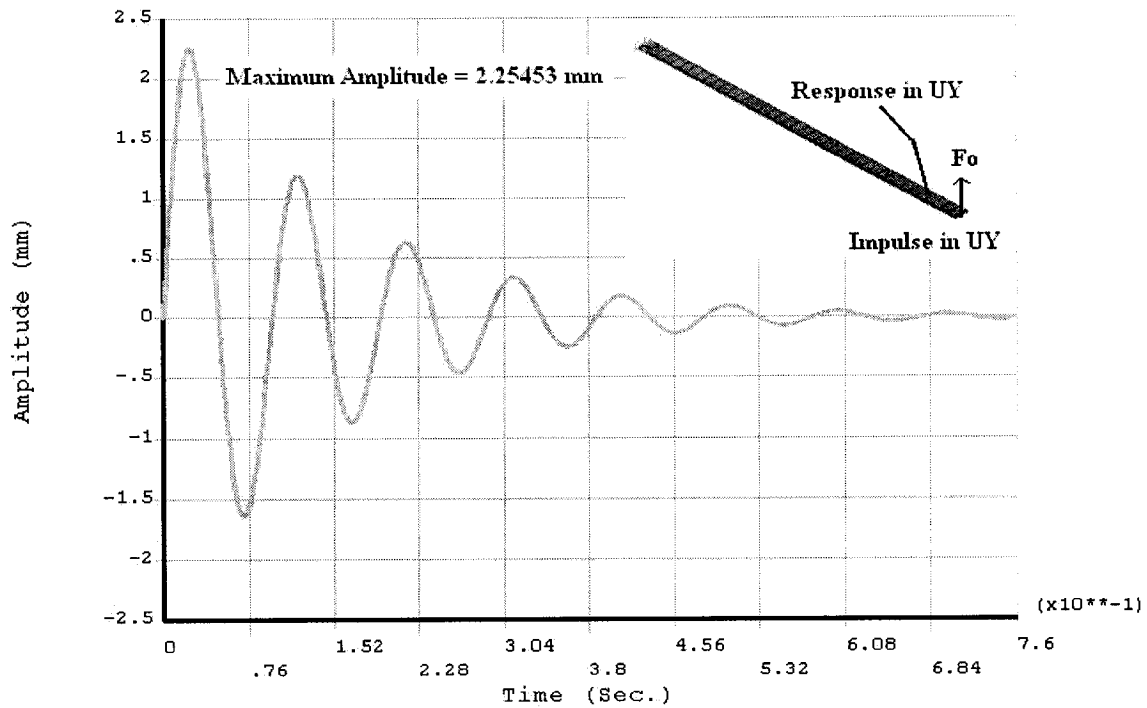


Fig. 2.13 Amplitude Response for  $\frac{1}{2}$  Scale Model Beam Under Impulse Excitation

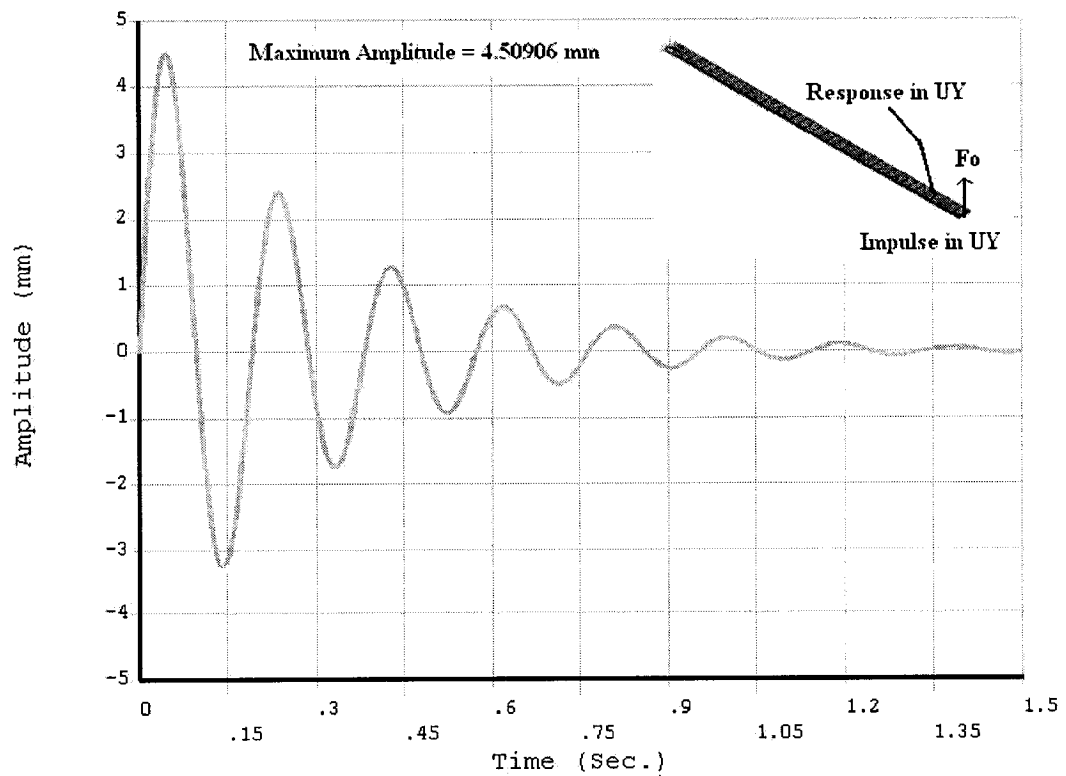


Fig. 2.14 Amplitude Response for Prototype Beam Under Impulse Excitation

Time for the model along the x-axis is expanded by  $\lambda_t$  and the amplitude response along the y-axis is expanded by  $\lambda_l$  to obtain the predicted response of prototype. The predicted response using model and the obtained prototype response are plotted in Fig. 2.15

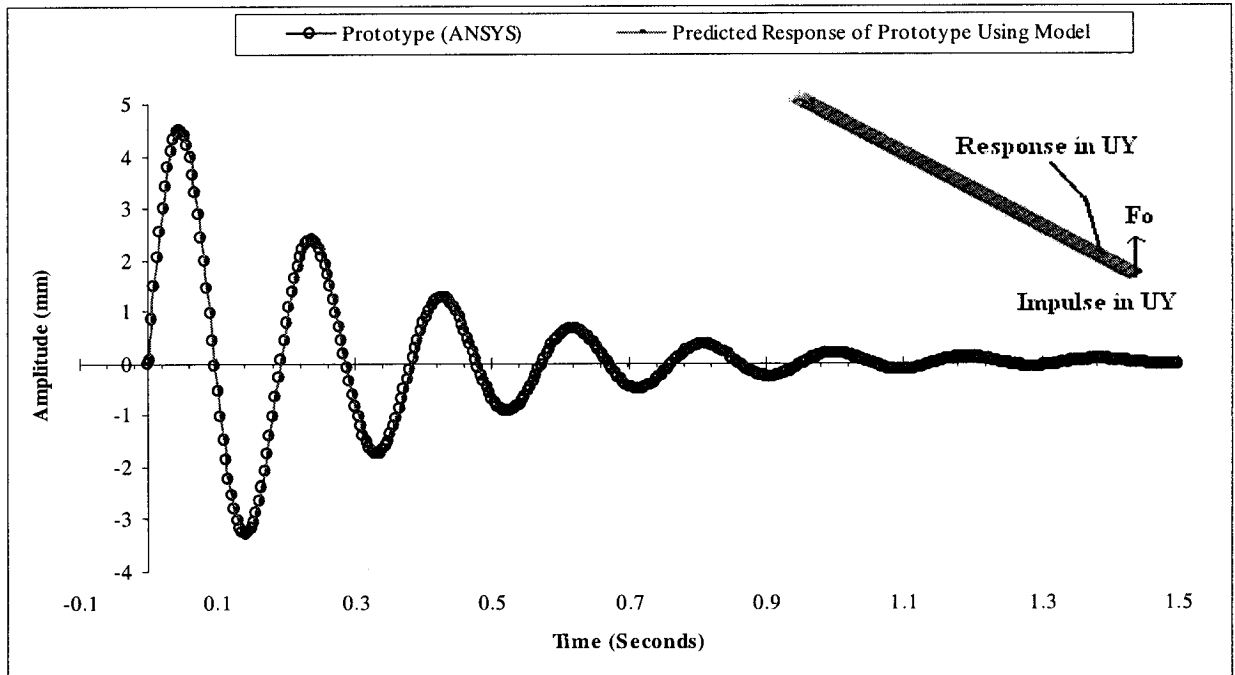


Fig. 2.15 Amplitude Response for Impulse Excitation (Analytical & Predicted Response Using Model)

The maximum amplitude obtained for  $\frac{1}{2}$  scale model is 2.25453 mm. To predict the maximum amplitude of prototype we have

$$\begin{aligned}
 \text{Predicted Amplitude of Prototype} &= \lambda_l \times \text{Amplitude of Model} \\
 &= 2 \times 2.25453 \\
 &= 4.50906 \text{ mm.}
 \end{aligned}$$

The harmonic analysis of the full scale prototype provides the maximum amplitude of 4.50906 mm which agrees very well with the predicted amplitude.

## 2.6.2 Using Dummy Masses to Avoid Violating Gravity Effects

### a) Calculation of Length Scale Factor $\lambda_l$

If a series of equally and closely spaced dummy weights are attached rigidly to the model structure, each section of the structure, with extra weight, can be considered to possess a density of  $\rho_m = \rho_{om} + \frac{\Delta m'}{\Delta v'}$ . Thus, the original restricting length scale factor relation given by

$$\lambda_E = \lambda_l \lambda_\rho \Rightarrow \lambda_l = \lambda_E / \lambda_\rho \Rightarrow \lambda_l = \frac{\lambda_E}{\rho_p} (\rho_{om} + \Delta m' / \Delta v') \text{ becomes more flexible.}$$

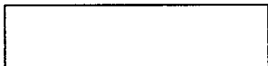
If aluminum dummy weights are used we get

$$\lambda_l = \frac{205e^{11}}{69e^9 \times 7870} (2700 + 2700) = 2.038561405$$

$$\Rightarrow \lambda_l = 2.038561405$$

The scaled parameters used for the 1/2.038561405 scale model is summarized in Table 2.6 below:

Table 2.6 Parameters used for Model Beam with Dummy Masses

PARAMETERS	1/2.038561405 Scale Model
Length of Beam	$L_m = 490.54500552 \text{ mm}$
Material Used for Beam	6061-T6 Aluminium
Modulus of Elasticity	$E_m = 69e^9 \text{ N/m}^2$
Original Density	$\rho_{om} = 2700 \text{ kg/m}^3$
Poisson's Ratio	$\nu_m = 0.29$
Cross Section	$\rightarrow 18.723988 \text{ mm} \leftarrow$  $\downarrow 3.129657 \text{ mm} \uparrow$

Scale Factors known are  $\lambda_l = 2.038561405$ ,  $\lambda_E = 2.97101449$ ,  $\lambda_\rho = 1.45707$ . Therefore other scale factors for dynamic analysis when dummy masses are used can be calculated as:

$$\lambda_t = \sqrt{\lambda_l} = 1.42778198$$

$$\lambda_\omega = \frac{1}{\sqrt{\lambda_l}} = 0.7003870398$$

$$\lambda_\sigma = \lambda_\rho \lambda_l = 2.97032666$$

$$\lambda_F = \lambda_l^3 \lambda_\rho = 12.3438833659$$

$$\lambda_a = 1$$

### b) Dummy Mass Calculation

For a line element such as beam, the amount of mass  $\mu_1$  to be added per unit length is given by [47]:

$$\mu_1 = \left[ \frac{1}{\lambda_E \lambda_l} - \frac{1}{\lambda_\rho \lambda_l^2} \right] \times \rho_p \cdot A_p \quad (2.36)$$

$$\mu_1 = \left[ \frac{69e^9}{205e^9 \times 2.038561405} - \frac{2700}{7870} \left( \frac{1}{2.038561405} \right)^2 \right] \times 38.17 \times 6.38 \times 10^{-6} \times 7870$$

$\mu_1 = 0.158219135589 \text{ kg/m}$  where  $\mu_1$  is define as

$$\mu_1 = \frac{\text{Mass}}{l_m} \times \text{Number of Dummy Masses} \quad (2.37)$$

If Number of Dummy Masses Used = 41 Then mass to be added is

$$\text{Mass} = 0.158219135589 \times \frac{0.49054200552}{41} = 0.001893 \text{ kg}$$

BEAM3 ANSYS 7.1 element has been used to model the beam.

For Dummy masses, MASS21 element has been used which a point element, having up to six degrees of freedom: translations in the nodal x, y, and z directions and rotations about the nodal x, y, and z axes.

The beam has been meshed with 40 BEAM3 elements and 41 MASS21 elements have been used as point masses to simulate dummy masses as shown in Fig. 2.16.

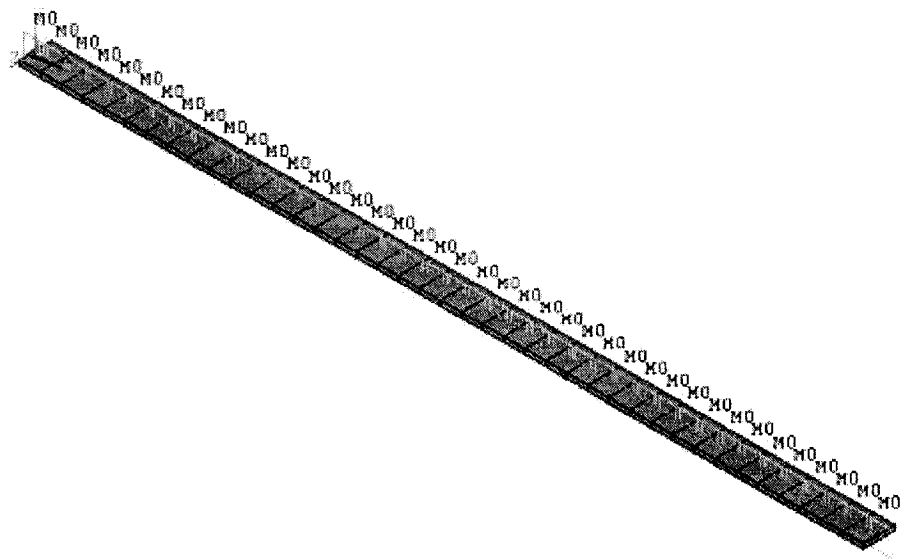


Fig. 2.16 Model Clamped Beam Meshed with Beam elements and Dummy Masses

#### 2.6.2.1 Modal Analysis

Modal analysis has been performed to locate the natural frequencies. Using the 1/2.038561405 scale model with dummy masses, the fundamental natural frequency is found to be 7.4637 Hz. Using the scaling laws the fundamental natural frequency of the full scale prototype has been predicted as:

$$\text{Predicted Natural Frequency of Prototype} = \lambda_{\omega} \times \text{Natural Frequency of Model}$$

$$= 0.7003870398 \times 7.4637$$

$$= 5.227479 \text{ Hz.}$$

The frequency analysis of the full scale prototype have also been conducted and the fundamental natural frequency has been found to be 5.26 Hz. Thus the predicted natural frequency using scaling law agrees with the natural frequency obtained from the full scale prototype beam parameters.

Table 2.7 summarizes the first ten natural frequencies and demonstrates that good correlation exists between the analytical and predicted natural frequencies, validating the frequency scale factor. Corresponding mode shapes are also shown in the last column of the Table 2.7 and they were found to be identical for the prototype and its  $1/2.038561405$  scale model with dummy masses, for the corresponding natural frequencies.

Sr. No.	Nat. Freq. (Hz) of 1/2 Scale Model ANSYS $(\omega_n)_M$	Predicted Nat. Freq. (Hz.) of full Scale Prototype $\lambda_\omega \cdot (\omega_n)_M$	Nat. Freq.(Hz.) of Full Scale Prototype ANSYS $(\omega_n)_P$	Corresponding Mode Shape (Prototype and Model with Dummy Masses)
1	7.4637	5.227479	5.26	
2	46.769	32.7564	32.962	
3	130.94	91.70868	92.289	
4	256.56	179.6913	180.83	
5	424.06	297.0061	298.88	

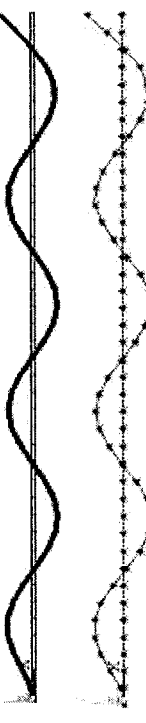
Sr. No.	Nat. Freq. (Hz) of 1/2 Scale Model ANSYS $(\omega_n)_M$	Predicted Nat. Freq. (Hz.) of full Scale Prototype $\lambda_\omega \cdot (\omega_n)_P$	Nat. Freq.(Hz.) of Full Scale Prototype $(\omega_n)_P$	Corresponding Mode Shape
6	633.39	443.6181	446.41	
7	884.52	619.5063	623.38	
8	1177.4	824.6357	829.76	
9	1512.1	1059.055	1065.5	
10	1888.4	1322.611	1330.7	

Table 2.7 Natural Frequencies and Mode Shapes with Aluminium Model and Steel  $\left( \lambda_\omega = \frac{1}{\sqrt{\lambda_i}} = 0.7003870398 \right)$

### 2.6.2.2 Harmonic Analysis

Base excitation is applied at the clamped end of the beam in UY direction and the response is also observed in UY direction near the free end. The input is applied as different amplitude ranges in different frequency bands as shown in Table 2.4.

For testing a 1/2.038561405 scaled model with dummy masses, this harmonic input is also scaled according to the scaling laws as shown in Table 2.8.

Table 2.8 Scaled Harmonic Input for Model

Frequency Range (Hz)	Amplitude in (meters)	No of substeps
0 to 21.41	0.000374	150
21.41 to 35.69	0.000249	100
35.69 to 47.11	0.000125	80
47.11 to 57.11	6.23E-05	70
57.11 to 71.38	3.74E-05	100

The amplitude response obtained for model using ANSYS 7.1 and is plotted in Fig. 2.17.

Constant damping ratio of 0.02 is used for the harmonic analysis.

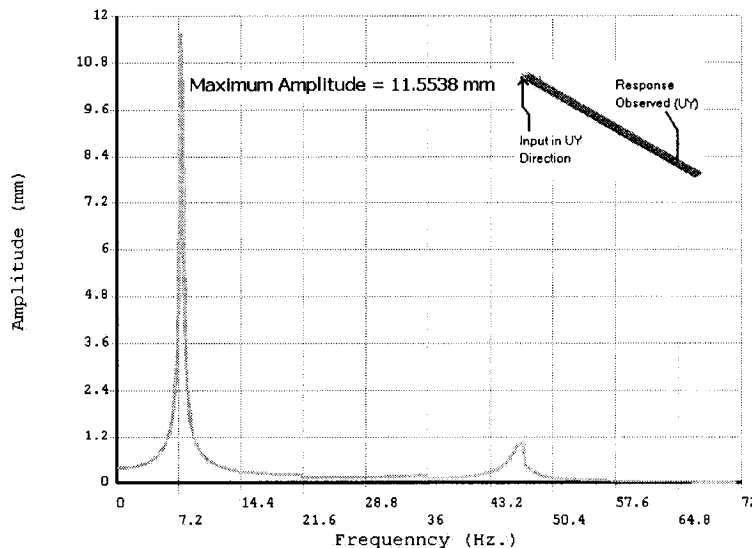


Fig. 2.17 Amplitude Response For Model with Dummy Masses Under Harmonic Excitation

The frequency axis of the model along the x-axis is expanded by  $\lambda_w$  and the amplitude response y-axis is expanded by  $\lambda_l$  to obtain the predicted response of prototype. The predicted response using model with dummy masses and response obtained from prototype are plotted in Fig. 2.18.

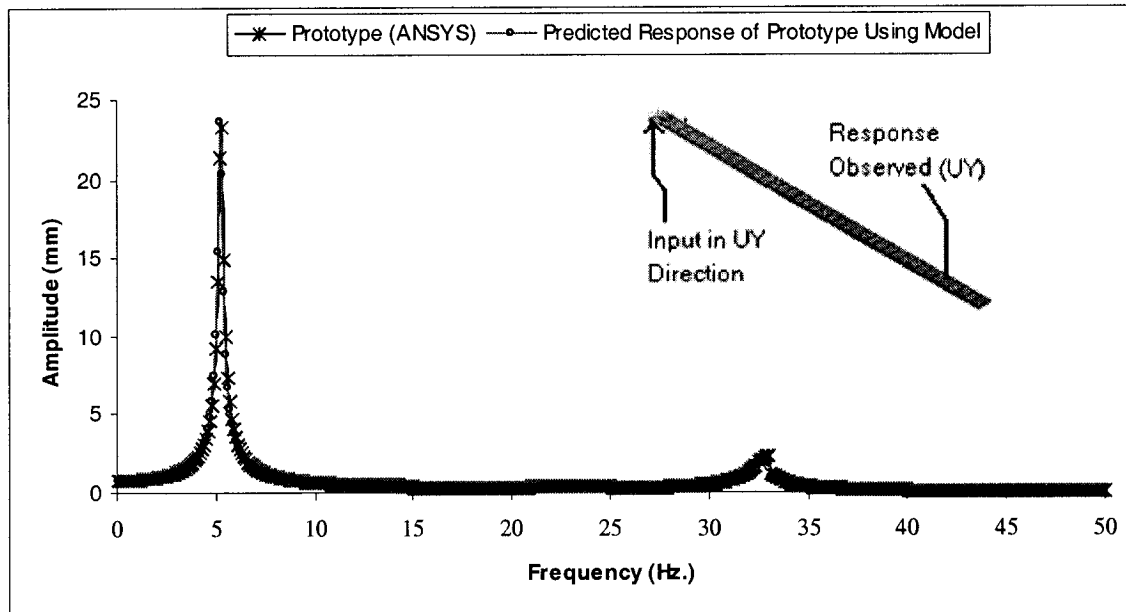


Fig. 2.18 Amplitude Response to Harmonic Excitation (Analytical & Predicted Response Using Model with Dummy Masses)

The maximum amplitude obtained for  $1/2.038561405$  scale model with dummy masses is 11.5538 mm. To predict the maximum amplitude of prototype we have

$$\begin{aligned}
 \text{Predicted Amplitude of Prototype} &= \lambda_l \times \text{Amplitude of Model} \\
 &= 2.038561405 \times 11.5538 \\
 &= 23.5531 \text{ mm.}
 \end{aligned}$$

The harmonic analysis of the full scale prototype has also been performed and maximum amplitude of 23.1732 mm was found confirming the predicted response using model with dummy masses.

### 2.6.2.3 Transient Analysis

For testing a 1/2.038561405 scale model with dummy masses the impulse parameters are scaled according to force and time scale factors as

$$(F_o)_m = \frac{(F_o)_p}{\lambda_F} = \frac{100}{12.3438833659} = 8.10117829N$$

$$(dt)_m = \frac{(dt)_p}{\lambda_t} = \frac{0.001}{1.42778198} = 7.0038703 e^{-4} \text{ sec.}$$

Stiffness proportional damping is used for transient analysis. In general, the mass and the stiffness proportional damping constant is expressed as  $\zeta_i = \frac{\alpha}{2\omega_i} + \beta\omega_i$ . Since we have only stiffness proportional damping,  $\zeta_i = \beta\omega_i$ . For model with dummy masses we have  $(\zeta_1)_m = \beta_m(\omega_1)_m$ . Therefore for 0.1 damping ratio in first mode, we have  $\beta_m = 0.00426422$ . The amplitude response obtained for model with dummy masses is plotted in Fig. 2.19.

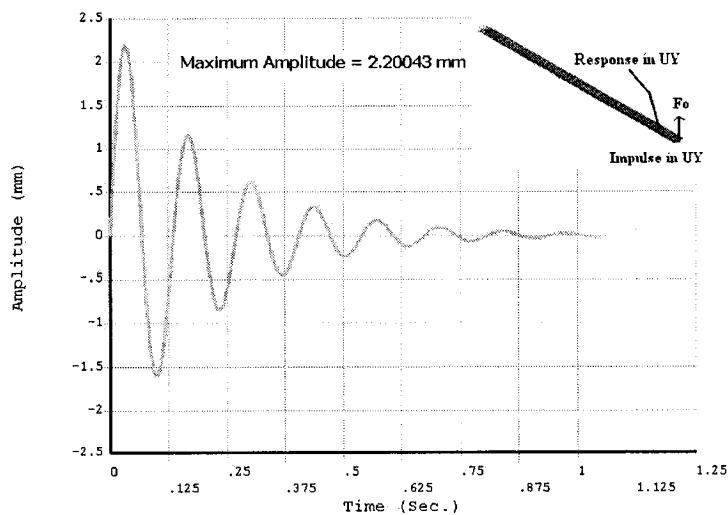


Fig. 2.19 Amplitude Response for Scale Model Beam with Dummy Masses Under Impulse Excitation

Again the x-axis which is time axis for the model with dummy masses is expanded by  $\lambda_i$  and the amplitude response y-axis is expanded by  $\lambda_i$  to obtain the predicted response of prototype. The predicted response using model and the obtained prototype response is plotted in Fig. 2.20.

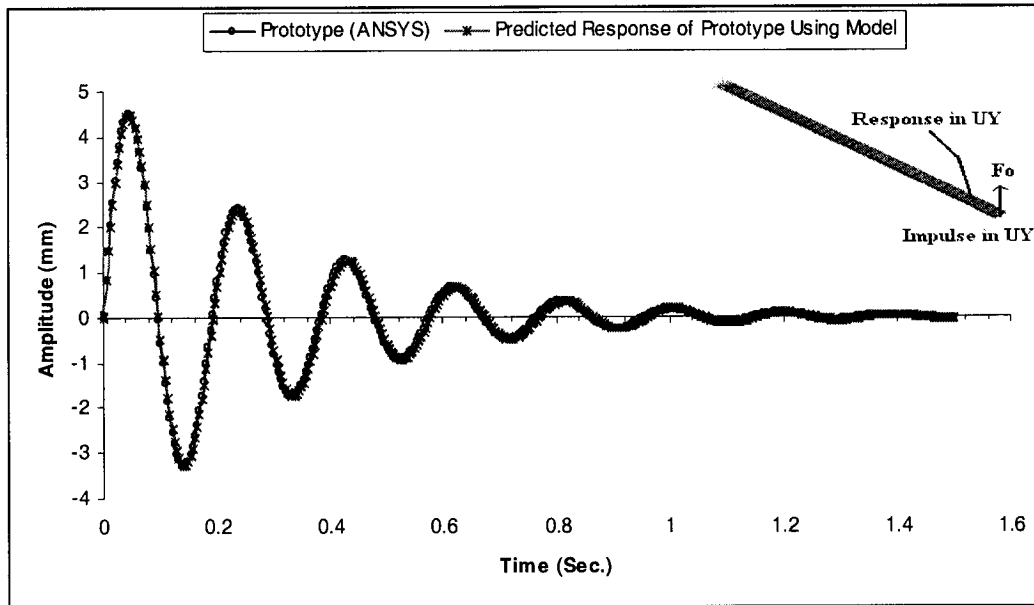


Fig. 2.20 Amplitude Response for Impulse Excitation (Analytical & Predicted Response Using Model)

The maximum amplitude obtained for the scale model with dummy masses is 2.20043 mm. To predict the maximum amplitude of prototype we have

$$\begin{aligned}
 \text{Predicted Amplitude of Prototype} &= \lambda_i \times \text{Amplitude of Model} \\
 &= 2.038561405 \times 2.20043 \\
 &= 4.85711672 \text{ mm.}
 \end{aligned}$$

Performing the transient analysis on full scale prototype, the maximum amplitude has found to be 4.50906 mm. As it can be seen good agreement exists between the predicted

amplitude using scaled model with dummy masses and the amplitude of the full scale prototype.

In the preceding chapter similitude theory has been discussed and scaling laws have been derived for dynamic analysis of structures. The derived laws are then validated on a simple beam structure by using ANSYS 7.1 and it has been shown that good correlation exist between the prototype and the model. In the following chapter, the scaling laws and simulation results obtained from ANSYS 7.1 are validated by carrying out experiments on the prototype and the model beam.

# CHAPTER 3

## EXPERIMENTAL VERIFICATION OF SCALING LAWS

### 3.1 INTRODUCTION

It has been analytically shown in the previous chapter that neglecting gravitational forces have negligible effect in vibrating structures and thus neglecting these forces in scale modeling is a valid relaxation. In order to verify the simulation and proof-of-concept of dynamic scaled modeling, as discussed in previous chapter, the prototype of the cantilever beam and its  $\frac{1}{2}$  scaled model without dummy masses has been experimentally tested in this chapter.

The prototype beam and its  $\frac{1}{2}$  scale model have been fabricated in the Machine Shop of Concordia University according to the parameters provided in Table 2.2. The necessary fixtures for the experiment have also been fabricated. An experiment for finding out the natural frequencies and mode shapes of cantilever prototype beam and its  $\frac{1}{2}$  scale model has been performed in order to validate the simulation results in chapter 2.

Dynamic testing typically consists of applying an excitation to the test object and monitoring the response and monitoring its response. The fundamental test set up for dynamic testing of an object is shown in Fig. 3.1.

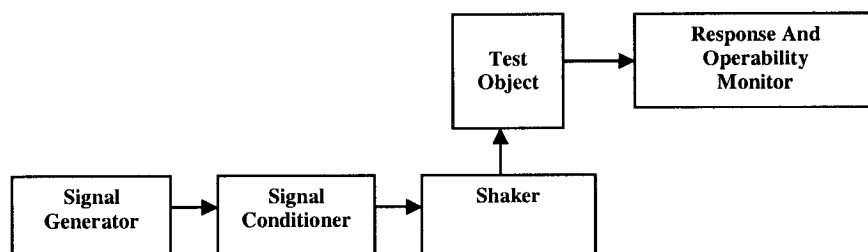


Fig. 3.1 Basic Test Setup in Dynamic Testing [1]

### **3.2 FABRICATION OF PROTOTYPE AND MODEL BEAM**

The prototype and its  $\frac{1}{2}$  scaled beam shown in Fig 3.2 were fabricated according to the specification tabulate Table 2.3.

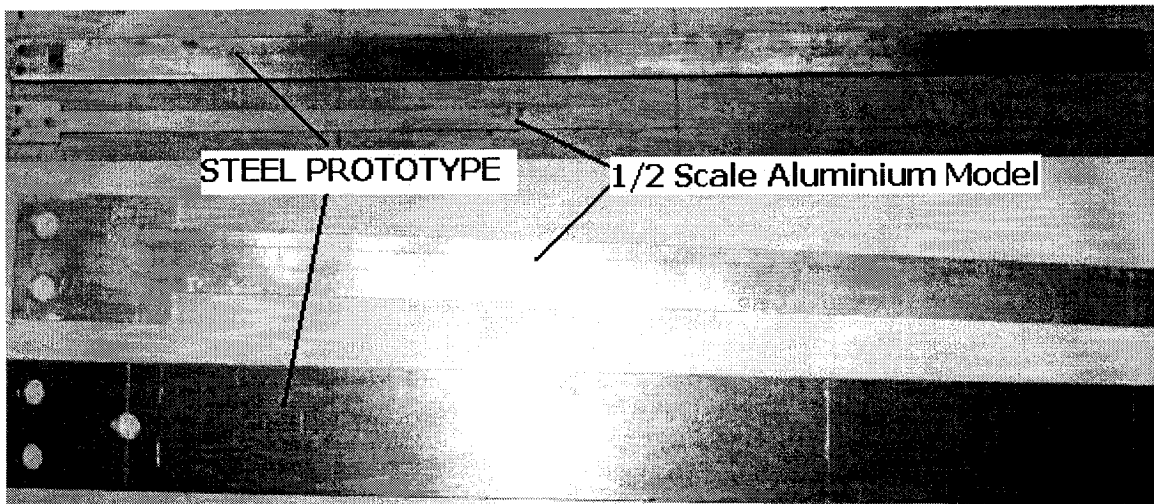


Fig. 3.2 Prototype 1018-Steel Beam and its  $\frac{1}{2}$  Scaled 6061-T6 Aluminium Beam

1018-Steel has been used for the fabrication of effective 1 meter long prototype beam and 6061-T6 Aluminium has been used for its  $\frac{1}{2}$  scaled effective 0.5 meter model beam. Extra length has been provided that was used for clamping the beam at one end for cantilever boundary condition. Fixture table as shown in Fig. 3.3 has also been designed and fabricated in order to provided cantilever support and the clearance for the beam to vibrate freely. Three holes have been drilled to screw the beam with the fixture table. Measurement lines have been marked on every 100 mm on the prototype beam and on every 50 mm on the model beam to provide homologous locations for measuring response.

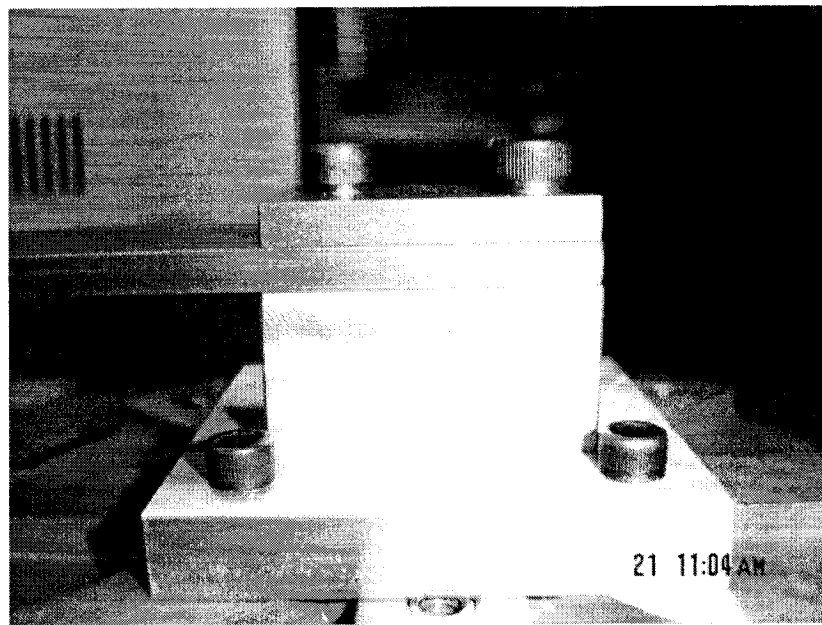


Fig. 3.3 Prototype Beam Clamped at One End to Achieve Cantilever Boundary Condition

### 3.3 EXPERIMENTAL SETUP AND RESULTS

The preliminary impulse hammer tests were performed on prototype and model beam to verify the natural frequencies with simulation results, and then roving impact test were performed to verify the mode shapes of prototype and model beam.

#### 3.3.1 Natural Frequency Measurement

In order to verify the simulation results and to validate scaling laws experimentally, frequency measurement has been conducted on both prototype and its  $\frac{1}{2}$  scale model beams with cantilever boundary conditions. A light impulse was applied to prototype with the impact hammer and the response motion was measured as acceleration at the free end with the help of an accelerometer as shown in Fig 3.4. The magnitude of receptance which is acceleration /force FRF was measured using two channels FFT Signal Analyzer Unit.

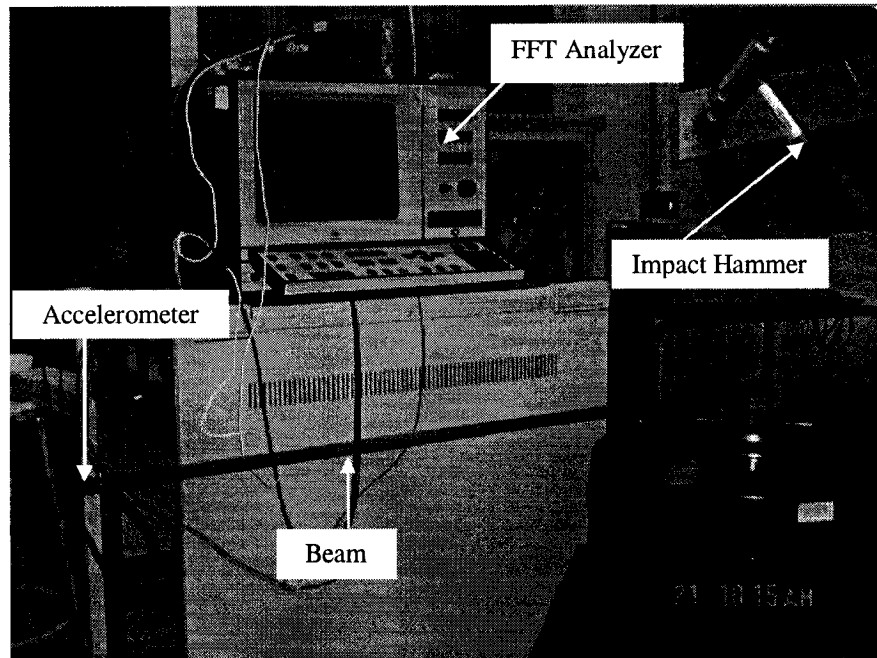


Fig. 3.4 Experimental Setup for Vibration Testing of Prototype Beam

The FRF of acceleration/receptance measured for the prototype beam is shown in Fig. 3.5. Examination of Fig. 3.5 reveals that the first three natural frequencies for the prototype are 5, 33 and 92.25 Hz which are in excellent agreement with those obtained analytically. The results of the experiment for the prototype and comparison with simulation are summarized in Table 3.1.

Table 3.1 Prototype Natural Frequencies obtained Experimentally and from Simulation

S. No.	Nat. Freq.(Hz.) of Full Scale Prototype (Simulation)	Nat. Freq.(Hz.) of Full Scale Prototype (Experiment)	Percentage Error in Nat. Freq. Experimental from Simulation results (%)
1.	5.26	5	5.2
2.	32.962	33	0.1151
3.	92.289	92.25	0.0422

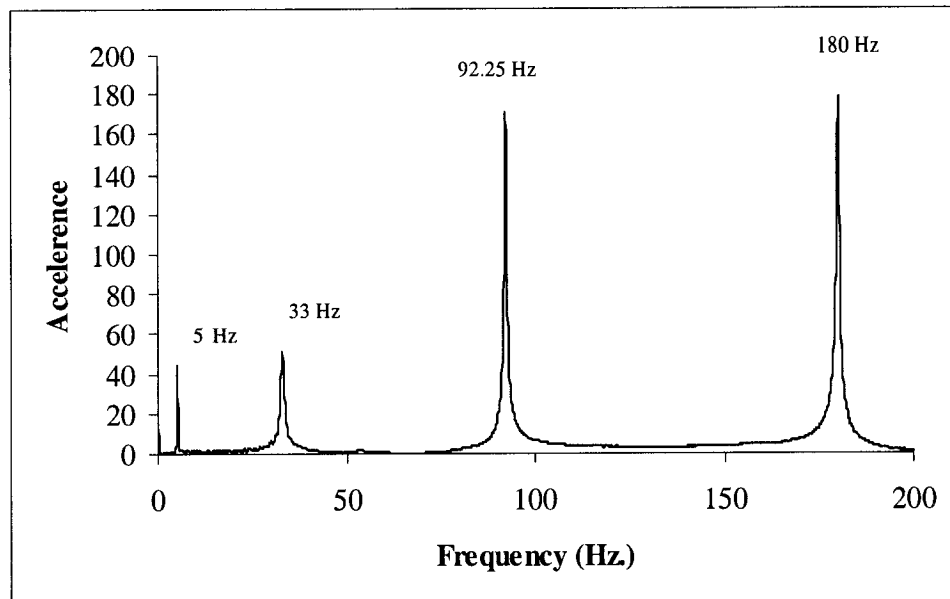


Fig. 3.5 FRF for Prototype

Since the weight of the accelerometer was found to be considerable for testing of the model beam, Electro optics Laser Vibrometer was used to measure the response velocity as shown in Fig. 3.6. Using FFT analyzer, derivative of the response velocity signal was measured to obtain the Receptance FRF as shown in Fig. 3.7.

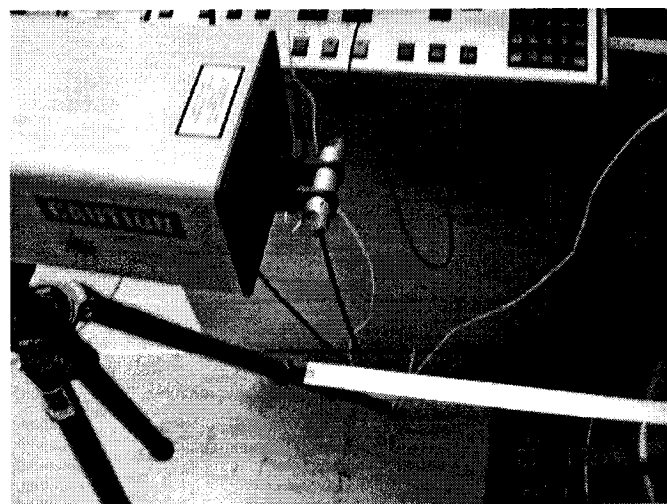


Fig. 3.6 Experimental Setup with Laser Vibrometer for Model Beam

According to Fig. 3.7 the first three natural frequencies of model beam are found to be 10.25, 64.75 and 182 Hz which are again in an excellent agreement with the simulated results obtained for the model beam. The experimental and simulation results for the first three natural frequencies are tabulated in Table 3.2.

Table 3.2 Model Natural Frequencies obtained Experimentally and from Simulation

S. No.	Nat. Freq.(Hz.) of $\frac{1}{2}$ Scale Model (Simulation)	Nat. Freq.(Hz.) of $\frac{1}{2}$ Scale Model (Experiment)	Percentage Error in Nat. Freq. Experimental from Simulation results (%)
1.	10.42	10.25	1.65
2.	65.598	64.75	1.309
3.	182.82	182	0.45

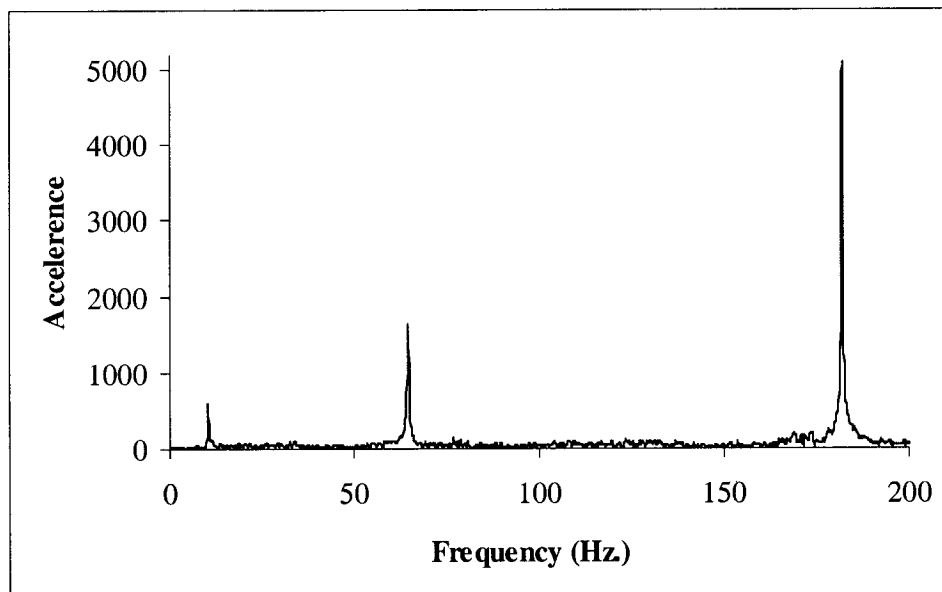


Fig. 3.7 FRF for Model

It is observed from this experiment that gravity effects are negligible for these vibrating structures and can be neglected in dynamic scaling because natural frequency of prototype predicted using model is found to be the same as the natural frequency

measured by testing the full scale prototype with a very small marginal error as shown in Table 3.3. Hence relaxation of neglecting gravity effects is justified.

Table 3.3 Comparison of the Predicted Natural Frequency using Experimental Results of the Model Beam with Experimental Natural Frequencies for Prototype

S. No.	Experimental Natural Frequency of Model Beam(Hz.) ( $\omega_n)_M$	Predicted Natural Frequency using Model Beam(Hz.) $\lambda_\omega \cdot (\omega_n)_M$	Experimental Natural Frequency of Prototype Beam(Hz.) ( $\omega_n)_P$	Percentage Error in Predicted and Simulated Nat. Freq. (%)
1	10.25	5.1741	5	3.482
2	64.75	32.685	33	0.954
3	182	91.87	92.25	0.411

The marginal percentage errors can be mainly attributed due to the following reasons:

1. The  $\frac{1}{2}$  scaled model is not exactly half in dimension due to manufacturing tolerance error.
2. The mass of the accelerometer is not accounted while measuring the prototype natural frequency.
3. The mass of hammer at the instance of the impact is also unaccounted.
4. The clamped boundary condition effects cannot be modeled.

### 3.3.2 Mode Shape Measurement

In order to verify corresponding mode shapes of prototype and its model beam, an impact rover test was carried out on the prototype and its  $\frac{1}{2}$  scale model beam with cantilever boundary conditions. The experimental set up and the procedure to obtain transfer functions is shown in Fig. 3.8. For mode shape measurement, continuous beam was discretized by taking measurement at 11 different equally spaced locations as shown

in Fig. 3.8. The imaginary part of FRF was measured on the free end (location 1) when the impact from hammer was applied at homologous locations (1, 2, 3..., and 11) i.e. after every 100 mm distance for prototype and 50 mm for model as shown in Fig. 3.8.

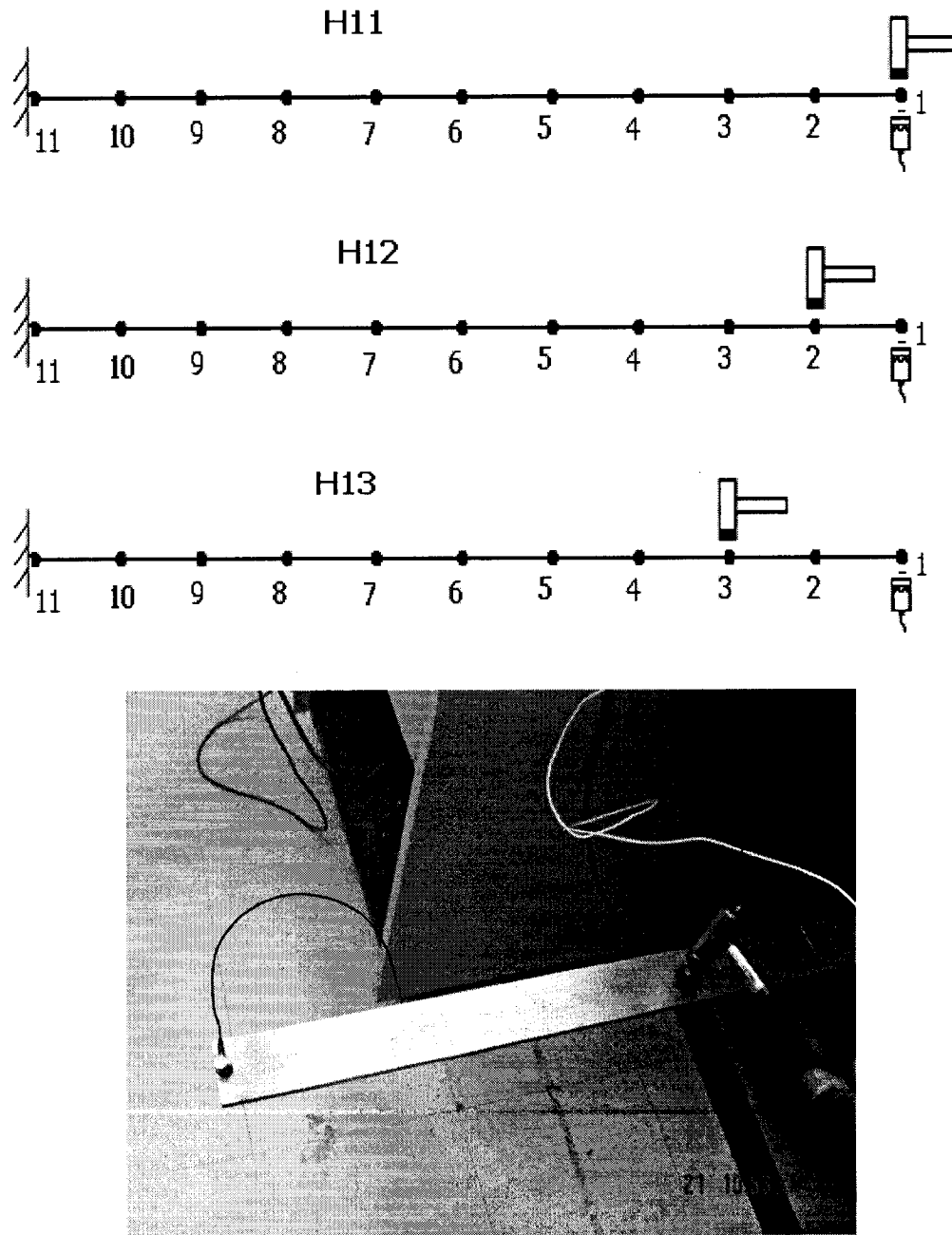


Fig. 3.8 Experimental Set up for Roving Impact Test to Obtain Mode Shape

There were 11 possible places where impact could be applied and 11 possible places where the responses could be measured. This means that there are a total of  $11 \times 11$  possible *complex-valued* frequency response functions that could have been acquired. The frequency response functions are usually described with subscripts to denote the input and output locations as,  $H_{out,in}$  (or with respect to typical matrix notation this would be  $h_{row,column}$ ). At first the beam was driven with a force from an impact hammer at the tip of the beam (location 1) and the response was also measured at the same location enabling to find  $H_{11}$  transfer function. This type of measurement is usually referred to as a drive point measurement. Some important characteristics of the drive point measurement are:

- All resonances (peaks) are separated by anti-resonances.
- The phase loses 180 degrees of phase as we pass over a resonance
- The phase gains 180 degrees of phase as we pass over antiresonance.
- The peaks in the imaginary part of the frequency response function must all point in the same direction.

The imaginary part of FRF of  $H_{11}$  for the prototype beam is shown in Fig. 3.9

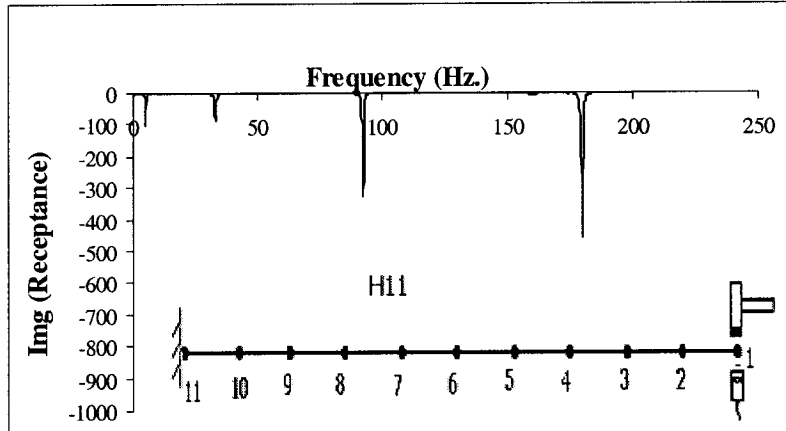


Fig. 3.9 Imaginary part of FRF ( $H_{11}$ ) for Prototype Beam

Similar measurements were taken by moving the impact force to point 2, 3..., and 11 and measuring the response at point 1 to obtain one complete row of  $H$  transfer function matrix. It is important to note that the frequency response function matrix is symmetric. This is due to the fact that the mass, damping and stiffness matrices that describe the system are symmetric. Hence we can see that  $h_{ij} = h_{ji}$  which is called the property of reciprocity. It is not required to actually measure all the terms of the frequency response function matrix later to obtain mode shapes, and only one row or column of the frequency response function matrix is enough [46]. For prototype the peak imaginary values of FRF obtained at first three resonant frequencies are tabulated for each  $H_{i,j}$  function to obtain the first three mode shapes as summarized in Table 3.4.

Same procedures were repeated for  $\frac{1}{2}$  scaled model beam and the peak imaginary values of FRF obtained at first three resonant frequencies are tabulated for each  $H_{i,j}$  function to obtain first three mode shapes of model beam as summarized in Table 3.5.

The mode shape is then obtained by plotting each row of Table 3.4 and 3.5 against 11 points (that represents location of impact measurement). The mode shapes obtained experimentally for model and prototype are shown in Fig. 3.10 which are

similar to those obtained from simulation in chapter 2. It is seen that both model and prototype have the same mode shapes for homologous frequency.

Table 3.4 Imaginary Values of FRF at obtained Experimentally at First Three Natural Frequencies for Prototype Beam

$\text{Frequency} \rightarrow A_t$	Peak Imaginary Value of FRF $\rightarrow$	$H_{11}$	$H_{12}$	$H_{13}$	$H_{14}$	$H_{15}$	$H_{16}$	$H_{17}$	$H_{18}$	$H_{19}$	$H_{110}$	$H_{111}$
5	-105	-86	-66.9	-59.8	-44.7	-33.7	-26.5	-14.8	-6.32	-2.74	-0.766	
33	-89.1	-45.7	-6.42	27.8	50.8	65.8	62.9	43.2	23.1	1.02	-6.46	
92.25	-319	-67.7	152	227	163	-13.9	-188	-261	-209	-65.7	11.9	

Table 3.5 Imaginary Values of FRF obtained Experimentally at First Three Natural Frequencies for  $\frac{1}{2}$  Scale Model Beam

$\text{Frequency} \rightarrow A_t$	Peak Imaginary Value of FRF $\rightarrow$	$H_{11}$	$H_{12}$	$H_{13}$	$H_{14}$	$H_{15}$	$H_{16}$	$H_{17}$	$H_{18}$	$H_{19}$	$H_{110}$	$H_{111}$
10.75	-1710	-1470	-1200	-979	-849	-675	-408	-247	-124	-37.3	-2.98	
64.75	-2260	-1180	119	1070	1590	1880	1370	669	210	17.1		
182	-2220	-183	1380	1950	1220	-254	-1610	-2010	-1490	-531	-11.1	

### Experimental Mode Shapes for Model

### Experimental Mode Shapes for Prototype

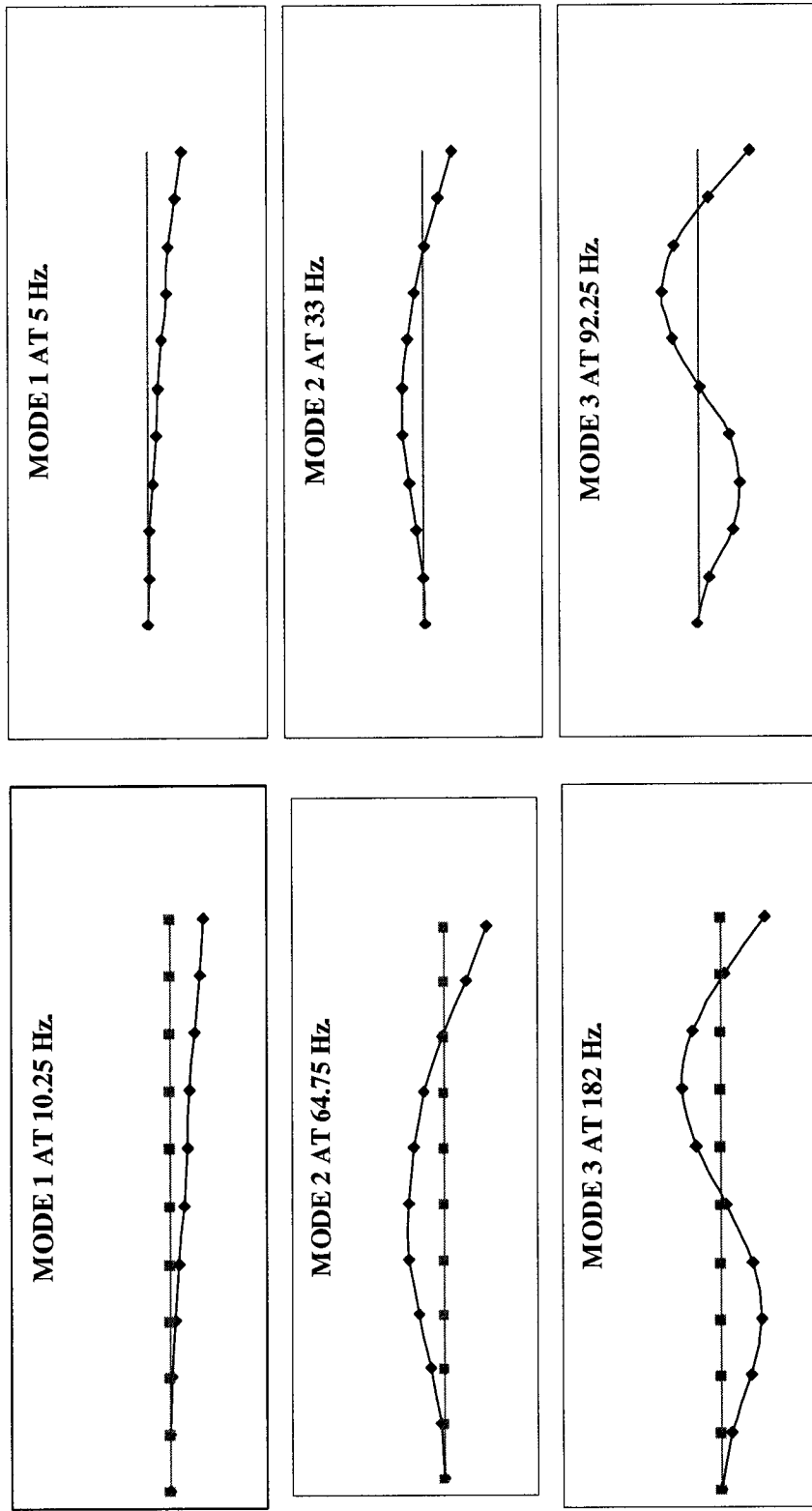


Fig 3.10 Mode Shapes obtained Experimentally for Prototype and its  $\frac{1}{2}$  Scale Model Beam

# **CHAPTER 4**

## **NAVAL SHIPBOARD CONSOLE VIBRATION AND SHOCK ANALYSIS USING SCALED MODEL**

### **4.1 GENERAL**

In the previous chapters the methodology has been developed for dynamic testing of structures using scaled models. The scaling laws are derived and has been validated both by carrying out finite element analysis using ANSYS 7.1 and by performing experiments for a simple structures. In this chapter the methodology has been applied to the real life structure. This chapter provides the detailed analysis and results of a thorough study carried out on a real life console for shipboard installation using a half scaled model. This dynamic analysis on the console was carried out under the specified shock and vibration levels. The predicted response of prototype from  $\frac{1}{2}$  scale model has been verified by simulation of full scale prototype.

### **4.2 DESCRIPTION OF THE SHIPBOARD MONITOR AND CONSOLE**

The Naval Shipboard Monitor and Console such as Bridge Control Console (BCC) shown in Fig. 4.1 and Machinery Control Console (MCC) provides the Man Machine interface. The main functions of the BCC are to provide the Man Machine Interface facilities with the capability to control and monitor the propulsion machineries from the bridge of the ship [42]. The main functions of the MCC are to provide facilities for one man control and monitoring of the propulsion, ancillary, auxiliary and electrical machinery on the frigates [43].

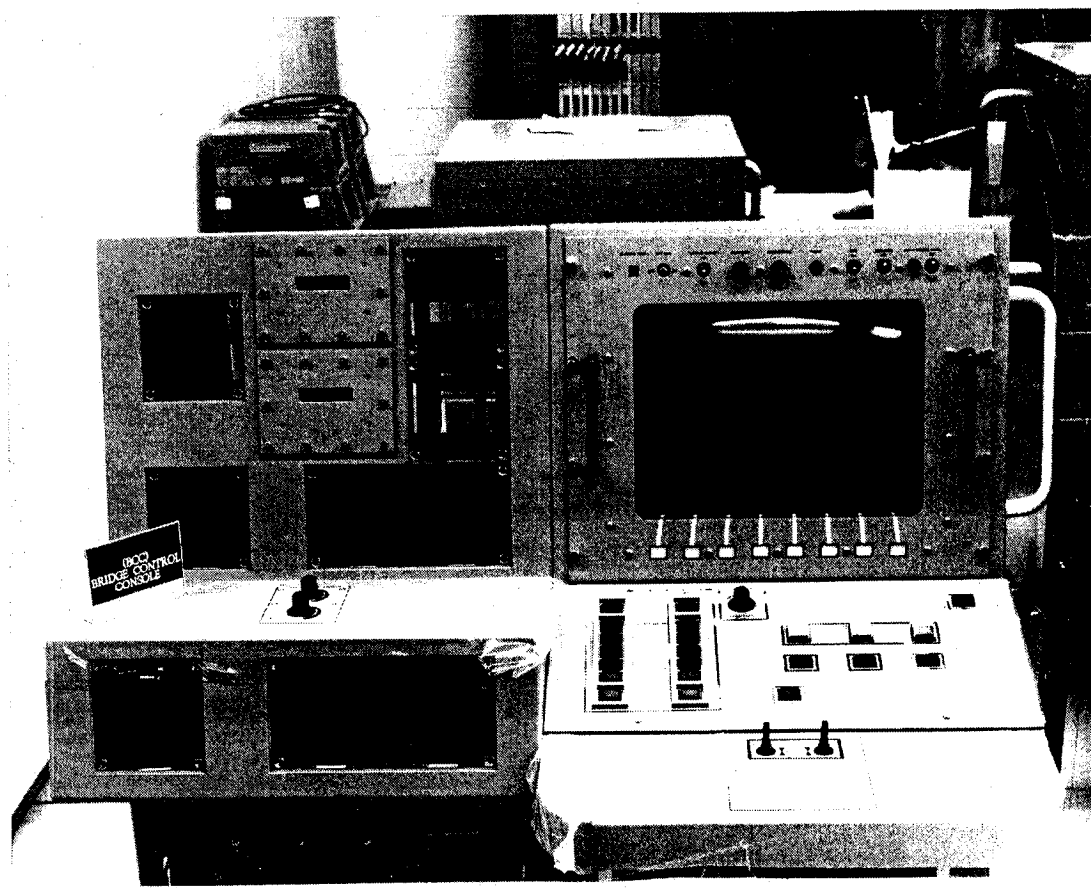


Fig. 4.1 Bridge Control Console Unit

The console under study consisted of three main sections:

1. **A base section** – where the electronic assemblies for interfacing with internal and external components of the consoles were housed,
2. **A bull nose section** – which provides mounting platform for the keyboard operator interface,
3. **A top section** – which provides the housing for a CRT based monitor which serves as the operator interface.

### 4.3 SCALING OF SHIPBOARD MONITOR AND CONSOLE

Every equipment, for use in ships, such as shipboard monitor and console, has to pass variable frequency test and shock test according to the specifications [44, 45]. Instead of testing the full scale prototype it is proposed to test  $\frac{1}{2}$  scale model. The developed scaling laws in Chapter 2 can be used to scale down the prototype into half size. As it is experimentally verified in Chapter 3 that gravitational effects in this type of vibrating structures is negligible. Considering this we can neglect the gravitational effects in scaling procedure and thus the following scaling factors can be employed:

$$\text{i. } \lambda_t = \lambda_l \sqrt{\frac{\lambda_\rho}{\lambda_E}}$$

$$\text{ii. } \lambda_\omega = \frac{1}{\lambda_l} \sqrt{\frac{\lambda_E}{\lambda_\rho}}$$

$$\text{iii. } \lambda_\sigma = \lambda_E$$

$$\text{iv. } \lambda_F = \lambda_l^2 \lambda_E$$

$$\text{v. } \lambda_a = \frac{\lambda_l \lambda_\rho}{\lambda_E}$$

Since same material is used for  $\frac{1}{2}$  scale model (i.e.  $\lambda_E = \lambda_\rho = 1$  and  $\lambda_l = 2$ ), the prototype is scaled according to the following scaling values

$$\lambda_t = \lambda_l \sqrt{\frac{\lambda_\rho}{\lambda_E}} = 2$$

$$\lambda_\omega = \frac{1}{\lambda_l} \sqrt{\frac{\lambda_E}{\lambda_\rho}} = 0.5$$

$$\lambda_\sigma = \lambda_E = 1$$

$$\lambda_F = \lambda_l^2 \lambda_E = 4$$

$$\lambda_a = \frac{\lambda_l \lambda_\rho}{\lambda_E} = 2$$

#### 4.4 FINITE ELEMENT MODELING AND MESHING

The console and the monitor system shown in Fig 4.2 have been modeled using Beam and Shell elements in ANSYS. The console has been modeled as a box with shell elements. The monitor has also been modeled as a box with shell elements. Monitor is made up of shell elements with the total weight being that of the monitor (59.1 kg for prototype and 7.38 kg for  $\frac{1}{2}$  scaled model) and with the same size as that of the monitor. All the edges of the console structure have been modeled using beam elements.

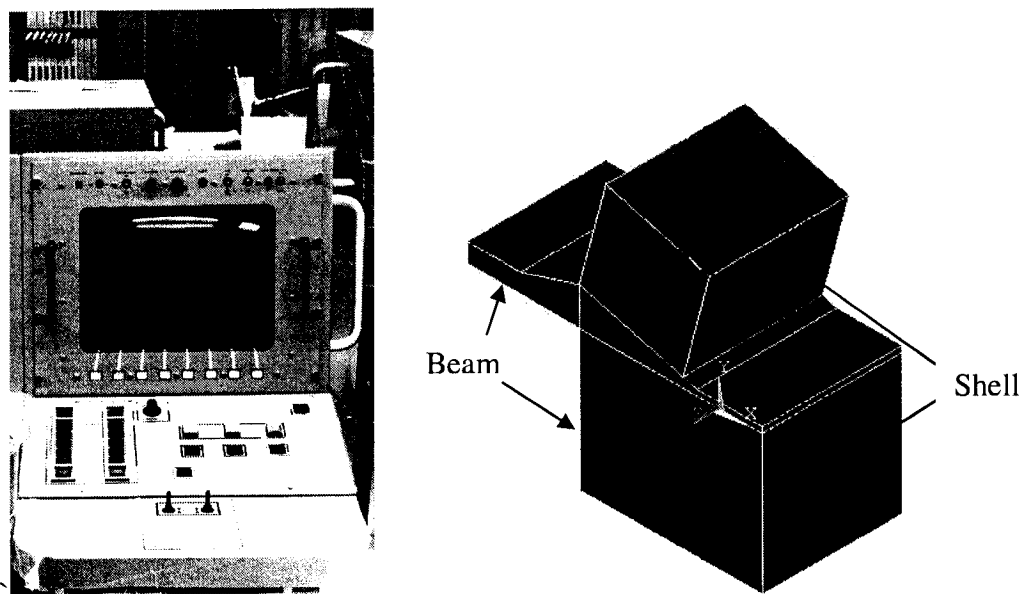


Fig. 4.2 Part of Bridge Control Console which is modeled for FEM Analysis

The shell part of the structure is meshed using SHELL63 element. This element has both bending and membrane capabilities and both in-plane and normal loads are permitted. The element has six degrees of freedom at each node: translations in the nodal x, y, and z directions and rotations about the nodal x, y, and z-axes. The edge of console is meshed with BEAM189 element which is suitable for analyzing slender to moderately

stubby/thick beam structures. This element is based on Timoshenko beam theory. Shear deformation effects are included. BEAM189 is a quadratic (3-node) beam element in 3-D and has six degrees of freedom per node. These include translations in the x, y, and z directions and rotations about the x, y, and z directions. Since both the SHELL63 and BEAM189 elements have same degrees of freedom at each node, they are compatible and there is no need of writing constraint equations for merging the nodes. Both prototype and its  $\frac{1}{2}$  scaled model have been identically meshed with equal number of elements as shown in Fig. 4.3

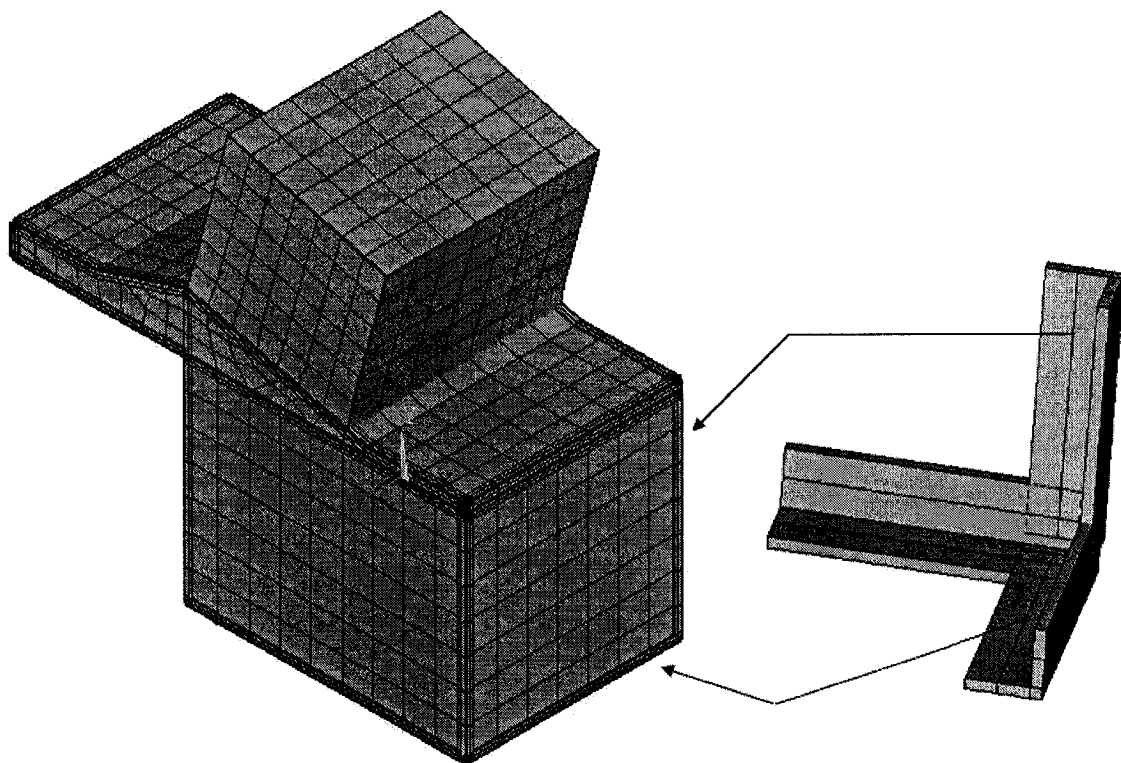


Fig. 4.3 FEM Model of Console with CRT Monitor and Beam Cross Section

## 4.5 ANALYSIS

Initially the console monitor system is analyzed for its natural frequencies using the modal analysis option in the ANSYS 7.1. Subsequently, it is analyzed for a harmonic displacement input at the base. Finally, the system is subjected to a transient input in the form of an impulse input. The impulse input is in the form of a hammer blow to the base of the system mounted on an anvil. The frequencies of interest are in the range of 0 – 50 Hz. The total impulse supplied by the hammer through the anvil, is modeled as a rectangular pulse with force acting through a duration that is calculated using the travel distance of the hammer, anvil and structure together.

### 4.5.1 Modal Analysis

Modal analysis is performed initially to determine the natural frequencies and mode shapes of the structure. The natural frequencies and mode shapes are important parameters to characterize the structural dynamic behavior. They are also required if spectrum analysis or a mode superposition harmonic or transient analysis is to be performed. Several mode extraction methods available in ANSYS 7.1 are: Block Lanczos (default), subspace, PowerDynamics, reduced, unsymmetric, damped, and QR damped. The default Block Lanczos modal analysis method has been used for both prototype and its  $\frac{1}{2}$  scale model. Modal analysis of the  $\frac{1}{2}$  scale model of the structure has been conducted and the fundamental natural frequency of 112.12 Hz has been identified. To predict the fundamental natural frequency of the full scale prototype from that of the scaled model using scaling laws we have:

$$\text{Predicted Natural Frequency of Prototype} = \lambda_{\omega} \times \text{Natural Frequency of Model}$$

$$= 0.5 \times 112.12$$

$$= 56.06 \text{ Hz.}$$

Conducting the modal analysis on the full scale prototype has revealed the fundamental natural frequency of 56.048 Hz which is in excellent agreement with above predicted frequency.

Table 4.1 summarizes the first 20 natural frequencies of the shipboard console structure and shows good correlation exists between the analytical and predicted natural frequencies.

Table 4.1 Comparison Between the Predicted Natural Frequencies using  $\frac{1}{2}$  Scale Model

$$\text{and Natural Frequencies of Full Scale Prototype } \left( \lambda_{\omega} = \frac{1}{\lambda_i} \sqrt{\frac{\lambda_E}{\lambda_p}} = 0.5 \right)$$

Sr. No.	Nat. Freq. (Hz) of $\frac{1}{2}$ Scale Model ANSYS $(\omega_n)_M$	Predicted Nat. Freq. (Hz.) of full Scale Prototype $\lambda_{\omega} \cdot (\omega_n)_M$	Nat. Freq.(Hz.) of Full Scale Prototype ANSYS $(\omega_n)_P$
1	112.12	56.06	56.048
2	131.9	65.95	65.92
3	138.65	69.325	69.29
4	148.12	74.06	74.021
5	157.19	78.595	78.596
6	158.82	79.41	79.408
7	175.19	87.595	87.594
8	194.02	97.01	97.007
9	198.87	99.435	99.394
10	206.21	103.105	103.04
11	218.38	109.19	109.27
12	220.86	110.43	110.42
13	221.97	110.985	110.96
14	226.63	113.315	113.3
15	247.56	123.78	123.76
16	254.91	127.455	127.45
17	260.62	130.31	130.31
18	280.2	140.1	140.05
19	293.26	146.63	146.62
20	310.92	155.46	155.46

### 4.5.2 Harmonic Analysis

According to military standard MIL-STD-177-1(SHIPS)[44], the equipment intended for shipboard application must be capable of withstanding the environmental vibration conditions which may be encountered aboard naval ships and should undergo variable frequency test. According to the standard, the prototype equipment should be vibrated from 4 Hz (or lowest attainable frequency) to 50 Hz. in discrete frequency intervals of 1 Hz at the amplitudes shown in Table 4.2 and Fig 4.4.

Table 4.2 Harmonic Input for Prototype

Frequency Range (Hz) $\omega_p$	Amplitude in (mm) $\delta_p$	No of Sub-steps
4 to 15	0.762	11
15 to 25	0.508	10
25 to 33	0.254	8
33 to 40	0.127	7
40 to 50	0.0762	7

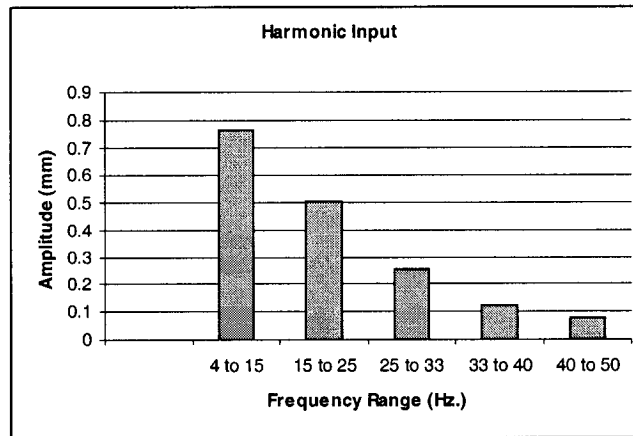


Fig. 4.4 Harmonic Input for Prototype

For testing a  $\frac{1}{2}$  scaled model, this harmonic input is scaled according to the scaling laws. The scaled harmonic input for the model is shown in Table 4.3 and Fig. 4.5.

Table 4.3 Scaled Harmonic Input for Model

Frequency Range (Hz) $\omega_m = \omega_p / \lambda_\omega$	Amplitude in (mm) $\delta_m = \delta_p / \lambda_l$	No of Sub-steps
8 to 30	0.381	11
30 to 50	0.254	10
50 to 66	0.127	8
66 to 80	0.0635	7
80 to 100	0.0381	10

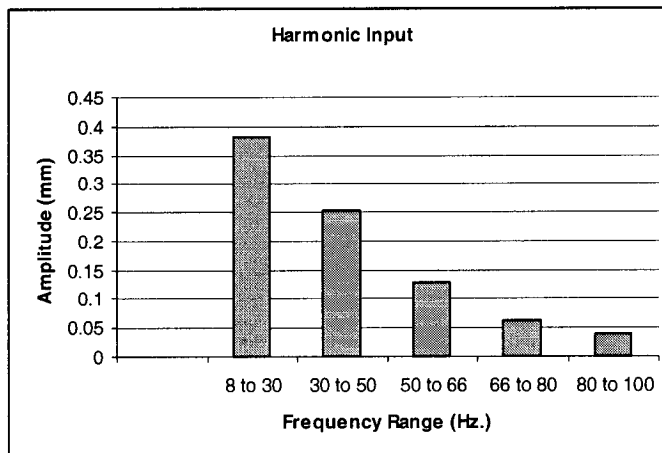


Fig. 4.5 Scaled Harmonic Input for Model

Variable frequency test is simulated in ANSYS 7.1 for prototype as well for its  $\frac{1}{2}$  scale model.

Three harmonic response analysis methods available in ANSYS are: *full*, *reduced*, and *mode superposition*. Full method has been used for harmonic analysis of shipboard monitor and control structure with the Base excitation applied at four corners of the console in UY direction according to Table 4.2 and Table 4.3 for prototype and model, respectively, and the response is observed on top of monitor and on the front of the console. Constant damping ratio of 0.01 is used for harmonic analysis in both model and prototype. The amplitude response obtained on top of the monitor for model and prototype is plotted in fig. 4.6 and Fig 4.7, respectively.

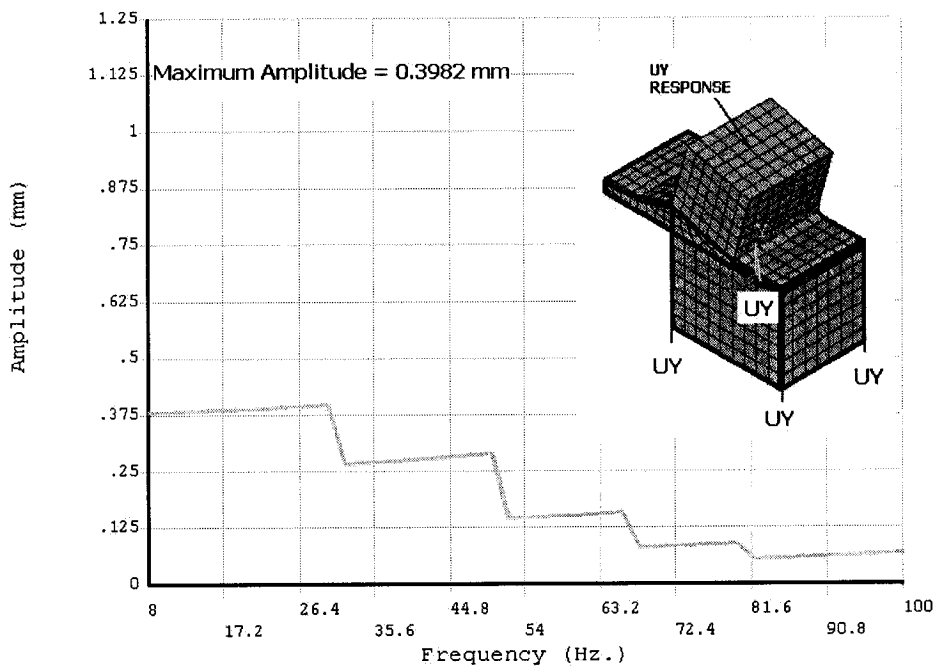


Fig. 4.6 Amplitude Response for  $\frac{1}{2}$  Scale Model under Harmonic Excitation

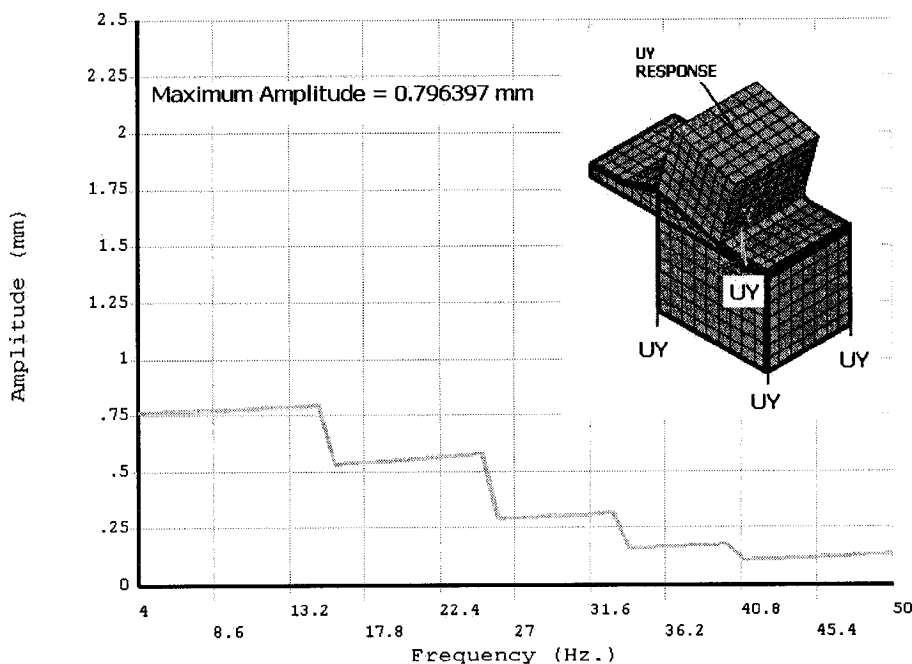


Fig. 4.7 Amplitude Response for Prototype under Harmonic Excitation

Examination of Fig. 4.6 and 4.7 reveals that, there is no model natural frequency between 8-100 Hz. and no prototype natural frequency between 4-50 Hz., and hence no peak is

observed in harmonic analysis. The maximum amplitude obtained for  $\frac{1}{2}$  scale model is 0.3982 mm. To predict the maximum amplitude of prototype we have

$$\begin{aligned}\text{Predicted Amplitude of Prototype} &= \lambda_l \times \text{Amplitude of Model} \\ &= 2 \times 0.3982 \\ &= 0.7964 \text{ mm.}\end{aligned}$$

The maximum amplitude obtained from prototype simulation is 0.796397 mm which is very close to the predicted value. The prototype response can be predicted by expanding the x-axis of model response which is obtained by multiplying frequency by  $\lambda_\omega$  and the amplitude response along y-axis by  $\lambda_l$ . The predicted response using model and response obtained from prototype is plotted in Fig.4.8.

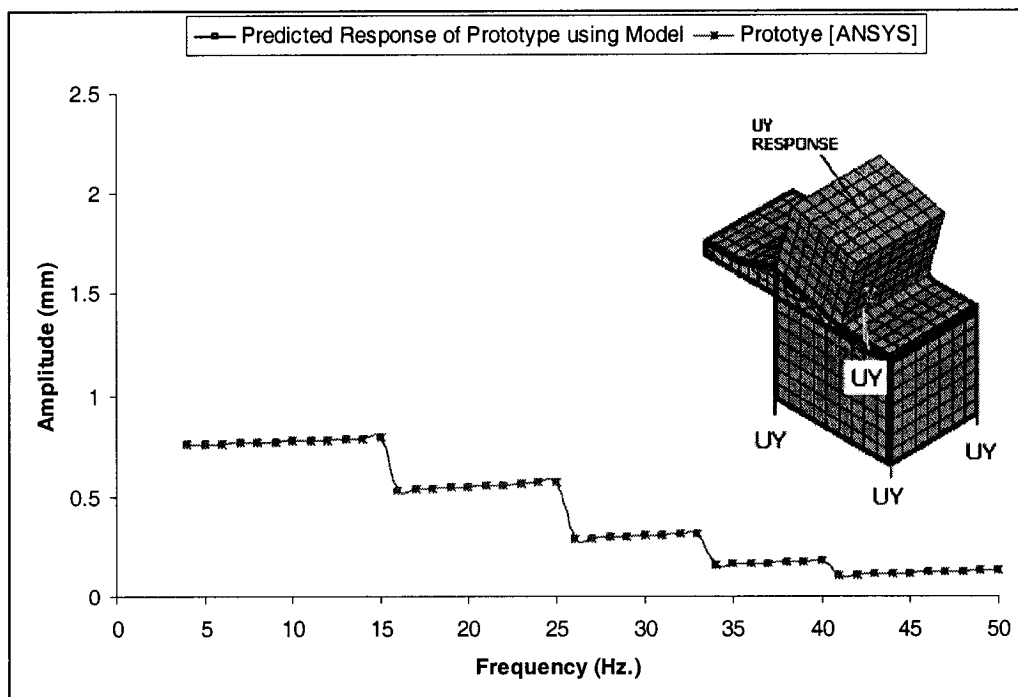


Fig.4.8 Amplitude Response for Harmonic Excitation (Analytical & Predicted Response using Model)

### 4.5.3 Shock Test

The shipboard monitor and console must withstand and satisfy the Specifications for Design and Test for Shock Resistant Equipment in Naval Ships [45]. It should pass through the shock machine test and remain operable to the equipment specification. Since this monitor console unit is between 114-2720 kg range, it has to pass medium weight test with test height specifications provided in Table 4.4.

This test consists of, two blows from 1360 kg hammer falling from the heights given in column 2, 3 and 4 of Table 4.4.

Table 4.4 Medium Weight Test Heights

Total Weight of Equipment and its mounting carried by anvil table (lb)	Height of Hammer drop with 3 inch anvil table travel (inch)	Height of Hammer drop with 1½ inch anvil table travel (inch)	Height of Hammer drop with 1½ inch anvil table travel (inch)
250-1000	11	15	24
1000-2000	13	17	28
2000-3000	14	19	31
3000-3500	16	21	34
<b>3500-4000</b>	<b>18</b>	<b>23</b>	<b>38</b>
4000-4400	20	27	45
4400-4600	22	29	48
4600-4800	24	31	51
4800-5000	26	33	55
5000-5200	29	37	62
5200-5400	32	41	69
5400-6000	35	45	72
6000-7500	36	46	72

In order to simulate the shock test in ANSYS 7.1, transient analysis is performed. Since it is not possible to produce an ideal shock or impulse force numerically, a load over a

discrete amount of time  $dt$  which generates the similar impulse has been used.

The required force and discrete amount of time can be calculated by the formulation as follows. The hammer falls through a height 'h', and impacts the base of the anvil on which the console-monitor assembly is mounted as shown in Fig 4.9. When the hammer impacts the anvil, the hammer –anvil –structure travels up through a distance 'd'. The impulse of the hammer is given by

$$I_H = M_H \cdot V_H \quad (4.1)$$

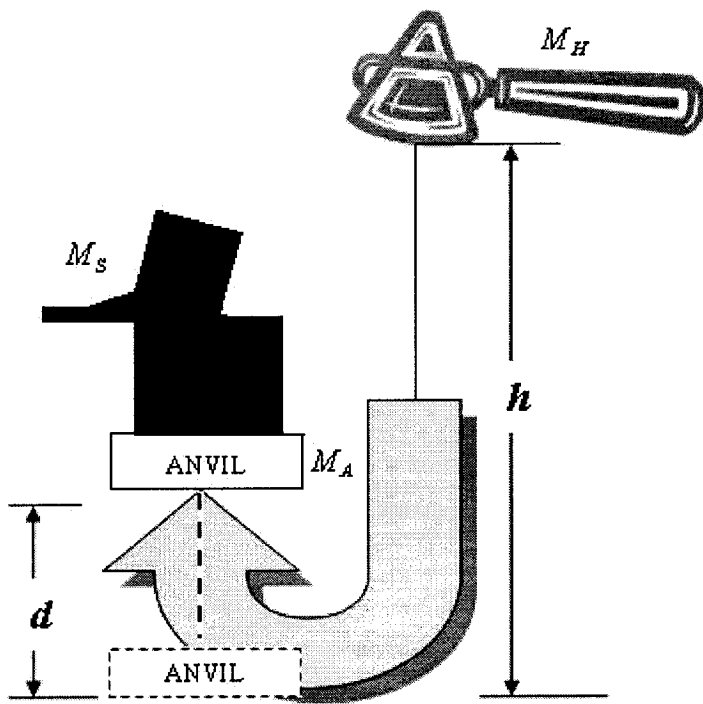


Fig. 4.9 Hammer Falls Through a Height 'h', and Impacts the Base of the Anvil on which the Console-Monitor Assembly is Mounted

This is equal to the momentum generated by the assembly of hammer-anvil-structure, and is given by

$$I_H = (M_A + M_H + M_S) \cdot V_C \quad (4.2)$$

Ignoring the energy loss during impact, the conservation of energy provides the force, which is given by

$$F.d = M_H \cdot g \cdot (h - d) - (M_A + M_S) \cdot g \cdot d \quad (4.3)$$

The impulse transmitted to the structure is

$$I_s = I_H - (M_A + M_H) \cdot V_c \quad (4.4)$$

The duration of the shock pulse is obtained as

$$\Delta t = \frac{I_s}{F} \quad (4.5)$$

Please refer to APPENDIX-2 regarding detailed calculation of force and time duration of impulse for Table 4.4.

Three methods are available to do a transient dynamic analysis: *full*, *mode superposition*, and *reduced*. Mode superposition method is used for simulation of shock test. The *mode superposition method* sums factored mode shapes (eigenvectors) from a modal analysis to calculate the structure's response. The first 50 modes have been used to calculate the transient response. For transient analysis, impulse force is applied at the base of the console and the response is taken on the top the monitor and on the bull nose section of the console.

The parameters for rectangular pulse calculated in APPENDIX-2 for 18" hammer drop and 3" Anvil travel are  $(F_o)_p = 50500N$  and  $(dt)_p = 0.0001sec$ . For testing a  $\frac{1}{2}$  scale model these parameters are scaled according to force and time scale factors as

$$(F_o)_m = \frac{(F_o)_p}{\lambda_F} = \frac{50500}{4} = 12625N$$

$$(dt)_m = \frac{(dt)_p}{\lambda_t} = \frac{0.0001}{2} = 0.00005 \text{ sec.}$$

Constant damping ratio of 0.01 is used in the analysis for both prototype and its  $\frac{1}{2}$  scale model. The amplitude response obtained from model and prototype is shown in Fig. 4.10 and Fig. 4.11 respectively.

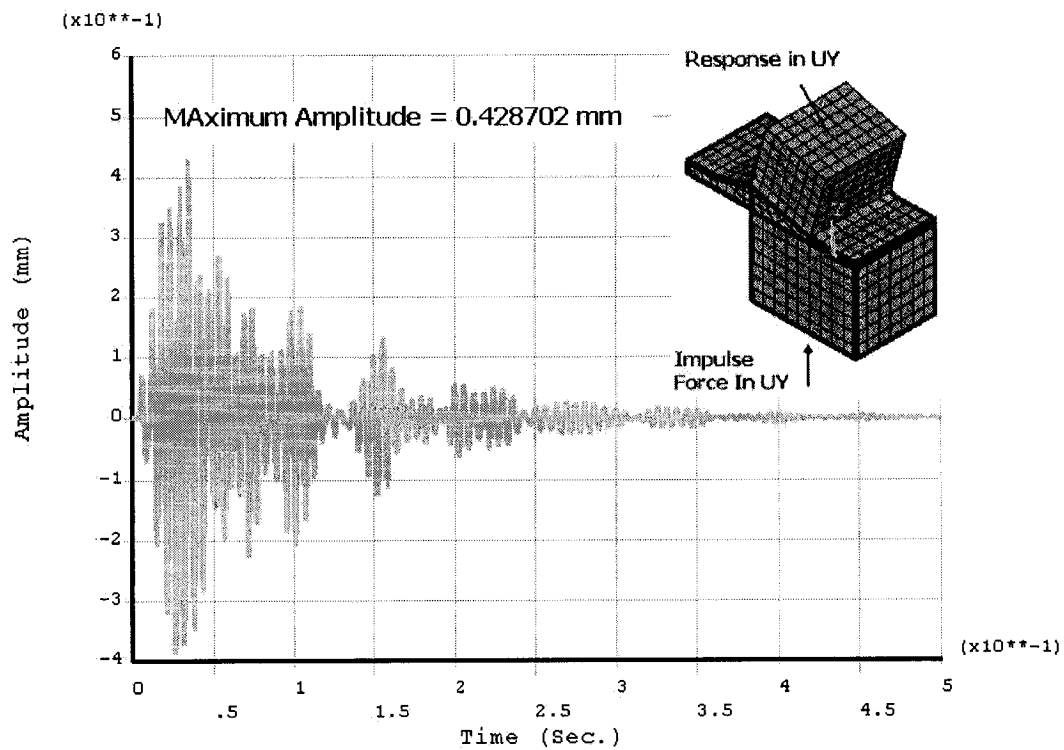


Fig. 4.10 Amplitude Response for  $\frac{1}{2}$  Scale Model under Impulse Excitation

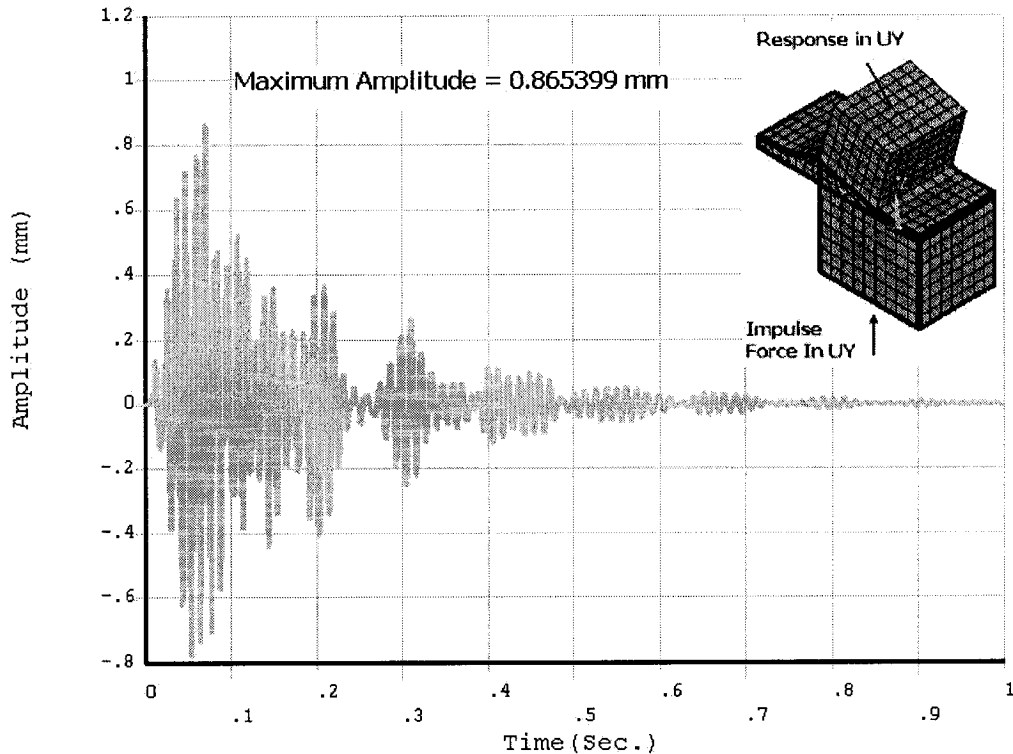


Fig. 4.11 Amplitude Response for Prototype under Impulse Excitation

The maximum amplitude obtained for  $\frac{1}{2}$  scale model is 0.428702 mm. To predict the maximum amplitude of prototype we have

$$\begin{aligned}
 \text{Predicted Amplitude of Prototype} &= \lambda_t \times \text{Amplitude of Model} \\
 &= 2 \times 0.428702 \\
 &= 0.857404 \text{ mm.}
 \end{aligned}$$

The maximum amplitude obtained from prototype simulation is 0.865399 mm which is very close to the predicted value. The prototype response can also be predicted by expanding the frequency along the axis by  $\lambda_\omega$  and the amplitude response along y-axis by  $\lambda_t$ . The predicted response using model and response obtained from prototype is plotted in Fig.4.12.

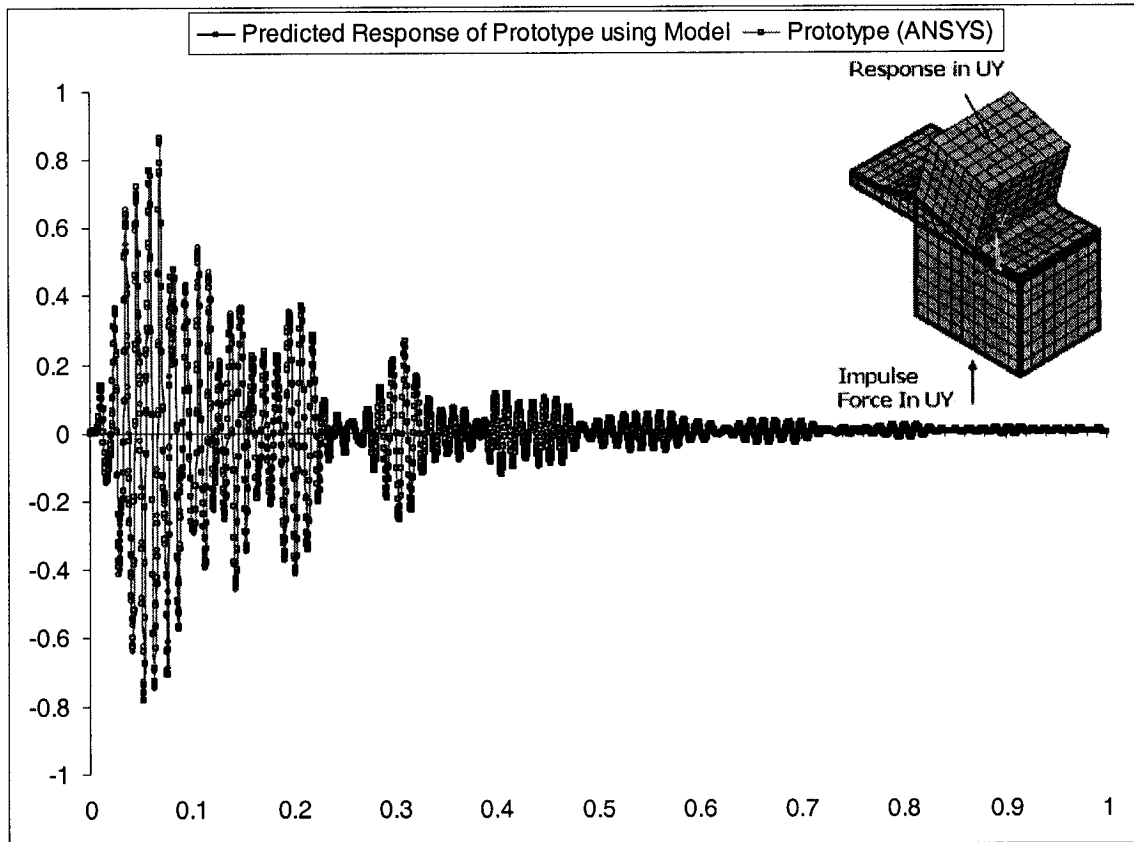


Fig. 4.12 Amplitude Response under Impulse Excitation (Analytical & Predicted Response using Model)

Please refer to the APPENDIX-3 for the result obtained for the bull nose section.

Simulation results of shock test for 23" Hammer Drop, 1.5" Anvil travel and 38" Hammer Drop, 1.5" Anvil Travel are also presented in the APPENDIX 3.

# **CHAPTER 5**

## **CONCLUSIONS AND FUTURE WORK**

### **5.1 SUMMARY**

The complete and comprehensive study on the methodology of dynamic scaled modeling has been treated in this thesis. Previous work on dynamic scaled modeling has been thoroughly reviewed and necessary modifications have been suggested. The theory of scaled modeling is studied and has been applied on dynamic testing of benchmark simple cantilever beam. Simulations of dynamic testing for model and prototype has been accomplished in ANSYS 7.1 to validate the scaling laws derived. Simulation results are then confirmed by experimentally testing of beam prototype and its  $\frac{1}{2}$  scale model.

Maintaining complete similarity becomes cumbersome and impractical in the area of scaled modeling dynamic scaling and relaxations are required to practically have a dynamic scaled model. Various relaxations are discussed to have a dynamic scaled model and it has been suggested that neglecting gravity effects in dynamic scaled model provides reasonably good results. Concept of using dummy masses has been discussed for dynamic scale modeling when the gravitational forces are significant and cannot be neglected and is applied on simple beam.

Finally the developed methodology is then applied on real life structure by studying the behavior of Naval shipboard Console under vibration and Shock using Scaled Model. Simulations of dynamic testing for full scale prototype of Naval Shipboard Monitor and Console and its  $\frac{1}{2}$  scale model has been carried out and demonstrated that results of  $\frac{1}{2}$  scale model can perfectly predict the behavior of the full scale prototype.

## 5.2 CONCLUSIONS

The following important conclusions can be drawn from the analytical and experimental studies undertaken in this research:

1. The study of scaled model methodology is found to be extremely useful for the dynamic testing of structures as it is convenient, economic and time saving.
2. Scaling laws are derived for dynamic testing using **Buckingham Pi Theorem** and **similarity conditions**, and good correlation is found between the properties of prototype and its  $\frac{1}{2}$  scale model in analytical studies by using finite element analysis as well as in experimental studies.
3. It is found that maintaining complete similarity for dynamic testing becomes very difficult due to practical limitations and hence relaxation or distortions are required to have a practical scaled model.
4. Relaxation of neglecting gravity effects is suggested for dynamic modeling and it is verified experimentally that the gravity does not significantly affect the model response.
5. Dummy masses can be attached to the model when the gravitational forces are significant in the structure.
6. Finite analysis results have found to provide good results and thus can be used confidently for dynamic analysis with scaled model.

### **5.3 FUTURE WORK**

Although this thesis has taken an important step towards the understanding of dynamic scaled modeling both analytically and experimentally, other important aspects are identified to complement an improved design of dynamic scaled model testing. These aspects can be summarized as follows:

1. Extending the experimental verification to more complex structures such as plates and shells.
2. Verifying the concept of dummy masses experimentally and extending the analytical formulation on complex structures such as plates.
3. Performing experimental verification for vibration excitation such as Harmonic, Shock and Random.
4. More investigation on the effect of scaling on damping.
5. Extending the idea of dynamic macro scaled modeling to micro electro mechanical structures (MEMS).

## REFERENCES

1. de Silva C.W., '*Dynamic Testing and Seismic Qualification Practice*', Lexington Books, D.C. Heath and Company Lexington, Massachusetts, Toronto, 1983.
2. David F.W. and Nolle H., '*Experimental modeling in Engineering*', Butterworths, 1982.
3. Abramson H.N., '*Some Modern Developments in the Application of Scale-Models in Dynamic Testing*', Colloquium on Use of Models and Scaling in Shock and Vibration, ASME Winter Annual Meeting , pp. 1-15, ASME, New York, November 1963.
4. Murphy G., '*Similitude in Engineering*', The Ronald Press Company, New York, 1950.
5. Dieterich J. Schuring, '*Scale Models in Engineering' fundamentals and applications*', Pergamon Press, 1977.
6. Young D.F., '*Basic Principles and Concepts of Model Analysis*', Experimental Mechanics, Vol. 11, No. 7, pp. 325-336, July 1971.
7. William G.S., '*Dynamic Modeling with Similar Material*', Colloquium on Use of Models and Scaling in Shock and Vibration, ASME Winter Annual Meeting, pp. 51-56, ASME, New York, November 1963.
8. Chen W.K., '*Algebraic theory of dimensional analysis*', Journal of the Franklin Institute, Vol. 292, No. 6, pp. 403-422, December 1971.
9. Higgins T. J., '*Electroanalogic Methods*', Applied Mechanics Reviews, Vol. 10, No. 8, pp. 331-335, August 1957.
10. Macagno E.O., '*Historico-Critical Review of Dimensional Analysis*', Journal of the Franklin Institute, Vol. 292, No. 6, pp. 391-402, December 1971.

11. Buckingham E., '*Physically Similar Systems; Illustrations of Use of Dimensional Equations*', Physical Review, Vol. 4, No. 4, pp. 345-376, June 1914.
12. Rayleigh J.W., '*The Principle of Similitude*', Nature, Vol. 95, No. 2389, pp. 66-68, and Vol. 95, No. 2373, pp. 202-203, and Vol. 95, No. 2389, pp. 644, March 1915.
13. Buckingham E., '*The Principle of Similitude*', Nature, Vol. 96, No. 2406, pp. 396-397, December 1915.
14. Bridgman P.W., '*Dimensional Analysis*', New Haven, Yale University Press, First published, November 1922.
15. Pankhurst R.C. ,'*Alternative Formulation of the Pi-Theorem*', Journal of the Franklin Institute, Vol. 292, No. 6, pp. 451-462, December 1971.
16. Baker W.E., Westine P.S., Dodge F.T., '*Similarity Methods in Engineering Dynamics, Theory and Practice of Scale Modeling*', Hayden Book Company, Inc., Rochelle Park, New Jersey, 1973.
17. Mansfield J.N., McGregor J., '*Contractual Acceptance Tests of Model Turbines*' , Proceedings of Symposium on "Model testing of Hydraulic Machinery and Associated Structures", Vol. 182, Part 3M, pp. 28-31, 1967-68.
18. Paterson I.S., Campbell G., '*Pump Intake Design Investigations*', Proceedings of Symposium on "Model testing of Hydraulic Machinery and associated Structures", Vol. 182, Part 3M, pp. 1-10, 1967-68.
19. Paterson I.S., McConnell T.A., '*Integrated Design of Pump and Adjacent System*', Proceedings of Symposium on "Model testing of Hydraulic Machinery and Associated Structures", Vol. 182, Part 3M, pp. 11-19, 1967-68.
20. Duggins R.K., '*Hydraulic Stability of a Model Hydroelectric Installation*', Proceedings of Symposium on "Model testing of Hydraulic Machinery and Associated Structures", Vol. 182, Part 3M, pp. 20-27, 1967-68.

21. Nixon R.A., Spencer E.A., '*Model Testing of High Head Pumps*', Proceedings of Symposium on "Model testing of Hydraulic Machinery and Associated Structures", Vol. 182, Part 3M, pp. 32-41, 1967-68.
22. Ward T., '*Thermodynamic Scale Effects on Pump Suction Performance*', Proceedings of Symposium on "Model testing of Hydraulic Machinery and Associated Structures", Vol. 182, Part 3M, pp. 42-47, 1967-68.
23. Vasallos D., '*Physical Modeling and Similitude of Marine Structures*', Ocean Engineering, Vol. 26, pp. 111-123, August 1998.
- 24.. Andrews J., Church J.W., '*A Model for the Simulation of Wave Impact Loads and Resulting Transient Vibration of a Naval Vessel*', Colloquium on Use of Models and Scaling in Shock and Vibration, ASME Winter Annual Meeting , pp. 16-28, ASME, New York, November 1963.
25. '*Wind Tunnel Studies of Buildings and Structures*', American Society of Civil Engineers Manuals and Reports on Engineering Practice No. 67, 1999.
26. Wardlaw R.L., Ponder C.A., '*An Example of the Use of Wind Tunnels for Investigating the Aerodynamic stability of Bridges*', Quarterly Bulletin Division of Mechanical Engineering and the National Aeronautical Establishment, Report No. DME/NAE 3, pp.13-34, July-September 1969.
27. National Research Council of Canada Quarterly Bulletin of the Division of Mechanical Engineering and the National Aeronautical Establishment, January 1 to March 31 1970.
28. Arthur A. Regier, '*The Use of Scaled Dynamic Models in Several Aerospace Vehicle Studies*', Colloquium on Use of Models and Scaling in Shock and Vibration, ASME Winter Annual Meeting , pp. 34-50, ASME, New York, November 1963.
29. Brooks G.W., '*The Application of Models to Helicopter Vibration and Flutter Research*', Proc. Ninth Annual Forum, American Helicopter Society, Washington, D.C., May 1953.

30. Sewall J.L., Herr R.W., and Igoe W.B., '*Flutter Investigation of a True-Speed Dynamic Model with Various Tip-Tank Configurations*', NASA TN D-178, March 1960.
31. Abbott F.T., Jr., Kelly H.N., and Hampton K.D., '*Investigation of Propeller-Power-Plant Auto-precession Boundaries for a Dynamic-Aeroelastic Model of a Four-Engine Turboprop Transport Airplane*', NASA TN D-1806, June 1963.
32. Runyan H.L., Morgan H.G., and Mixson J.S., '*Role of Dynamic Models in Launch Vehicle Development*', Experimental Techniques in Shock and Vibration, ASME, New York, pp. 55-69, November 1962.
33. Ferritto J., '*Dynamic test of Model Concrete*', Dynamic Modeling of Concrete Structures, SP73-2, Publication SP-73 American Concrete Institute Detroit, pp. 23-33, 1982.
34. Clough R.W., '*Earthquake Simulator Research on Arch Dam Models*', Dynamic Modeling of Concrete Structures, SP73-5, Publication SP-73 American Concrete Institute Detroit, pp. 83-105, 1982.
35. Abrams D.P., '*Behavior of Small Scale Reinforced Concrete Model Structures*', Dynamic Modeling of Concrete Structures, SP73-4, Publication SP-73 American Concrete Institute Detroit, pp. 65-82, 1982.
36. Takanashi K., Ohi K., '*Response observation of scaled model structures to strong earthquakes*', Journal of Constructional Steel Research, Volume 13, Issues 2-3, pp. 189-210, 1989.
37. Godden W.G., '*Seismic Modeling of Long-Span Bridges*', Dynamic Modeling of Concrete Structures, SP73-6, Publication SP-73 American Concrete Institute Detroit, pp. 107-123, 1982.
38. Priyadarsini R., Cheong K.W., Wong N.H., '*Enhancement of natural ventilation in high-rise residential buildings using stack system*', Energy and Buildings, Vol. 36, pp. 61-71, 2004.

39. Hegvold L.W., 'A 1:8 Scale Model Auditor', Applied acoustics, Vol. 4, pp. 237-256, 1971.
40. Dobrzynski W., Gehlhar B., Büchholz H., 'Model and full scale high-lift wing wind tunnel experiments dedicated to airframe noise reduction', Aerospace Science and Technology, Vol. 5, Issue 1, pp. 27-33, January 2001.
41. S. Tavakoli, M. Tavakoli, 'Optimal Tuning of PID Controllers for First Order Plus Time Delay Models Using Dimensional Analysis', The Fourth International Conference on Control and Automation (ICCA'03), 10-12, Montreal, Canada June 2003.
42. CAE Inc., "Environmental Qualification Testing of A Bridge Control Console, Machinery/Ship Control System", CPF, Project No. XT 250, Report No. 70/91, 10081-2711-4 (DMES 4-3-2), Jan 1991.
43. CAE Inc., "Shock Testing of A Machinery Control Console", Project No. XT 187, Report No. 1/89, 10081-2711-4 (DGMEM/RM 3-2), March 1988.
44. Military Standard MIL-STD-167-1(SHIPS), "Mechanical Vibrations of Shipboard Equipment (Type I- Environment and Type II- Internally Excited")", pp 5, May 1 1974.
45. Specification for Design and Test Criteria for Shock Resistant Equipment in Naval Ships, D-03-003-007/SF-000, Section 6, pp 24, June 19 1972.
46. A. Peter, "Experimental Modal Analysis a Simple Non-Mathematical Presentation", Sound and Vibration, pp. 1-11, January 2001
47. P.D. Mocarz, H. Krawinkler, "Similitude Requirements for Dynamic Models", Dynamic Modeling of Concrete Structures, SP73-1, Publication SP-73 American Concrete Institute Detroit, pp. 1-22, 1982.

# APPENDIX-1

## HARMONIC TEST RESULTS

The amplitude response obtained on bull nose section of the console for model and prototype from ANSYS 7.1 is plotted in fig. 6.1 and Fig 6.2 respectively.

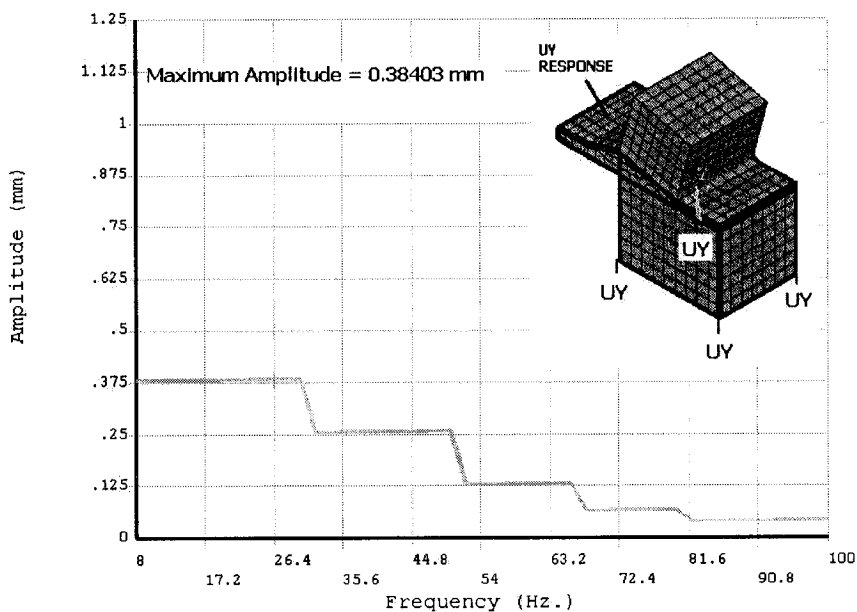


Fig 6.1 Amplitude Response for  $\frac{1}{2}$  Scale Model under Harmonic Excitation

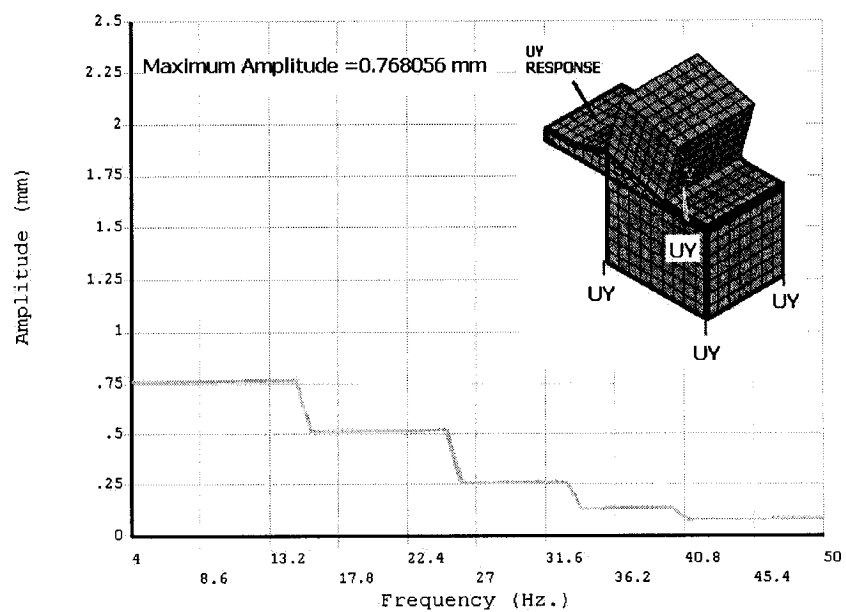


Fig 6.2 Amplitude Response for Prototype under Harmonic Excitation

## **APPENDIX-2**

### **CALCULATION OF SHOCK PULSE PARAMETERS**

*Mass of Anvil*( $M_A$ ) = 1820 Kg , *Mass of Hammer*( $M_H$ ) = 1360 Kg

*Mass of Structure*( $M_S$ ) = *Mass of Console + Mass of Monitor*  $\approx$  300 kg

1.) For 18" Hammer Height, 3" Anvil travel

$$h = 18" = 0.4572 \text{ m} \quad , \quad d = 3" = 0.0762 \text{ m}$$

a.)  $I_H = M_H \cdot V_H$

$$V_H = \sqrt{2 \cdot g \cdot h} = 2.995 \text{ m/sec}$$

$$I_H = 4073.2 \text{ N.Sec}$$

b.)  $I_H = (M_A + M_H + M_S) \cdot V_C$

$$V_C = 1.1704597 \text{ m/sec}$$

c.)  $F \cdot d = M_H \cdot g \cdot (h - d) - (M_A + M_S) \cdot g \cdot d$

$$F = 50423.4 \text{ N} \approx 50500 \text{ N}$$

d.)  $I_S = I_H - (M_A + M_H) \cdot V_C$

$$I_S = 351.138154 \text{ N.Sec}$$

e.)  $\Delta t = \frac{I_S}{F} = 0.006953 \text{ sec.}$

2.) For 23" Hammer Height, 1½" Anvil travel

$$h = 23" = 0.5842 \text{ m} , \quad d = 1\frac{1}{2}" = 0.0381 \text{ m}$$

a.)  $I_H = M_H \cdot V_H$

$$V_H = \sqrt{2 \cdot g \cdot h} = 3.3855 \text{ m/sec}$$

$$I_H = 4604.35 \text{ N.Sec}$$

$$b.) I_H = (M_A + M_H + M_S).V_C$$

$$V_C = 1.323089 \text{ m/sec}$$

$$c.) F.d = M_H.g.(h-d) - (M_A + M_S).g.d$$

$$F = 170432.4 \text{ N} \approx 170500 \text{ N}$$

$$d.) I_S = I_H - (M_A + M_H).V_C$$

$$I_S = 396.92698 \text{ N.Sec}$$

$$e.) \Delta t = \frac{I_S}{F} = 0.002328 \text{ sec.}$$

3.) For 38" Hammer Height, 1½" Anvil travel

$$h = 38" = 0.9652 \text{ m}, d = 1\frac{1}{2}" = 0.0381 \text{ m}$$

$$a.) I_H = M_H.V_H$$

$$V_H = \sqrt{2.g.h} = 4.351 \text{ m/sec}$$

$$I_H = 5918.3012 \text{ N.Sec}$$

$$b.) I_H = (M_A + M_H + M_S).V_C$$

$$V_C = 1.7006 \text{ m/sec}$$

$$c.) F.d = M_H.g.(h-d) - (M_A + M_S).g.d$$

$$F = 303848.4 \text{ N} \approx 303900 \text{ N}$$

$$d.) I_S = I_H - (M_A + M_H).V_C$$

$$I_S = 510.3932 \text{ N.Sec}$$

$$e.) \Delta t = \frac{I_S}{F} = 0.0016794 \text{ sec.}$$

## APPENDIX-3

### SHOCK TEST RESULTS

#### 1.) For 18" Hammer Height, 3" Anvil travel

The amplitude response obtained on bull nose section of the console for model and prototype from ANSYS 7.1 is plotted in fig. 6.3 and Fig 6.4 respectively.

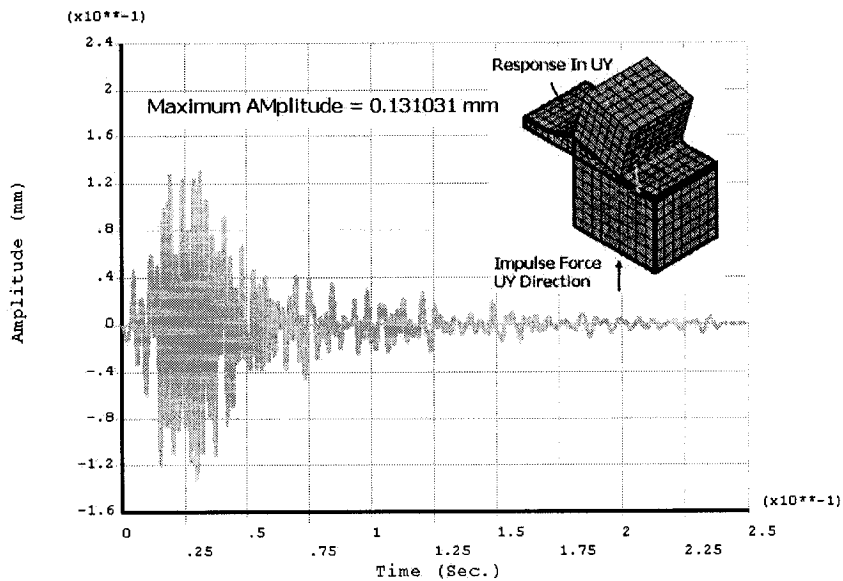


Fig 6.3 Amplitude Response for  $\frac{1}{2}$  Scale Model under Impulse Excitation

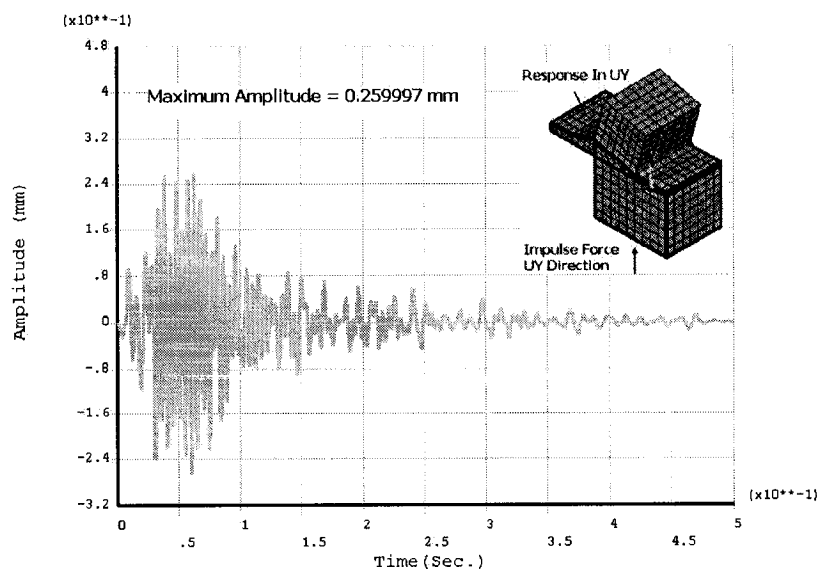


Fig 6.4 Amplitude Response for Prototype under Impulse Excitation

2.) For 23" Hammer Height,  $1\frac{1}{2}$ " Anvil travel

The amplitude response obtained on top of monitor for model and prototype from ANSYS 7.1 is plotted in fig. 6.5 and Fig 6.6 respectively

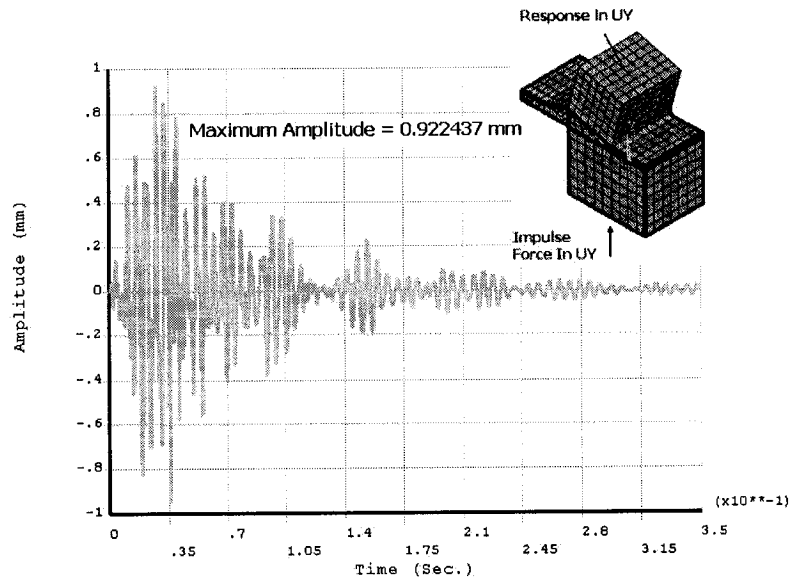


Fig 6.5 Amplitude Response for  $\frac{1}{2}$  Scale Model under Impulse Excitation

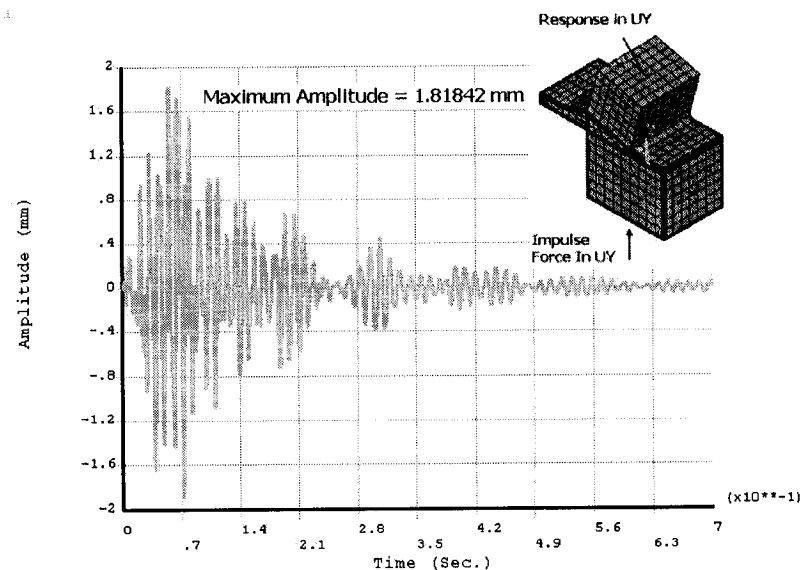


Fig 6.6 Amplitude Response for Prototype under Impulse Excitation

The amplitude response obtained on bull nose section of the console for model and prototype from ANSYS 7.1 is plotted in fig. 6.7 and Fig 6.8 respectively.

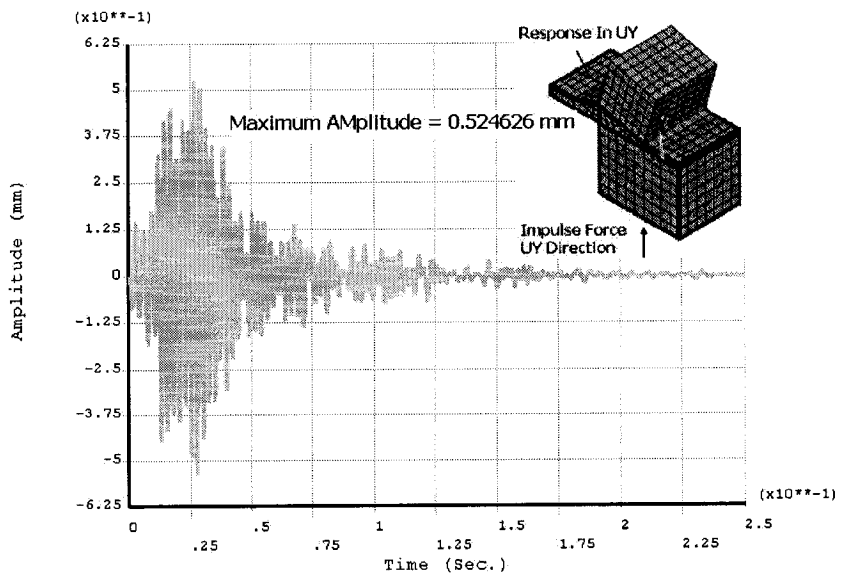


Fig 6.7 Amplitude Response for  $\frac{1}{2}$  Scale Model under Impulse Excitation

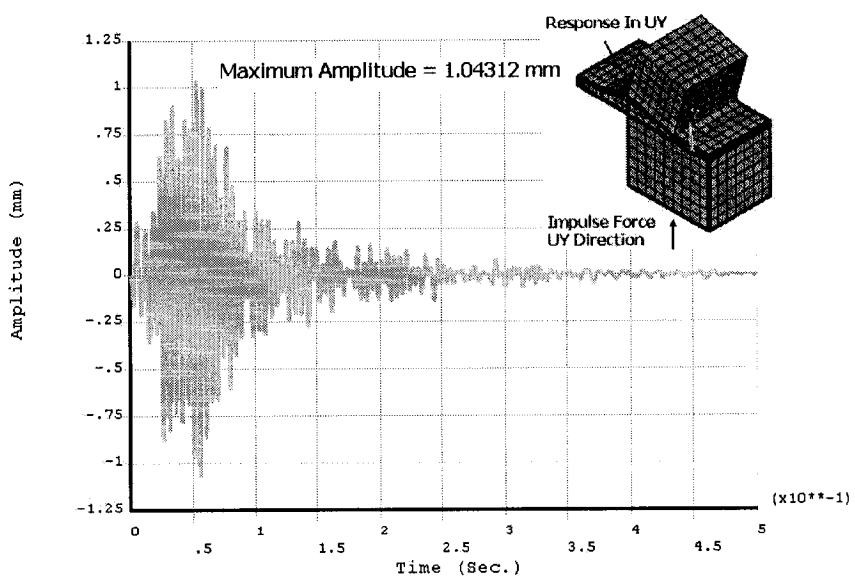


Fig 6.8 Amplitude Response for Prototype under Impulse Excitation

3.) For 38" Hammer Height,  $1\frac{1}{2}$ " Anvil travel

The amplitude response obtained on top of monitor for model and prototype from ANSYS 7.1 is plotted in fig. 6.9 and Fig 6.10 respectively.

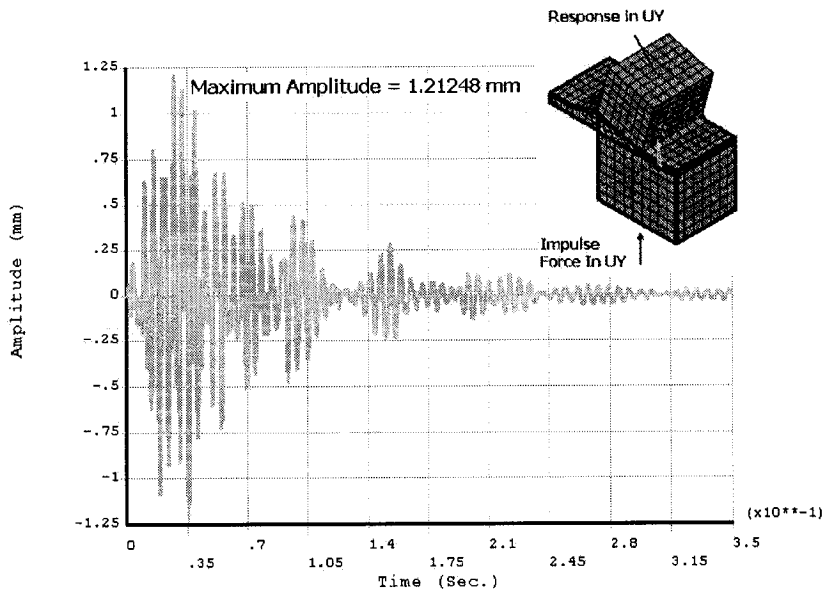


Fig 6.9 Amplitude Response for  $\frac{1}{2}$  Scale Model under Impulse Excitation

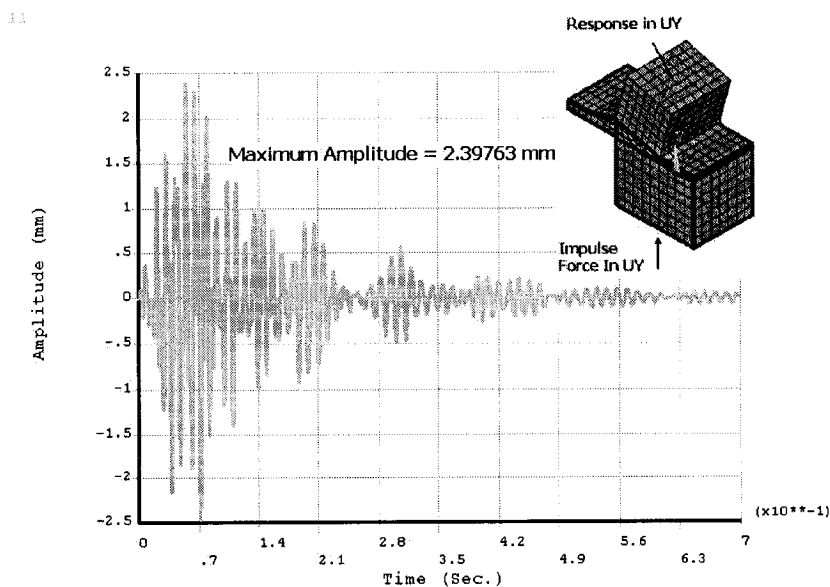


Fig 6.10 Amplitude Response for Prototype under Impulse Excitation

The amplitude response obtained on bull nose section of the console for model and prototype from ANSYS 7.1 is plotted in fig. 6.11 and Fig 6.12 respectively.

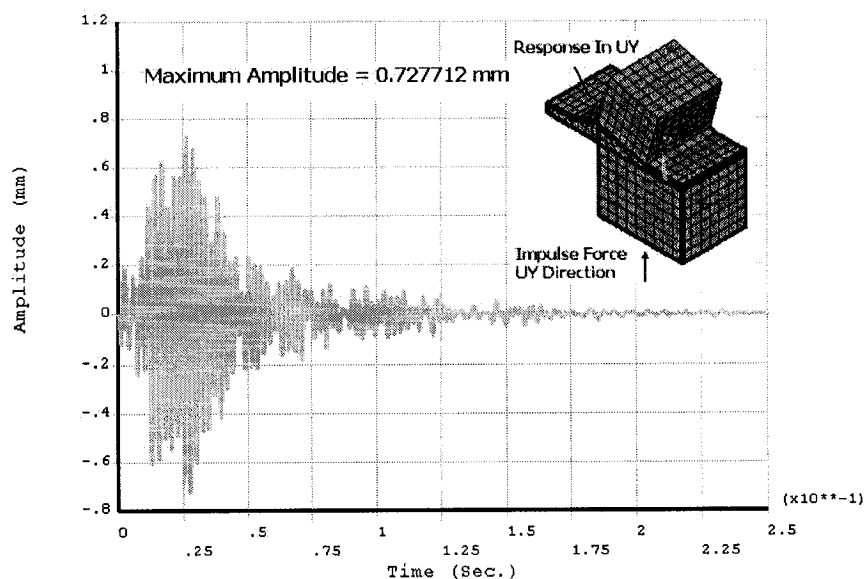


Fig 6.11 Amplitude Response for  $\frac{1}{2}$  Scale Model under Impulse Excitation

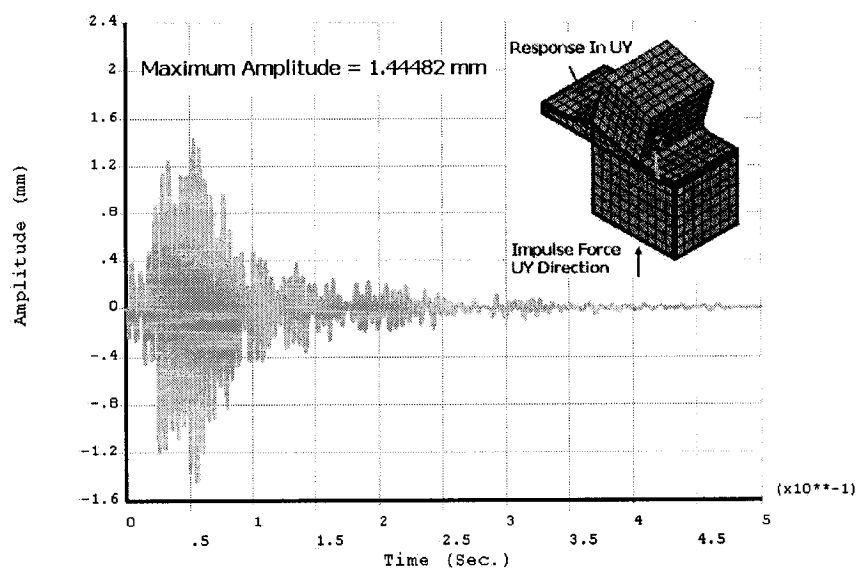


Fig 6.12 Amplitude Response for Prototype under Impulse Excitation